Svoluji k zapůjčení své diplomové práce ke studijním účelům a prosím, aby byla vedena přesná evidence vypůjčovatelů. Převzaté údaje je vypůjčovatel povinen řádně odcitovat.

**Univerzita Karlova**

**Přírodovědecká fakulta**

Studijní program: Biologie

Studijní obor: Genetika, molekulární biologie a virologie


**Bc. Maroš Kompas**

# Vliv metabolismu hemu na reversi latence HIV-1

Effects of heme metabolism on HIV-1 latency reversal

Diplomová práce

Školitel: MUDr. Zora Mělková, PhD.

Praha, 2022

**Prohlášení**

Prohlašuji, že jsem závěrečnou práci zpracoval samostatně a že jsem uvedl všechny použité informační zdroje a literaturu. Tato práce ani její podstatná část nebyla předložena k získání jiného nebo stejného akademického titulu.

V Praze, 04.01.2022

Podpis

First and foremost, I would like to express my sincere gratitude to my supervisor MUDr. Zora Mělková, PhD. for all the guidance, patience, and invaluable scientific insights that helped me during my studies.

I cannot express enough thanks to my family and friends who supported me both financially and emotionally in the time of need. I would like to specifically express my deepest gratitude to MUDr. Matej Rúra and Mgr. Róbert Reiberger for their unconditional support that allowed me to finish this work.

Last but not least, I would like to thank my collegues for their bright ideas, advices, and motivation they provided me with during my work in laboratory.

**Abstract**

Progression of HIV infection in HIV-positive patients can now be successfully controlled by the combined antiretroviral therapy. However, due to persistence of the latent reservoir, HIV infection cannot be cured. The immune system nor current therapeutic approaches can target the pool of latently infected cells, thus strategies aiming at reactivation and subsequent elimination of the reservoir cells are recognized as possibly curative.

This thesis has examined previously demonstrated latency-reversing capacity of heme arginate (HA), another redox modulator, and their synergism with Protein Kinase C inducer phorbol myristate acetate (PMA) to reactivate HIV-1 in the context of heme metabolism. HIV-1 reactivation was assessed by the intensity of green fluorescence in the model Jurkat cell line clone (A2), containing HIV-1 *"mini-virus"* (LTR-Tat-IRES-EFGP-LTR), as well as in the A2 cells stably transfected with plasmid vectors encoding cDNA for specific factors of heme metabolism and for control luciferase. While the administration of redox modulator alone did not stimulate expression from the HIV-1 LTR and HA reactivated the *"mini-virus"* only slightly, both compounds revealed a synergy with PMA in all cell lines studied. Basal and induced expression of EGFP was found variable in cells transfected with plasmids encoding cDNA for the individual factors examined. The results provided in this work suggest that studied genes are potentially significant for HIV-1 reactivation and that heme metabolism might play an important role in HIV-1 latency reversal and maintenance.

**Keywords:** HIV-1 latency, heme metabolism, heme arginate, redox modulator, latency-reversing agents

**Abstrakt**

Progresi infekce virem lidské imunodeficience u HIV-pozitivních pacientů je dnes možné úspěšně kontrolovat pomocí kombinované antiretrovirové terapie. Avšak, pro perzistenci latentního rezervoáru, není možné HIV infekci zcela vyléčit. Imunitní systém ani současné terapeutické postupy nedokážou rozpoznat latentně infikované buňky, a proto se strategie zaměřující na reaktivaci a následnou eliminaci těchto buněk pokládají za potenciálně terapeuticky využitelné.

Tato práce zkoumala vliv dříve popsaného latenci revertujíciho agens hem arginátu (HA), jiného redox modulátoru, a jejich součinnost s aktivátorem protein kinázy C forbol myristátem acetátem (PMA) při reaktivaci latence HIV-1 v kontextu metabolizmu hemu. V modelové T-lymfocytární linii obsahující integrovaný HIV-1 *„mini-virus“* (LTR-Tat-IRES-EFGP-LTR, Jurkat klon A2) a v A2 buňkách stabilně transfekovaných plasmidy kodújícimi cDNA pro faktory participující na metabolismu hemu či pro luciferázu, byla studována míra reaktivace HIV-1 pomocí intenzity fluorescence EGFP. Zatímco samotný redox modulátor nestimuloval expresi z HIV-1 LTR a HA reaktivoval *„mini-virus“* jen mírně, obě látky jevily synergické efekty s PMA ve všech studovaných liniích. V jednotlivých liních transfekovaných plasmidy kódujícími cDNA pro studované faktory byla bazální a indukovaná exprese EGFP rozdílná. Výsledky uvedené v této práci naznačují, že sledované geny jsou potenciálně důležité pro reaktivaci HIV-1, a že metabolizmus hemu muže hrát klíčovou roli při reverzi či udržování HIV-1 latence.

**Klíčová slova:** HIV-1 latence, metabolismus hemu, hem arginát, redox modulátor, latenci revertující agens

# Table of contents

## List of abbreviations

| Abbreviation | Full name |
|---|---|
| - | Negative |
| + | Positive |
| A2 | A2 clone of Jurkat cells |
| AIDS | Acquired Immune Deficiency Syndrome |
| AP-1 | Activator Protein 1 |
| ARE | Antioxidant response element |
| BACH2 | BTB And CNC Homolog 2 |
| bp | Base pairs |
| BR | Bilirubin |
| BTB | Broad complex–Tramtrack–Bric-a-brac domain |
| BV | Biliverdin |
| BVR, BVRA, BVRB | Biliverdin Reductase (A, B) |
| CA | Capsid protein |
| cART | Combined antiretroviral therapy |
| cART | Combined antiretroviral therapy |
| CA-US RNA | Cell-associated unspliced RNA |
| CCR5 | C-C chemokine receptor type 5 |
| CD4 | Cluster of differentiation 4 |
| CNC | Cap'n'collar |
| CO | Carbon monooxide |
| CRF | Circulating recombinant form |
| CXCR4 | C-X-C chemokine receptor type 4 |
| DC | Dendritic cell |
| DNMT | DNA methyltransferases |
| DNMTi | DNA methyltrasnferase inhibitor |
| DPP | 12-deoxyphorbol-13-phenylacetate |
| DSF | Disulfiram |
| EGFP | Enhanced Green Fluorescent Protein |
| *Env,* Env | Envelope (gene, polyprotein) |
| *Gag,* Gag | Group-specific antigen (gene, polyprotein) |
| GAPDH | Glyceraldehyde-3-Phosphate Dehydrogenase |
| HA | Heme arginate |
| HAART | Highly active antiretroviral therapy |
| HAT | Histone acetylase |
| HDAC | Histone deacetylase |
| HDACi | Histone deacetylase inhibitor |
| HEXIM1 | Hexamethylene Bisacetamide Induced Protein 1 |
| HIV, HIV-1 | Human immunodeficiency virus, HIV type 1 |

| | |
|---|---|
| HMT | Histone methyltransferase |
| HMTi | Histone methyltransferase inhibitor |
| HO-1 | Heme Oxygenase-1 |
| IN | Integrase |
| IκB | Inhibitor of κB |
| LC | Langenhars cell |
| LN | Lymphatic node |
| LRA | Latency-revensing agent |
| LT | Lymphatic tissue |
| LTR | Long terminal repeats |
| LUC | Luciferase |
| MA | Matrix protein |
| Maf | Musculoaponeurotic Fibrosarcoma |
| MAPK | Mitogen-activated Protein Kinase |
| mRNA | Messenger RNA |
| NC | Nucleocapsid protein |
| *Nef,* Nef | Negative regulatory factor (gene, protein) |
| NFAT | Nuclear Factor For Activated T cells |
| NF-E2 | p45 Nuclear Factor Erythroid-derived 2 |
| NF-κB | Nuclear Factor κB |
| Nrf | NF-E2-related factor |
| ORF | Open reading frame |
| p.i. | Post-infection |
| PB | Peripheral blood |
| PBMC | Peripheral Blood Mononuclear Cell |
| pDNA | Plasmid DNA |
| PIC | Pre-integration complex |
| PKC | Protein Kinase C |
| *Pol,* Pol | Polymerase (gene, polyprotein) |
| PR | Protease |
| PR | Protease |
| P-TEFb | Positive Transcription Elongation Factor |
| PTEN | Phosphatase And Tensin Homolog |
| qPCR | Quantitative polymerase chain reaction |
| *Rev,* Rev | Regulator of expression of virus (gene, protein) |
| RT | Reverse transcriptase |
| RT-qPCR | Reverse transcriptase quantitative polymerase chain reaction |
| SIV | Simian Immunodeficiency Virus |
| Sp1 | Specificity Protein 1 |
| SU | Surface protein |
| TAR | Transactivating response region |
| *Tat,* Tat | Transactivator of transcription (gene, protein) |
| TBP | TATA-binding Protein |

| | |
|---|---|
| $T_{CM}$ | Central memory T-cell |
| TF | Transcription factor |
| $T_H$ | Helper T-cell |
| $T_M$ | Memory T-cell |
| TM | Transmembrane protein |
| TNFα | Tumor necrosis factor α |
| $T_{TM}$ | Transitional Memory T-cell |
| UNAIDS | Joint United Nations Programme on HIV/AIDS |
| URF | Unique Recombinant Forms |
| *Vif,* Vif | Viral infectivity factor (gene, protein) |
| *Vpr,* Vpr | Viral protein R (gene, protein) |
| *Vpu,* Vpu | Viral protein U (gene, protein) |
| vRNA | Virus RNA |
| YY1 | Yin Yang 1 |

# 1. Introduction

Human immunodeficiency virus (HIV) is the causative agent of Acquired Immune Deficiency Syndrome (AIDS), a lethal disease defined by a progressive decline in the number of Cluster of differentiation 4-positive (CD4+) T-lymphocytes. There are two genetically distinct types of HIV, namely HIV-1 and HIV-2, and several groups and subtypes that are differentially co-distributed around the world (Li *et al.*, 2015). Considering its predominant prevalence and superior clinical significance, current research focuses primarily on the HIV-1 type. Despite the extensive research that has started on the brink of HIV-1 epidemics in the early 1980s, it is still one of the most prevalent viruses in the human population. In 2021, the Joint United Nations Programme on HIV/AIDS (UNAIDS) reported 37.6 million active cases worldwide, with an annual increase of approximately 1.5 million new infections. The number of HIV/AIDS-related deaths until the year 2019 was roughly estimated to 690 000 (UNAIDS, 2020). These statistics strongly underline the threat imposed by HIV on public health and depict a perpetual need for the development of an effective cure or vaccine against HIV.

To date, the main challenge to the HIV-1 cure is the establishment of a latent reservoir, which is formed very early during the acute phase of the infection in permissive cells of the host. HIV-1 latency is described as a phenomenon when reversely transcribed HIV-1 DNA undergoes an integration into the host cell genome and becomes transcriptionally inactive but replication-competent. As such, it remains concealed to host immune surveillance and cannot be eliminated by adaptive immunity (Donahue* and Wainberg, 2013). Latency reversal and elimination of HIV-1 provirus from the pool of latently infected cells became a subject of comprehensive research efforts after the combined antiretroviral therapy (cART) was introduced globally to the millions of affected patients. The cART, or highly active antiretroviral therapy (HAART), has proven to be efficient in limiting the plasma viremia below the detectable levels (<50 HIV-1 RNA copies/ml) (Perelson *et al.*, 1997), but it fails to target and eradicate the latently infected cells (Finzi *et al.*, 1999). Also, although the cART is able to profoundly ameliorate the ongoing HIV-1 infection, reducing the transmissibility and morbidity, the medication is required to be taken in a life-long manner and may produce a myriad of adverse effects.(Chen *et al.*, 2013). Contrarily, cessation of the therapy leads to a rapid relapse of HIV-1 viremia, subsequent deterioration of the immune system, and progression to AIDS (Deeks *et al.*, 2001; Grant *et al.*, 2001; Pinkevych *et al.*, 2015). Current therapeutic approaches are incapable of directing the components of humoral and cellular

immunity on the pool of latently infected cells. Thus the development of novel curative strategies is required to overcome HIV-1 infection *in vivo.*

In the last decades, several approaches attempting to cure HIV-1 have been intensively studied. Among these, a strategy termed „shock and kill" or "kick and kill" aims to reactivate the HIV-1 provirus in the latently infected cells and simultaneously eliminate them by the action of cytotoxic CD8+ T-lymphocytes, the cytopathic effects caused by the virus or by therapeutics. Reactivation of HIV-1 provirus has been achieved both in primary model cell lines in the latent stage of HIV-1 infection and *in vivo* with chemical compounds collectively named latency-reversing agents (LRA)(Melkova* *et al.*, 2017). Various LRAs have been reportedly efficient in the reactivation of the HIV-1 provirus *in vitro,* but only a limited number of them were administered to the HIV+ patients on cART in the pilot clinical studies. Although it has been demonstrated that some LRAs can reactivate the HIV-1 provirus from infected cells *in vivo*, the decrease in the size of the pool of latently infected cells was, so far, clinically irrelevant (Archin *et al.*, 2012; Gutiérrez *et al.*, 2016; Søgaard *et al.*, 2015; Spivak *et al.*, 2014).

The research team of Dr. Mělkova previously demonstrated that Normosang (heme arginate, HA), a registered drug used to treat acute hepatic porphyria, synergizes with Protein Kinase C (PKC) inducer phorbol myristate acetate (PMA) to reactivate HIV-1. Conversely, administration of HA alone was shown to limit the infection of bystander cells in primary cell lines by inhibiting reverse transcription during acute infection (Shankaran, 2016; Shankaran *et al.*, 2011). Human iron-containing porphyrin heme, incorporated in HA molecule, is degraded by heme oxygenases into ferrous iron ($Fe^{II+}$), carbon monoxide (CO), and biliverdin (BV). BV is in turn catabolized into bilirubin (BR) by the action of Biliverdin Reductase (BVR). Considering these processes play an integral part in the cellular redox-signaling, which is intrinsically involved in HIV-1 reactivation, it was hypothesized that the observed HA dichotomy might be attributed to differing redox conditions under particular stimulatory settings (Melkova* *et al.*, 2017; Shankaran *et al.*, 2017). Also, while the latency-reversing effect of DSF was observed before in a few independent studies (Doyon *et al.*, 2013; Kula *et al.*, 2019; Melkova *et al.*, unpublished results), it was only recently characterized as a putative inhibitor of BVR (van Dijk *et al.*, 2017). To our knowledge, the latency-reversing ability of disulfiram in the context of heme metabolism has not been addressed yet.

## 2. Aims of the thesis

This work aims to:

- Examine the inhibitory effect of disulfiram on Biliverdin Reductase A (BVRA)

- Evaluate the latency-reversing capacity of HA and DSF in the model of HIV-1 latency, A2 clone of Jurkat cells

- Verify synergistic effect of HA and PMA on HIV-1 reactivation

- Characterize the influence of BVRA and BTB Domain And CNC Homolog 2 (BACH2) overexpression on the reactivation of HIV-1 *"mini-virus"*

- Assess the phenotype of transfected cells overexpressing genes of interest upon treatment with PMA, HA, and DSF or their combinations in terms of cellular viability and degree of HIV-1 reactivation

# 3. Review of literature

## 3.1. Human immunodeficiency virus 1 (HIV-1)

HIV-1 belongs to the family of *retroviridae,* subfamily of *orthoretrovirinae,* and to the genus *lentivirus*. HIV-1 virions are enveloped and approximately of spherical shape with an average diameter of 145nm. Beneath the envelope, conical capsid encases 2 identical copies of genomic single-stranded RNA, as well as several proteins required for the initiation of the virus life cycle (Briggs *et al.*, 2003, 2006) The proviral genome size is 9.7 kbp and it encodes 15 genes within 9 open reading frames (ORF). While 9 out of 15 genes are essential in terms of virus reproduction, the remaining 6 genes encode accessory proteins with various regulatory functions. Similar to other retroviruses, transcription of the HIV-1 genetic information is preceded by the generation of proviral DNA through the mechanism of reverse transcription and the integration into the host cell genome. As a part of this process, long terminal repeats (LTR) are synthesized at both ends of proviral DNA from non-coding regions of the HIV-1 RNA genome. Following the reverse transcription, HIV-1 DNA undergoes an integration into the host genome. A schematic diagram of the HIV-1 DNA genome is shown in figure 1.

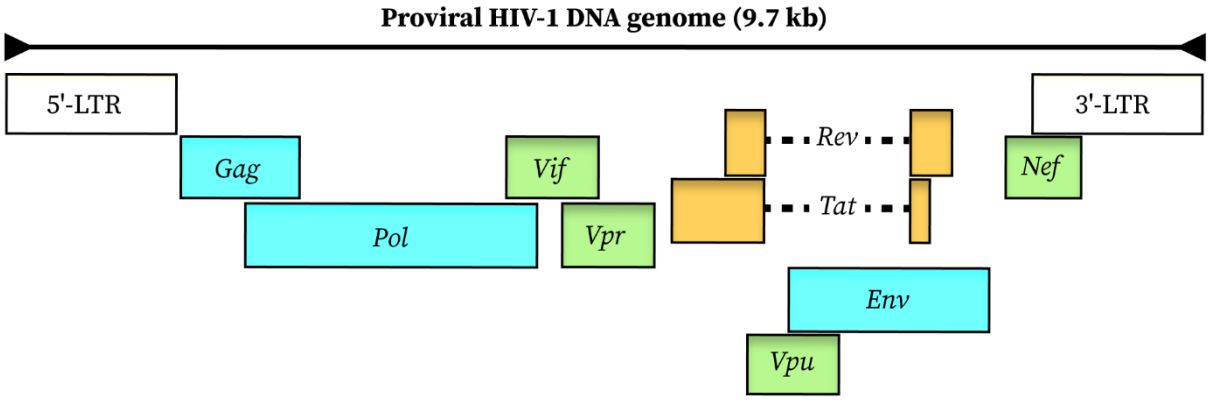


**Figure 1 | A schematic diagram of the HIV-1 DNA genome.**
The length of the proviral HIV-1 DNA genome is 9.7 kbp. The position of virus-encoded genes is depicted with regard to the relative localization of genes in the HIV-1 genome. LTR flanking coding regions of the genome are shown in white squares. Essential (*Gag, Pol,* and *Env*), regulatory (*Tat, Rev*), and accessory (*Vif, Vpr, Vpu, Nef*) genes are represented by blue, orange, and green squares, respectively. Dotted lines illustrate RNA splicing. ***Gag*** - group-specific antigen; ***Pol*** - polymerase; ***Env*** - envelope protein; ***Tat*** - transactivator of transcription; ***Rev*** - regulator of expression of virus proteins; ***Vif*** - viral infectivity factor; ***Vpr*** - viral protein R; ***Vpu*** - viral protein U; ***Nef*** - negative regulatory factor. Adapted from (Nkeze *et al.*, 2015).

Once successfully integrated, proviral DNA can be transcribed by the action of host DNA-dependent RNA polymerase from the promoter located in 5'-LTR. Gene products of the essential genes, *Gag, Pol,* and *Env*, are encoded within 3 major ORFs. The primary transcripts of essential genes are translated into 3 polypeptide intermediates Gag, Gag-Pol, and Env, which are then further processed by the cellular and virus-encoded proteases into the final protein products common to all retroviruses. Cleavage of the Pol polyprotein leads to the formation of 3 functional proteins with crucial enzymatic activities that are vital for the virus replication, namely RT (reverse transcriptase), IN (integrase), and PR (protease). On the other hand, post-translational processing of Gag and Env polyproteins gives rise to 6 structural proteins. Four structural proteins derived from the Gag, MA (matrix), CA (capsid), NC (nucleocapsid), and p6 (p6 protein), associate together to form virion core, whereas 2 Env proteins, TM (gp41, transmembrane protein) and SU (gp120, surface protein) are present on the virion surface (Frankel* and Young, 1998; Nkeze *et al.*, 2015). Unlike essential proteins that arise from aforementioned ORFs, gene products of HIV-1 regulatory genes (*Tat* and *Rev*) and accessory genes (*Vif, Vpr, Vpu, Nef*) are translated individually from different ORFs. A schematic representation of HIV-1 virion is shown in figure 2.

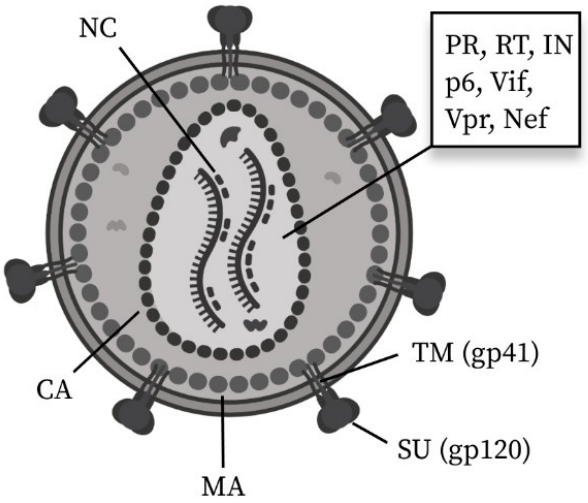


**Figure 2 | A schematic representation of the HIV-1 virion.**
Lines protruding from the virion depict the localization of proteins within the HIV-1 particle. Proteins located in the HIV-1 nucleocapsid are listed in the adjacent table. **NC** – nucleocapsid, **CA –** capsid, **MA –** matrix**, SU (gp120) –** surface protein, **TM (gp41) –** transmembrane protein, **PR** – protease, **RT** - reverse transcriptase, **IN** – integrase, **p6** – p6 protein, **Vif** - viral infectivity factor, **Vpr** – viral protein R, **Nef** - negative regulatory factor. In addition to proteins, the nucleocapsid contains two genomic RNA molecules. Adapted from (Frankel* and Young, 1998).

### 3.1.1. HIV-1 emergence, epidemiology, and evolution

According to the genetic and phylogenetic analyses, HIV-1 has reportedly originated from a zoonotic retrovirus known as Simian immunodeficiency virus (SIV) in a cross-species transmission event between chimpanzee *Pan troglodytes* and human (Gao *et al.*, 1999; Huet *et al.*, 1990; Keele *et al.*, 2006; Peeters *et al.*, 1989). It has been proposed that zoonotic transmission of HIV-1 resulted from hunting, manipulation, and trading of primates in the West and Central Africa (Aghokeng *et al.*, 2010; Wolfe *et al.*, 2004). A rigorous investigation of sequences circulating in Central Africa and archival HIV-1 samples from 1960 has provided compelling evidence, suggesting that primary transmission of HIV-1 had occurred in Kinshasa in the early 1920s (Faria *et al.*, 2014). Within a few decades, HIV-1 has spread from Africa to Haiti and later to North America, where it caused a deadly epidemic in the early 1980s (Gilbert *et al.*, 2007). On the verge of the new millennium, HIV-1 has become ubiquitous in most parts of the world (UNAIDS, 2000).

It should be noted that circulating HIV-1 specimens do not represent a uniform population of viruses, but rather several genetically incoherent lineages of HIV-1, including groups abbreviated M, N, O, and P. These lineages have originated independently of each other in separate cross-species transmission events (Plantier *et al.*, 2009). The prevailing HIV-1 M-group viruses cause up to 90 % of all HIV-1 infections and can be further subdivided into 9 clades (A–D, F–H, J, and K) and multiple circulating recombinant forms (CRF) and unique recombinant forms (URF)(Hemelaar *et al.*, 2019). A genome-wide study of 1705 HIV-positive (HIV+) patients has estimated an average genomic nucleotide sequence diversity between particular groups and M-group clades to 37.5% and 14.7%, respectively (Li *et al.*, 2015). Such broad genetic variability of the virus observed in HIV+ patients is a combined result of multiple zoonotic transmission events (Plantier *et al.*, 2009), high mutation rate introduced by error-prone reverse transcriptase (Bebenek *et al.*, 1989), and recombination events that occur during productive infection (Charpentier *et al.*, 2006; Zhuang *et al.*, 2002).

The high mutation rates and recombination events virtually cause the heterogeneity of HIV-1 specimens to be observable also the individual level (Charpentier *et al.*, 2006; Fisher *et al.*, 1988). Following the acute infection, reservoir cells within the host and in between distinct anatomical compartments harbor slightly genetically altered versions of HIV-1 proviruses. These virus strains or *quasispecies* mostly arise from a single virus genotype, termed “founder” virus, which is, as implied, responsible for transmission and outgrown of the variable progeny in the patient (Kearney *et al.*, 2009; Keele *et al.*, 2008; Salazar-Gonzalez *et*

*al.,* 2009). Besides the high mutation rates and recombination events, early virus evolution is also driven by a selective pressure induced by the host immune responses (Liu *et al.,* 2006; Richman *et al.,* 2003). In the context of compartment-specific adaptations, competition between residing virus strains results in the outgrown of a predominant population with the highest survival advantage. Unsurprisingly, the interplay between these factors determines the pool of *quasispecies* found in the reservoir sanctuaries at the time of latency establishment via the mode of natural selection. The highest sequential variations between *quasispecies* in individual patients have been identified in the genomic region encoding the Env polyprotein (Li *et al.,* 1999; McDonald *et al.,* 1997). This is consistent with the presence of five hypervariable regions $V_1$-$V_5$ on the HIV-1 SU protein (gp120)(Starcich *et al.,* 1986), where substitution of single amino acid may allow the virus particle to evade neutralizing antibodies (Park *et al.,* 1998; Schreiber *et al.,* 1996), T-cell responses (Borrow *et al.,* 1997) or confer the particular virus strain a change of tropism (Bunnik *et al.,* 2011). These findings collectively demonstrate that immune responses towards HIV-1 lead to the positive selection of a narrow group of *quasispecies,* which are able to escape from the host immunological effectors by employing surface epitopes diversification (i.e. escape mutants)(Richman *et al.,* 2003; Wood *et al.,* 2009) or by expanding the target cells repertoire (Eckstein *et al.,* 2001). In the absence of the treatment, the combination of high adaptability and variability of virus strains render immune response to the infection inadequate, thus permitting the infection to progress to AIDS in a few years.

Indeed, the dynamics of HIV-1 evolution within a host can be considerably hindered by a prompt therapeutic intervention in the form of cART. Nonetheless, dissemination of the virus to distinct anatomical compartments occurs very early after the HIV-1 transmission and remains a clinical issue. As demonstrated in patients non-adherent to the therapy, continual selective pressure imposed by antiretroviral drugs in suboptimal concentration favors the acquisition of the drug-resistant mutations over their fitness cost. Moreover, some studies show that low-level, but persistent replication (Bailey *et al.,* 2006; Dornadula *et al.,* 1999; Sahu *et al.,* 2009) and slow-paced evolution of new *quasispecies* also appear in patients with no recorded cessation of therapy (Dampier *et al.,* 2016; Raymond *et al.,* 2014). Supported by a mathematical model, evolution towards the drug-resistance in patients on HAART might be relevant in the case of reservoir cells in lymphoid tissue due to the insufficient penetration of the antiretroviral drugs into these compartments (Lorenzo-Redondo *et al.,* 2016). A more recent study conducted by Rosenbloom and colleagues argues that samples on which this mathematical model was based, were taken before, three months, and six months after an

adherence to cART, and therefore "represent an artifact of rapidly decaying viral populations" (Rosenbloom *et al.*, 2017). An absence of clear evidence of virus evolution in 20 adult patients treated since the onset of infection was also observed by Abdi *et al.* These researchers have shown that during and after 5 years of virological control, there were no significant sequential differences between early and late viral populations (Abdi *et al.*, 2020). It remains controversial whether residual replication in well-adherent patients can lead to long-term evolution or acquisition of drug resistance, as it is only a rarely encountered phenomenon (Martinez-Picado* and Deeks, 2016). High variability and pace of the virus evolution thereby impose an astounding challenge to prophylaxis and treatment targeted against HIV/AIDS.

### 3.1.2. HIV-1 transmission and entry

The HIV-1 infection arises from exposure of host mucosal membranes to infectious virus particles or when inoculated parenterally. Statistically, most of the new infections in Europe are attributed to exposure of mucosal surfaces to the virus during sexual intercourse. The second most prevalent route of transmission is intravenous drug use, followed by congenital infections accounting for roughly 1% of all reported cases (World Health Organization, 2019). Transmission of HIV-1 during a coital act is mediated through genital secretions of an infected person and can be greatly influenced by the use of a condom, choice of a partner, and preferred sexual practice (Varghese *et al.*, 2002). Aside from behavioral factors, stage of the disease (Hollingsworth *et al.*, 2008), treatment status (Loutfy *et al.*, 2013; del Romero *et al.*, 2015), the integrity of the exposed site (Coplan *et al.*, 1996; Paz-Bailey *et al.*, 2010) and male circumcision (Quinn *et al.*, 2000) have been also confirmed to profoundly influence transmission hazards. While sexual intercourse with an infected person might not necessarily lead to transmission, the risk of contracting HIV-1 is substantially increased in the absence of a condom (Varghese *et al.*, 2002). Under these circumstances, the highest per-act transmission probability is estimated at 1.4% for individuals engaging in receptive anal sex. Unprotected penile-vaginal intercourse is considered less hazardous, with female-to-male and male-to-female transmission risk estimates being at 0.04% and 0.08%, respectively (Boily *et al.*, 2009). Alternatively, chances of contracting HIV-1 via oral fellatio are close to zero. A study on 135 individuals whose only potentially infective exposure to HIV-1 occurred through orogenital contact with HIV+ partner, recorded no seroconversions during 10 years of follow-up (del Romero *et al.*, 2002).

However, the transmission hazards can be significantly increased in the case of the former (up to 1:3; 1 transmission per 3 exposures) when other risk factors are present (Powers *et al.*, 2008). For this reason, men having sex with men (MSM) are at increased risk of contracting HIV-1 and represent a large fraction of HIV/AIDS patients in developed countries (up to 60%). Regardless, approximately 70% of new HIV-1 infections result from heterosexual intercourse, and it remains the most prevalent route of HIV-1 transmission worldwide (Shaw* and Hunter, 2012).

Virus entry to a cell is mediated through the interaction between virus envelope protein gp120 and cellular CD4 receptor and C-C chemokine receptor type 5 (CCR5) or C-X-C chemokine receptor type 4 (CXCR4) coreceptors. These are present on the surface of major cellular targets of HIV-1, namely CD4+ T-cells, dendritic cells, monocytes, and tissue macrophages (Lee *et al.*, 1999). Depending on the molecule which serves as a coreceptor, virus strains are referred to as CCR5-tropic (R5), CXCR4-tropic (X4), or when both molecules can be used to enter a cell as dual or mixed-tropic (DM). Besides the two, several studies show that in the case of some virus strains, chemokine receptors CCR3, CCR2b, or others (Connor *et al.*, 1997; Doranz *et al.*, 1996) can virtually serve as minor coreceptors too. The presence of both, receptor and coreceptor molecules on the surface of the cell, therefore renders it permissive to infection by virus strain with the corresponding tropism. Nonetheless, the vast majority of new infections are caused by the R5 strains. In fact, it is assumed that R5 strains have a selective transmission advantage due to their unparalleled predominance in the early stages of infection (Keele *et al.*, 2008; Salazar-Gonzalez *et al.*, 2009). Contrarily, X4 strains originate from R5 strains later during the chronic phase of infection in around 50% of HIV/AIDS patients (Koot *et al.*, 1999; Shepherd *et al.*, 2008) as a consequence of virus evolution orchestrated on the basis of the *Env* gene mutagenesis (Bunnik *et al.*, 2011). It is believed that the emergence of X4 strains in previously R5 exclusive patients allows the infection to spread to naïve CD4+ T-cells expressing solely CXCR4 (Eckstein *et al.*, 2001) and predicts disease progression as indicated by a further decline in CD4+T-cell counts and increased viral load (Blaak *et al.*, 2000; Connor *et al.*, 1997; Daar *et al.*, 2007). Consistent with this notion, it has been demonstrated that the survival rate after AIDS diagnosis in 4-year follow up of R5 exclusive patients is markedly increased (Koot *et al.*, 1999) and that slow progressors, defined by CD4+ T-cell count ≥ 200 cell/µl and by the absence of AIDS-related illness for ≥11 consecutive years, were less likely to harbor X4 tropic strain (Shepherd *et al.*, 2008). Moreover, it has been shown that adherence to cART substantially reduces the probability of X4 strain development and prolongs the time frame

within which such phenotypic shift occurs (Seclén *et al.*, 2010; Weiser *et al.*, 2008). Expansion of permissive cell repertoire thus provides a plausible explanation for accelerated disease progression in patients infected with both virus strains and could be its primary determinant (Eckstein *et al.*, 2001). Nonetheless, palpable scientific evidence linking the emergence of X4 strains to rapid loss of CD4+ T-cells is still missing and despite the progress in the understanding of HIV-1 tropism, its impact on HIV-1 latency remains largely unsolved.

### 3.1.3. Early cellular targets

If transmitted via sexual contact, virus particles must invade epithelial barriers of the genital or gastrointestinal tract to infect initial cellular targets that reside within or beneath them. These include CD4+ T-lymphocytes (Gupta *et al.*, 2002) and various professional antigen-presenting cells (APC), such as tissue macrophages (Kacani *et al.*, 1998), intraepithelial Langerhans cells (LC)(Sivard *et al.*, 2004), and other types of dendritic cells (DC)(Granelli-Piperno *et al.*, 1999). Depending on the exposed site, virions must traverse either multicellular stratified squamous epithelium covering the genital tract or single-layer cylindric epithelium in the rectum. In both types of epithelia, virions may be captured by DCs and translocated to subepithelial compartments of skin (i.e. *lamina propria*), or they can migrate across independently if abrasions compromise the integrity of the epithelium. Mechanisms of HIV-1 entry across the vaginal epithelium are depicted in figure 3. Additionally, the invasion of HIV-1 through rectal epithelium may also be mediated by transcytosis, which refers to spontaneous relocation of cell-free virions through tight junctions of the monolayered epithelium (Carias* and Hope, 2019).

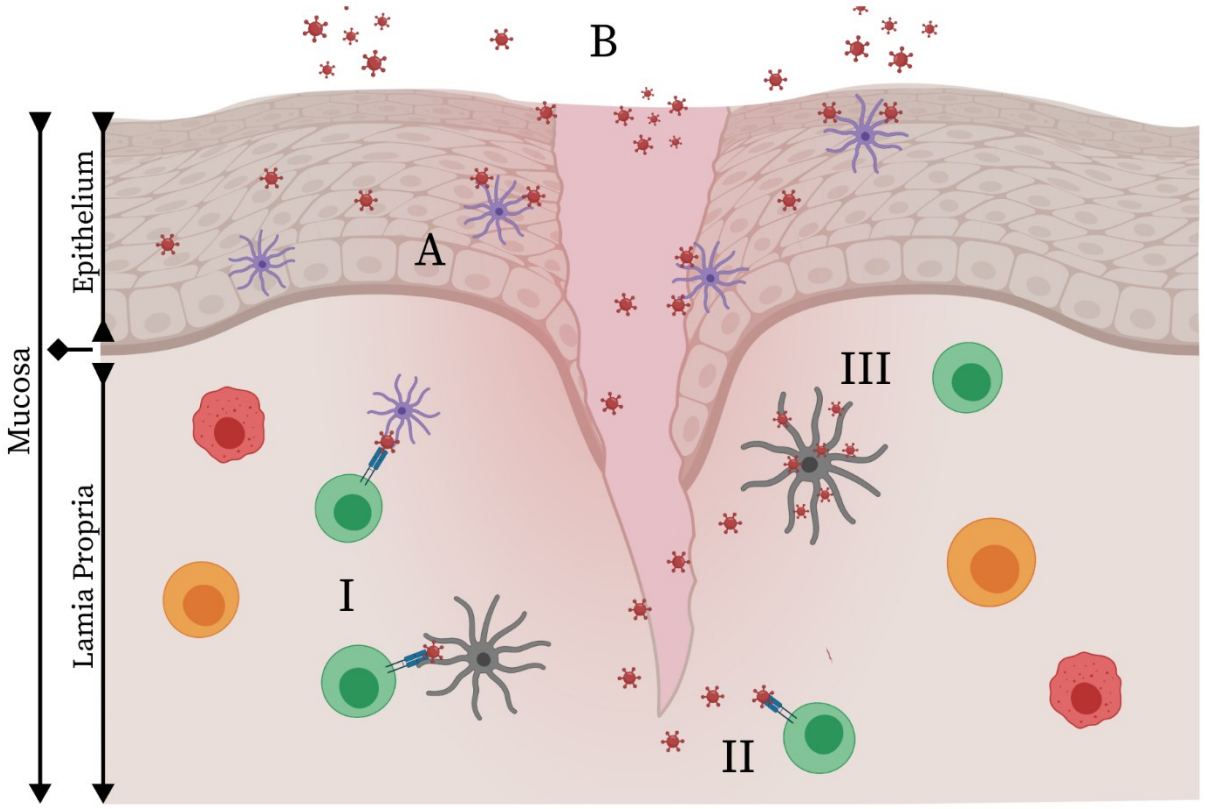


**Figure 3 | The vaginal entry of HIV-1 and means of transport.**
Vertical lines represent first two layers of mucosa. (◆—) marks basal membrane. **(A)** Translocation of virions to the subepithelial compartment of the mucosa by Langenhars cell (blue). **(B)** Spontaneous entry of cell-free virions through abrasion. **(I)** Trans-infection of resting T-cell (green) by intramucosal Dendritic cells (grey) or Langenhars cell. **(II)** Direct infection of mucosal resting T-cell. **(III)** Progeny-mediated cis-infection of resting T-cell by Dedritic cell. Infected T-cells and tissue macrophages are shown in orange and red, respectively. Adapted from (Carias* *et al.*, 2019).

#### 3.1.3.1. Dendritic cells

Since localized in the uppermost layers of mucosa (Sivard *et al.*, 2003), LCs are considered to be one of the first cells to encounter HIV-1 in the stratified epithelium of vaginal mucosa, penile foreskin, and ectocervix (McCoombe and Short, 2006; Sivard *et al.*, 2004). Here, LCs utilize binding and internalization of virions through the interaction of C-type lectin langerin with viral envelope protein gp120, followed by their deposition and pH-dependent degradation in Birbeck granules, the LC-specific cytoplasmic organelle associated with antigen processing (Valladeau *et al.*, 2000; de Witte *et al.*, 2007). Based on this finding, it has been hypothesized that under low virus doses, virus clearance by LCs represents a natural barrier that prevents the transport of infectious particles deeper into mucosae, hence prohibiting transmission of HIV-1 to other permissive cells (de Witte *et al.*, 2007). Notwithstanding, because LCs express both CD4 receptor and CCR5/CXCR4 coreceptor

molecules, it cannot be excluded that virions occasionally enter these cells by membrane fusion (Kawamura *et al.*, 2003; Sivard *et al.*, 2004) rather than undergo internalization by endocytosis. Noteworthy, the frequency of such event would be dramatically increased upon full saturation of the surface langerin by virions or when inhibited otherwise (de Witte *et al.*, 2007). Provided the virus gains entry to LC by membrane fusion, the cell will become productively infected (Kawamura *et al.*, 2003) and will support the transmission of HIV-1 progeny to other permissive CD4+ T-cells (*cis*-infection) localized at proximal sites of mucosa (Sivard *et al.*, 2004) and to local lymph nodes (LN)(Blauvelt *et al.*, 2000). A considerable body of evidence also indicates that *trans*-infection of T-cells by LCs can be facilitated in a non-productive fashion (Ballweber *et al.*, 2011; Cavrois *et al.*, 2007; Hladik *et al.*, 2007). As shown by Hladik and colleagues, despite LCs may not be infected themselves, internalized virions are fit to infect adjacent T-cells during migratory movement (Hladik *et al.*, 2007). Nonetheless, more recent data suggest that propagation of HIV-1 from LCs to T-cells occurs predominantly in *cis* (Peressin *et al.*, 2014), possibly due to exhaustion of free surface langerin. Also, a narrow group of preferentially transmitted HIV-1 variants, known as founder viruses, have been shown to resist langerin-mediated control of transmission (Hertoghs *et al.*, 2019).

Besides superficial LCs, other subsets of mucosal DCs have been shown to transport HIV-1 virions from exposed mucosal site to T-cells in secondary lymphoid organs, both non-productively (Geijtenbeek *et al.*, 2000; Kwon *et al.*, 2002) or when infected (Burleigh *et al.*, 2006; Granelli-Piperno *et al.*, 1999). In contrast to LCs, other DCs subsets do not express langerin but bind gp120 protein by their surface DC-specific C-type lectin (DC-SIGN; DC-Specific Intercellular adhesion molecule-3-Grabbing Non-integrin)(de Witte* *et al.*, 2008). It has been demonstrated that binding and internalization of virions into membrane-bound vesicles may lead to non-productive transmission of virions to T-cells through the formation of "infectious synapse" on the interface of DC and T-cell junction (Kwon *et al.*, 2002; McDonald *et al.*, 2003). Moreover, captured virions were also shown to remain tethered on DC surface, and it was proposed that these particles may be subsequently trafficked in an infectious state to permissive CD4+ T-cells (Burleigh *et al.*, 2006; Cavrois *et al.*, 2007; Geijtenbeek *et al.*, 2000). Although it is clear that professional APCs are pertinent to the mucosal transmission of HIV-1, their presence is not a prerequisite for the dissemination of HIV-1. This is evident from several *in vitro* and *ex vivo* studies, where direct infection of CD4+ T-cells by founder viruses have been observed independently of DCs (Gupta *et al.*, 2002; Hladik *et al.*, 2007).

### 3.1.3.2. CD4+ T-cells

To better understand HIV-1 pathogenesis, it is crucial to recognize the distinctive biology of CD4+ T-cells subsets in terms of their maturation and activation. A naïve CD4+ T-cells (CD4+ $T_N$) arises from immature, double-positive (CD4+CD8+) thymocytes in the process of thymopoiesis. As such, CD4+ $T_N$ cells may be triggered into an activated phenotype by virtue of antigen recognition, which is presented by a DC. Followed by their stimulation, activated CD4+ T-cells are clonally expanded and mount an immune response against the corresponding antigen. The majority of these cells will perish shortly, however, a small fraction of activated CD4+ T-cells will be reverted back into quiescence to become CD4+ memory cells (CD4+ $T_M$). Provided the organism re-encounters the same antigen in the future, CD4+ $T_M$ will briskly recall the effector phenotype to promote an enhanced immune response. As exemplified in figure 4, the term resting CD4+ T-cell commonly refers to either CD4+ $T_N$ or CD4+ $T_M$. Conversely, an activated CD4+ T-cell describes an effector cell that arose from resting CD4+ T-cell upon primary or secondary exposition to a particular antigen (Donahue* and Wainberg, 2013; Thome *et al.*, 2014).

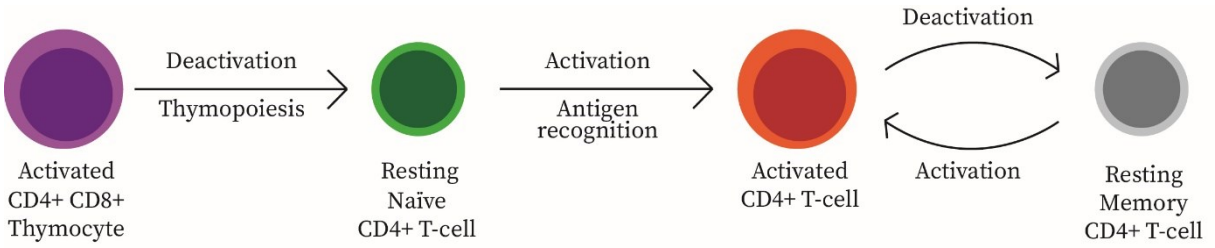


**Figure 4| Maturation of Thymocyte into resting memory CD4+ T-cell.**
The naïve CD4+ T-cell is generated from the transcriptionally active CD4+CD8+ Thymocyte following thymopoiesis. The naïve CD4+ T-cell can become activated upon primary antigen recognition. The resting memory CD4+ T-cell is generated from the activated CD4+ T-cell following deactivation. Resting memory CD4+ T-cell can revert to activated CD4+ T-cell upon secondary antigen priming. Adapted from (Donahue* and Wainberg, 2013).

Both CD4+ $T_M$ and activated T-cell populations comprise subsets that are distinguished by differential expression of phenotypic markers and functional properties. The population of CD4+ $T_M$ cells can be further subcategorized into central memory (CD4+ $T_{CM}$), transitional memory (CD4+ $T_{TM}$), and effector memory (CD4+ $T_{EM}$) cells depending on their function, proliferative capacity, localization, and degree of maturation. The CD4+ $T_{CM}$ subset represents a textbook example of quiescent cells that convey long-lasting immunological memory,

thanks to their proliferative capacity and their localization in secondary lymphoid organs. Here, CD4+ $T_{CM}$ cells await secondary priming by antigen-carrying DC to promote their activation and subsequent proliferation. The CD4+ $T_{EM}$ cells are, in contrast, delineated by their increased activation state, ability to produce pro-inflammatory molecules, and their proximal localization to tissues where a preponderance of microbial agents are encountered and their effector functions can be immediately enacted (Donahue* and Wainberg, 2013; Fritsch *et al.*, 2005; Sallusto *et al.*, 1999). As for the CD4+ $T_{TM}$, these cells have been described as an intermediary maturational stage between CD4+ $T_{CM}$ and CD4+ $T_{EM}$, because their cytokine expression profile corresponds to that of CD4+ $T_{EM}$, but they are not yet irreversibly maturated into CD4+ $T_{EM}$ (Fritsch *et al.*, 2005). On the other hand, activated T-cells may differentiate into various subsets, including helper T-cells ($T_H$) such as $T_H1$, $T_H2$, $T_H17$, and others, based on the type of antigenic stimulus (Donahue* and Wainberg, 2013). Unsurprisingly, distribution and frequencies of resting and activated CD4+ T-cell subsets vary in particular anatomical compartments (Campbell *et al.*, 2001; Thome *et al.*, 2014) with regard to immunological status, age, and ongoing infections. For example, throughout early childhood, CD4+ $T_N$ and regulatory T-lymphocytes constitute the major T-cell populations, whereas, in young adults, the highest proportion of CD4+ T-cells can be classified as CD4+ $T_M$ (Thome *et al.*, 2016). Considering their role in immune response, activated CD4+ T-cell normally represent only a small fraction of all CD4+ T-cells, predominantly circulating in peripheral blood (PB) and lymphatic tissues (LT)(Thome *et al.*, 2014, 2016).

Activated CD4+ T-cells are considered more permissive to the HIV-1 infection than resting CD4+ T-cells, because, as shown by several lines of evidence, T-cell activation is crucial for HIV-1 replication *in vitro* (Stevenson *et al.*, 1990; Zack *et al.*, 1990, 1988). Besides, activated CD4+ T-cells are particularly susceptible to HIV-1 infection because they express high amounts of CCR5 (Bleul *et al.*, 1997; Wu *et al.*, 1997). In a model of human cervicovaginal tissue, productive infection was preferentially supported within a fraction of T-cells expressing marker of activation (Saba *et al.*, 2010). Nevertheless, productive infection of resting CD4+ T-cell, though at a lower rate, has been demonstrated *in vivo* upon intravaginal inoculation of SIV into rhesus macaques (Zhang *et al.*, 1999). A study on *in vitro* cultured human tonsillar tissue by Eckstein *et al.* also shows that productive infection of nonproliferating CD4+ $T_N$ and CD4+ $T_M$ cells is possible, yet they argue that the contribution of these cells to HIV-1 pathogenesis is more significant during later stages of the infection (Eckstein *et al.*, 2001). These findings insinuate that the activation status of the host cell strongly influences the course and outcome of the infection. The role of resting CD4+ T-cells

in mucosal transmission and latency establishment will be briefly discussed in the following chapters.

### 3.1.4. Initial stages of the infection

Once HIV-1 virions penetrate through physical barriers and establish local infection at the mucosal site or elsewhere, dissemination of virus to late tissue sanctuaries occurs and systemic infection occurs in a matter of days. Within the first 7 days post-infection (p.i.), HIV-1 gradually disseminates throughout the exposed mucosal sites and to distal LT (Miller *et al.*, 2005). During this time and up to 21 days p.i., the presence of HIV-1 in the bloodstream may not be clinically detectable, and so scientific literature refers to this stage of infection as to the ecliptic phase (Shaw* and Hunter, 2012). At first, infection is locally restricted at the portal of entry, and although HIV-1 can be detected at distal LT as soon as 1-4 days p.i., a low quantity of virus particles or infected cells migrating to these sites are, presumably, unable to support productive infection of resident cells. However, upon sufficient expansion of infection at the exposed mucosal site and due to continuous seeding of these compartments, the virus systematically disseminates to draining LN and through the bloodstream to distal LT where self-propagating infection (*R0 ≥ 1) typically occurs in 7-10 days p.i. Following the systemic spread of HIV-1, peak viremia usually appears within 10-21 days p.i. as a result of explosive viral reproduction at distal LT. By the end of the month, viral load and the number of infected cells decline (Miller *et al.*, 2005) due to a massive elimination of CD4+ $T_M$ in multiple tissues (Mattapallil *et al.*, 2005). This is ensured mainly by the action of cytotoxic CD8+ T-lymphocytes (Goonetilleke *et al.*, 2009) and the cytopathic effect of the virus (Mattapallil *et al.*, 2005). At the same time, a small pool of CD4+ $T_M$ cells and other permissive cells will become latently infected, heralding entry to the chronic stage of infection (Shan *et al.*, 2017; Terahara *et al.*, 2019).

In contrast to PB and LN, an early loss of CD4+ T-cells is particularly substantial in extra-lymphoid effector sites of mucosae (Vajdy *et al.*, 2001), where CD4+ $T_{EM}$ represent the major memory T-cell subset (Veazey *et al.*, 2003; Mehandru *et al.*, 2004). Preferential depletion of mucosal CD4+ T-cells has been observed in both distal LT, like lung or gut-associated lymphoid-tissue (Gordon *et al.*, 2010; Mehandru *et al.*, 2004; Vajdy *et al.*, 2001), and at portals of HIV-1 entry (rectal/vaginal mucosa)(Clayton *et al.*, 1997; Saba *et al.*, 2010; Veazey *et al.*, 2003). In addition, the CD4+ $T_{EM}$ cells express HIV-1 functional coreceptor CCR5 at higher frequencies than CD4+ $T_{CM}$ and CD4+ $T_N$, which reside predominantly in PB

and LN (Anton *et al.*, 2000; Veazey *et al.*, 2003). In support of this, the CD4+ $T_{EM}$ were shown to be more susceptible to infection by HIV-1 R5 strain in DC-mediated transmissions (Groot *et al.*, 2006). Considering that gut-associated lymphoid-tissue is the largest lymphoid organ of the body, harboring vast amounts of T-cells, it can be reasoned that the gastrointestinal tract is critically important for the early virus outgrowth (Li *et al.*, 2005; Mehandru *et al.*, 2007). Combined these data suggest that mucosal CD4+ $T_{EM}$ populations rather than other CD4+ T-cell subsets support HIV-1 propagation during the first days of infection.

From a clinical point of view, the initial phases of HIV-1 infection are best described by the sequential appearance of virological and immunological markers in a patient's blood like HIV-1 RNA, p24 antigen, and HIV-1 specific antibodies. Based on the markers, Fiebig and colleagues have devised a staging model that characterizes periods of acute and early stage of HIV-1 infection (Fiebig *et al.*, 2003; Shaw* and Hunter, 2012). The laboratory staging model of HIV-1 infection is shown ins figure 5. The acute HIV-1 infection typically lasts for 3 weeks and is defined by an exponential increase in HIV-1 RNA copy number and by the appearance of p24 antigen. On the other hand, the early stage of HIV-1 infection is distinguished by the presence of HIV-1 specific antibodies, which emerge later in the natural history of the infection. The beginning of the early stage is therefore marked by seroconversion and the establishment of the virus load set point. The viral load setpoint refers to an initial steady-state decrease in viral load following peak viremia (Pilcher* *et al.*, 2004), which, together with CD4+ T-cell count, represent a significant prognostic marker of disease progression (Mellors *et al.*, 1997; Pedersen *et al.*, 1997). The prompt clinical diagnostics and the early treatment of HIV+ patients with cART were shown to enhance the virological control of HIV-1 during primary infection and to potentiate reconstitution of CD4+ and CD8+ T-lymphocytes afterward (Davy-Mendez *et al.*, 2018; Oxenius *et al.*, 2000).

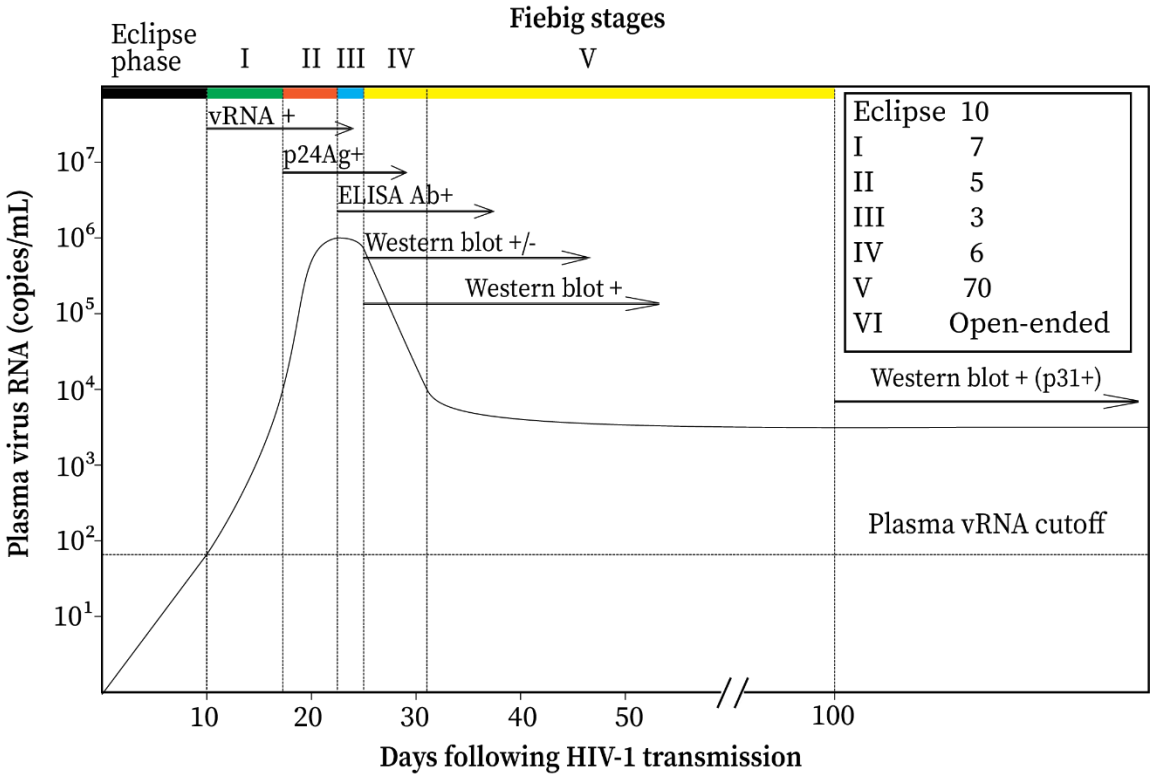


**Figure 5| Laboratory staging model of the acute and early-stage of HIV-1 infection.**
The natural history of the HIV-1 infection as defined by the appearance of immunological and virological markers. The inlet shows the average duration of the eclipse phase and Fiebig stages (Fiebig *et al.*, 2003) in days. **vRNA** - plasma virus RNA. Adapted from (Lee *et al.*, 2009).

## 3.2. HIV-1 latency

Not to be confused, integration of the HIV-1 genome alone does not usually lead to latency but instead to the productive infection that often culminates with the destruction of the host cell (Folks *et al.*, 1986). The HIV-1 latency is, by definition, a rare event, which occurs when the integrated provirus ceases to produce virus-encoded proteins due to transcriptional silencing but remains competent to do so under particular stimulatory settings (Donahue* and Wainberg, 2013). When examined in patients on cART within the first year of infection, most proviruses are found defective (Bruner *et al.*, 2016; Ho *et al.*, 2013). In fact, it was shown that only 1-5% of CD4+ T-cells harboring HIV-1 cDNA contain replication-competent provirus that is reactivable upon the adequate stimulation (Hermankova *et al.*, 2003; Hiener *et al.*, 2017). Since these cells are probably unable to support a productive infection, they do not contribute to the latent HIV-1 reservoir *per se* (Bruner *et al.*, 2016) and will not be addressed here.

The presence of intact HIV-1 provirus has been confirmed in many cell types, including CD4+ $T_N$, CD4+ $T_M$, activated CD4+ T-cells, CD34+ hematopoietic progenitor cells, CD4+ memory stem cells (CD4+ $T_{MS}$), γδ T cells, macrophages, microglia, astrocytes, dendritic cells, and possibly others. To a greater or lesser extent, permissive cells containing integrated, replication-competent provirus together form the latent HIV-1 reservoir that is detectable in multiple anatomical sites of the body. The significance of a particular permissive cell type for HIV-1 latency is difficult to assess *in vivo* because HIV-1 research is largely based on experimental *in vitro* platforms, such as immortalized HIV-1 infected cell lines, e.g. J-Lat, ACH-2, or U1 and primary cell lines derived from human donors, namely peripheral blood mononuclear cells (PBMC) and purified resting CD4+ T-cells. Besides, the magnitude of the HIV-1 reservoir in patients on cART is typically only about approximately one million of infected cells, making research on human primary cell lines and clinical trials very problematic. Current *in vivo* models of the HIV-1 infection are best represented by multiple strains of humanized mice or *rhesus macaques* infected with HIV, SIV, or their chimeric alternatives. Although the research on model organisms has played an inseparable role in understanding HIV-1 pathogenesis and latency establishment, it has considerable limitations, which are well-reviewed in (Melkova* *et al.*, 2017). Because the HIV-1 reservoir resides predominantly within CD4+ T-cell populations (Chomont *et al.*, 2009), the following chapters will focus primarily on this cell type.

### 3.2.1. Latency establishment and persistence

Given the CD4+ T-cells characteristics, it was rationalized that HIV-1 latency may be established through two distinctive ways. First, a more feasible scenario is that latency is established in thymocyte or activated effector CD4+ T-cell during their transition into naïve or resting memory CD4+ T-cell, respectively (Brooks *et al.*, 2001; Shan *et al.*, 2017). The second pathway to latency is via a direct infection of resting CD4+ T-cell. Albeit, the latter is considered very unlikely because resting CD4+ T-cells restrict the HIV-1 life cycle at various stages from entry to integration (Donahue* and Wainberg, 2013). At any rate, it has been previously demonstrated that latency can be established directly in both resting and activated CD4+ T cells early after infection (Swiggard *et al.*, 2005; Chavez *et al.*, 2015; Agosto *et al.*, 2018). The possible modes of the HIV-1 latency establishment are depicted in figure 6. A study performed by Saleh and colleagues also implies that resting CD4+ T-cells may become more permissive to the infection due to a cytokine and chemokine stimulation (Saleh *et al.*, 2007).

Interestingly, it has been hypothesized that this mechanism may be important in the lymphoid tissue microenvironment as immunomodulating compounds may sensitize resting CD4+ T-cells to the HIV-1 infection (Eckstein *et al.*, 2001; Kinter *et al.*, 2003).

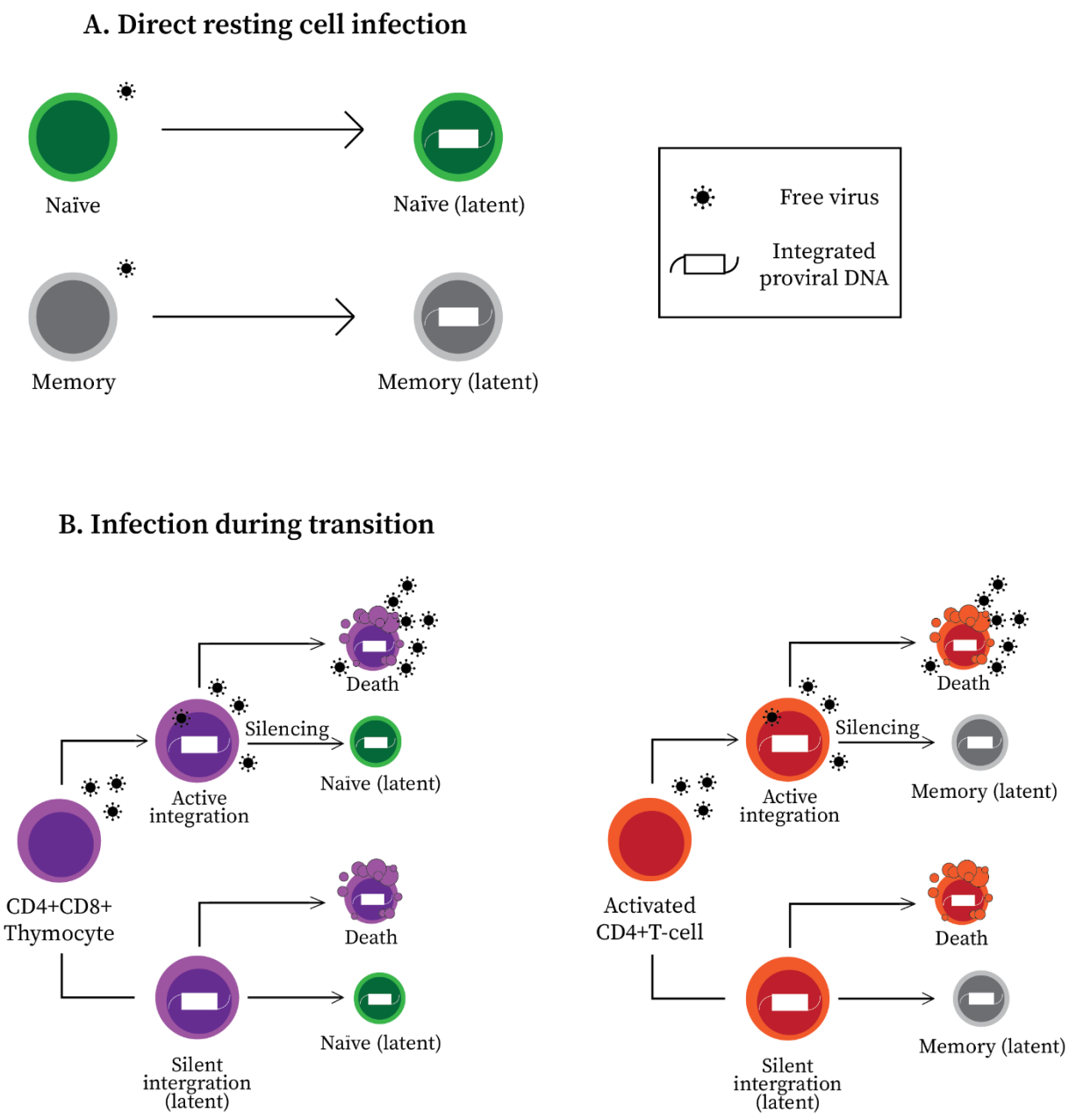


**Figure 6| Modes of the latent HIV-1 infection establishment in resting CD4+ T-cells**
**(A)** illustrates direct infection and latency establishment in resting naïve CD4+ T-cell (green) or resting memory CD4+ T-cell (grey). **(B)** exemplifies entry into the HIV-1 latency in activated CD4+CD8+ Thymocyte (purple) and activated CD4+ T-cell (orange) during their transition into resting CD4+ T-cells. Adapted from (Donahue* and Wainberg, 2013).

The increasing knowledge on HIV-1 latency strongly suggests that resting CD4+ T-cells, and CD4+ $T_M$ cells in particular, represent the largest and most significant reservoir of the virus in patients receiving cART (Brenchley *et al.*, 2004; Chomont *et al.*, 2009; Chun *et al.*, 1997; Hiener *et al.*, 2017; Terahara *et al.*, 2019). When comparing CD4+ $T_N$ versus CD4+ $T_M$, the former are less permissive for the HIV-1 infection, and as such, they are normally designated as the minor population to carry latent HIV-1 (Dai *et al.*, 2009; Hiener *et al.*, 2017). Current views on different CD4+ $T_M$ subsets suggest that while all CD4+ $T_M$ cells may harbor the HIV-1 provirus (Baxter *et al.*, 2016; Soriano-Sarabia *et al.*, 2014), CD4+ $T_{CM}$ are the predominant memory CD4+ T-cell population to preserve intact and replication-competent provirus (Chomont *et al.*, 2009; Soriano-Sarabia *et al.*, 2014). Unbeknownst to the host immune defenses, these long-lived cells not only retain latent reservoir but also maintain it over time by homeostatic proliferation (Chomont *et al.*, 2009; Jaafoura *et al.*, 2014). By contrast, reactivation of latent provirus was more readily induced in CD4+ $T_{EM}$ (Baxter *et al.*, 2016; Kulpa *et al.*, 2019). Alternatively, a different study by Hiener *et al.* identified the highest distribution of intact proviruses in the CD4+ $T_{EM}$ subset (Hiener *et al.*, 2017). Considering that the studies were based on a limited number of subjects with different immunological backgrounds and CD4+ $T_{EM}$ are a terminal maturational stage of CD4+ $T_M$ cells, these disparate experimental outcomes may not be mutually exclusive.

Regarding the HIV-1 provirus integration site, multiple sources corroborate that the pre-integration complex (PIC) aims for the actively transcribed genomic *loci* (Brady *et al.*, 2009; Ikeda *et al.*, 2007; Kok *et al.*, 2021; Schröder *et al.*, 2002). The targeting of PIC to these sites is controlled by lens-epithelium derived growth factor protein, which can tether PIC to the chromosomal DNA and facilitate the integration of HIV-1 DNA into the regions that are recognized by it (Ciuffi *et al.*, 2005; Marshall *et al.*, 2007). Besides the chromatin-reader, other characterized integration co-factors include GC-rich regions, CpG islands, and interspaced *Alu* elements (Brady *et al.*, 2009; Ikeda *et al.*, 2007). Because integration and active transcription of virus-encoded genes are crucial for the completion of the virus life cycle, the selection of integration sites within these hotspots is no coincidence. From this viewpoint, latency establishment is believed to be rather an outcome of a biological error than a strategy of an intracellular parasite. Accordingly, it has been demonstrated that active transcription units are favored in both activated and resting CD4+ T-cells, however, when compared to each other, a statistically significant proportion of proviruses in resting CD4+ T-cells were detected in repressed chromatin regions (Brady *et al.*, 2009). The integration of provirus in resting CD4+ T-cells has been observed in the absence of consequent activation (Dai *et al.*, 2009).

Moreover, Trejbalova *et al.* show that the HIV-1 latency is further reinforced by progressive CpG methylation of the HIV-1 5'-LTR promoter *in vitro* and in patients on long-term cART (Blazkova *et al.*, 2009; Trejbalova *et al.*, 2016). Also of note, the provirus in cART-suppressed patients was, among a few other genes, preferentially integrated within the *BACH2* gene *locus* (Cesana *et al.*, 2017; Ikeda *et al.*, 2007; Maldarelli *et al.*, 2014; Wagner *et al.*, 2014). Recent *in vitro* studies on the Jurkat cell line provide new evidence suggesting that if integrated into *BACH2 locus,* the HIV-1 promoter becomes gradually silenced as a consequence of promoter methylation (Hamann *et al.*, 2021; Inderbitzin *et al.*, 2020). Based on these data, it was hypothesized that localization of the provirus into preferred genes promotes the persistence of HIV-1 in self-renewing cells. Together, these findings elucidate some of the biological aspects underlying HIV-1 latency establishment and the longstanding persistence of the HIV-1 reservoir.

### 3.2.2. Reactivation and latency reversal

Predictably, if provirus integrates inside transcriptionally silent regions, the production of viral proteins is abrogated. However, in relation to HIV-1 latency, such transcriptional silencing is not irreversible and the provirus might be reactivated. Unlike in the case of the natural course of infection, the reactivation of HIV-1 can be orchestrated artificially by the administration of LRA. Since the expression of HIV-1 from its promoter segment in 5'-LTR is dependent on the arrangement of chromatin and host transcriptional machinery, these compounds usually enforce latency reversal by epigenetic modifications or recruitment of transcription factors (TF)(Donahue* and Wainberg, 2013). Among the well-described TFs that bind to *cis*-regulatory elements of HIV-1 LTR are the Nuclear Factor For Activated T-cells (NFAT)(Kinoshita *et al.*, 1998), nuclear factor κB (NF-κB)(Pyo *et al.*, 2008), Specificity Protein 1 (Sp1)(Perkins *et al.*, 1993; Suñé and García-Blanco, 1995) and TATA-binding protein (TBP)(Raha *et al.*, 2005). Other TFs like Actirvator protein 1 (AP-1) (Hokello *et al.*, 2021) and Yin Yang 1 (YY1)(Yu *et al.*, 2020) have been also shown to coordinate the activity of the HIV-1 promoter. Besides the host TFs, HIV-1 trans-activator of transcription (Tat) protein is vital for efficient HIV-1 gene expression, because it recruits the positive transcription elongation factor (P-TEFb; CDK9/Cyclin T1) to TAR (transactivating response region) element on newly transcribed leader sequence of HIV-1 RNA (Garber *et al.*, 2000). This interaction facilitates subsequent hyperphosphorylation of the C-terminal domain of RNA polymerase II (Isel and Karn, 1999), in preinitiation complex with other canonical TFs,

allowing for successful transcript elongation (Yamada *et al.*, 2006). Provided Tat protein fails to execute its function, HIV-1 transcription and replication cannot be properly concluded (Lalonde *et al.*, 2011; Rustanti *et al.*, 2017). Due to this, the presence of Tat in latently infected cells is integral for HIV-1 reactivation (Turner* and Margolis, 2017). On the other hand, the expression of HIV-1 is impacted by the accessibility of chromatin (Battivelli *et al.*, 2018). The chromatin structure is generally regulated by ATP-dependent chromatin remodeling complexes or covalent modifications of histone proteins. In the framework of the virus, the Tat protein was shown to cooperate with a component of the SWItch/Sucrose Non-Fermentable remodeling complex during HIV-1 reactivation in latently infected ACH-2 cell line (Agbottah *et al.*, 2006). As for the histones modifications, these are carried out by histone acetylases (HAT) or deacetylases (HDAC), histone methyltransferases (HMT), and kinases. The functional relation of these enzymes to HIV-1 latency reversal will be discussed below.

In light of previously addressed observations, it is believed that upon cessation of cART, latently infected cells will become progressively activated, and once sequestered TFs and factors associated with gene expression will coordinate global HIV-1 reactivation, permitting the dissemination of the virus to other permissive cells. By contrast, the idea behind the shock and kill strategy is to reactivate the virus and eliminate reservoir cells in treated patients, thus avoiding the infection of bystander cells (Archin *et al.*, 2012; Deeks*, 2012). Depending on their mechanism of action, the main categories of LRA will be briefly described in the following subchapters.

#### 3.2.2.1. Histone deacetylases inhibitors

Histone deacetylases mediate the removal of neutral acetyl groups from N-terminal domains of DNA-bound histones. Hence, the positive charge of histones tails is no longer mitigated by nonpolar groups and negatively charged DNA molecule winded around nucleosomes becomes more tightly packed thanks to electrostatic interactions. Under these circumstances, TFs and other components of host transcriptional machinery are unable to access the particular part of chromatin and effective gene expression cannot transpire. In this regard, reactivation of the virus is functionally dependent on the recruitment of HATs to the HIV-1 LTR. Conversely, their antagonists HDACs are mobilized to the promoter region when the latency is established, and thus HDACs inhibitors (HDACi) became a subject of the HIV-1 latency reversal research (Turner* and Margolis, 2017). As one of the most extensively studied LRAs, HDACi have shown a great promise in a model *in vitro* systems (Archin *et al.*, 2009;

Spina *et al.*, 2013), but exhibited only limited efficacy in mice (Spina *et al.*, 2013; Tsai *et al.*, 2016), HIV-infected cells from patients cultured *ex vivo* (Archin *et al.*, 2012; Lu *et al.*, 2014; Wei *et al.*, 2014), and in clinical studies (Archin *et al.*, 2010, 2014; Siliciano *et al.*, 2007). Up to 2017, 18 HDACsi have been characterized (Turner* and Margolis, 2017), including valproic acid (Siliciano *et al.*, 2007), Vorinostat (Archin *et al.*, 2014), Panobinostat (Rasmussen *et al.*, 2014; Tsai *et al.*, 2016), Romidepsin (Wei *et al.*, 2014) and others. Moreover, a very recent study using a virtual screening has identified 60 novel compounds which might serve as HDACi (Divsalar *et al.*, 2020). Even though administration of HDACsi alone proved ineffective in clinical settings, it is believed that they might still induce HIV-1 expression in reservoir cells in combination with other mechanistically different LRAs or sterilizing approaches (Turner* and Margolis, 2017).

#### 3.2.2.2. Inhibitors of methyltransferases

DNA methylation is an epigenetic modification facilitated by cellular DNA methyltransferases (DNMT), which aid to maintain a repressive chromatin environment (Donahue* and Wainberg, 2013). As described above, methylation of HIV-1 promoter at CpG-rich regions attenuates the HIV-1 expression, reinforcing latency and virus persistence in reservoir cells (Blazkova *et al.*, 2009; Trejbalova *et al.*, 2016). Current research on provirus methylation suggests that epigenetic silencing is more robust in aviremic patients (Kint *et al.*, 2020; Trejbalova *et al.*, 2016), occurs in intragenic regions (Kint *et al.*, 2020), and acts together with other limiting factors of a host cell to restrict HIV-1 expression (Duverger *et al.*, 2009). Understandably, inhibitors of DNA methyltransferases (DNMTi) represent another class of chemical compounds with latency-reversing ability. Most intensively studied DNMTi, 5-aza-2′-deoxycytidine, also known as Decitabine, was shown to reactivate HIV-1 in combination with HDACi *in vitro* and *ex vivo* (Bouchat *et al.*, 2016). The Decitabine also synergized with NF-κB activators, prostratin and Tumor necrosis factor α (TNFα), to reactivate HIV-1 in latently infected J-Lat cell lines (Kauder *et al.*, 2009). Another class of demethylation agents that reactivate HIV-1 from latency are HMT inhibitors (HMTi) like chaetocin, BIX-01294, or GSK343 (Melkova* *et al.*, 2017). In consideration of provirus silencing, several specific histone methylation markers were described, such as trimethylation of lysine residues at positions 9 and 27 of histone H3 (Pearson *et al.*, 2008) or monomethylation of lysine 20 at histone H4 (Boehm *et al.*, 2017). Treatment of latently infected cells by aforementioned HMTsi was shown to nullify methylation of histones at these sites and enabled subsequent reactivation of HIV-1 (Imai *et al*, 2010; Tripathy *et al.*, 2015). The latency-reversing effect of chaetocin and

BIX-01294 has been also confirmed in *ex vivo* cultured resting CD4+ T-cells and CD8+ depleted PBMCs from treated HIV+ patients (Bouchat *et al.*, 2012).

#### 3.2.2.3. PKC inducers

In contrast to previously described classes of LRAs, the activation of the PKC signalization axis enables the reactivation of latent provirus through the release of host TFs, such as NF-κB and P-TEFb. Since NF-κB and P-TEFb represent major limiting factors of the HIV-1 expression, PKC agonists became widely recognized as potent LRAs (Melkova* *et al.*, 2017). Among other PKC inducers, phorbol esters and their derivatives, like PMA (Shankaran *et al.*, 2017), prostratin, 12-deoxyphorbol-13-phenylacetate (DPP)(Beans *et al.*, 2013), and macrolide lactone bryostatin (Díaz *et al.*, 2015), and ingenol (Jiang *et al.*, 2015) demonstrated robust latency-reversing capacity both *in vitro* and *ex vivo.* These PKC agonists stimulate HIV-1 reactivation via the PKC-NF-κB arm, as they functionally substitute the role of diacylglycerol, an upstream second messenger of the PKC (Beans *et al.*, 2013; Díaz *et al.*, 2015; Jiang *et al.*, 2015; Kedei *et al.*, 2004). In addition, the P-TEFb and NF-κB can be successfully rescued from their inhibitors, hexamethylene bisacetamide induced protein 1 (HEXIM1) and inhibitor of κB (IκB), respectively, in a PKC-independent manner (Barboric *et al.*, 2007; Pyo *et al.*, 2008). In the latter case, treatment of latently infected cell lines with oxidizing chemicals like $H_2O_2$ led to IκB sequestration, translocation of NF-κB to the nucleus, and subsequent reactivation of HIV-1 (Pyo *et al.*, 2008). Moreover, the production or administration of TNFα was shown to create a positive feedback loop to NF-κB signalization due to its pro-oxidative properties, potentiating HIV-1 expression. On the contrary, co-treatment of cultures with antioxidizing agents has markedly downsized the effect of LRAs on HIV-1 reactivation (Westendorp *et al.*, 1995). Because NF-κB is a redox-sensitive TFs and a limiting factor of HIV-1 expression, it has been hypothesized that oxidative stress plays an integral role in the HIV-1 latency reversal.

#### 3.2.2.4. Disulfiram

Disulfiram, an inhibitor of alcohol dehydrogenase used for the treatment of chronic alcoholism, was first characterized as LRA in the year 2011 (Xing *et al.*, 2011). The mechanism of action was later proposed by Doyon and colleagues, who, based on their empirical data, have suggested that the latency-reversing effect of DSF is mediated via inhibition of Phosphatase And Tensin Homolog (PTEN), activation of the protein kinase B, and subsequent release of NF-κB from its inhibitory protein IκB (Doyon *et al.*, 2013; Jeong *et al.*, 2005). Besides,

disulfiram was also shown to act as DNMTi, inhibiting DNMT1 and reducing the global content of methylated cytosines (Lin *et al.*, 2011). Unlike some other LRAs, DSF also reactivated HIV-1 without undesirable global T-cell activation, making it an ideal candidate for shock and kill strategy (Xing *et al.*, 2011). The reactivation of latent HIV-1 by DSF was, so far, reported in several monocyte-derived cell lines, including U1, THP89GPF, CHME-5/HIV, and in primary PBMCs, resting CD4+ T-cells, and Bcl-2-immortalized CD4+ T-cells, but not in model HIV-1 latency cell lines, such as ACH-2, J89GFP or J-Lat 9.2 ect on HIV-1 reactivation when administered alone to treated HIV+ patients in pilot clinical studies (Elliott *et al.*, 2015; Spivak *et al.*, 2014). The lack of desired DSF effect on the HIV-1 reactivation in Jurkat cells was explained by the absence of PTEN expression (Doyon *et al.*, 2013). The unavailability of PTEN in unstimulated reservoir cells might explain insufficient latency-reversing ability observed *in vivo*.

## 3.3. Heme metabolism

Heme, or iron protoporphyrin IX, is a linear tetrapyrrole molecule containing a central atom of ferrous iron ($Fe^{2+}$). In cells, heme is found as a prosthetic group in catalytic centers and binding sites of proteins that facilitate vital cellular processes like bioenergetics, metabolism, signaling, and transcriptional regulation. In terms of organismic homeostasis, heme also represents a major component of the oxygen transport and storage system, since, thanks to its redox characteristics, it enables cyclic capture and release of oxygen from hemoglobin and myoglobin proteins. The synthesis of the heme molecule occurs in a series of eight consecutive enzymatic reactions that take place in mitochondria and cytoplasm. Hereditary or acquired conditions disrupting heme anabolism lead to the development of serious illnesses known as porphyrias. On the other hand, excessive levels of heme were shown to be implicated in several inflammatory pathologic conditions, including sickle cell disease, malaria, sepsis, vascular endothelium injury, acute lung injury, acute kidney injury, and others (Ryter*, 2021).

The degradation cascade of heme is initiated by the NADPH-dependent microsomal heme oxygenase 1 (HO-1), which catalyzes the oxidation of heme by molecular oxygen to form equimolar amounts of biliverdin, ferrous iron, and CO. Next, biliverdin is converted into bilirubin in a spatiotemporally coupled reaction catalyzed by BVR (Tenhunen *et al.*, 1969). The BR is an important cellular quencher of free radicals and its antioxidative properties are essential in terms of redox homeostasis. As such, BR can be reversibly oxidized to BV and then recycled back by the action of BVR. Indeed, the multitude of *in vitro* evidence suggests that the fine-tuned redox cycling of BR exerts powerful cytoprotective effects in various tissues (Barañano *et al.*, 2002; Doré *et al.*, 1999; Jansen *et al.*, 2010; Sedlak *et al.*, 2009). The heme degradation cascade is shown in figure 7. By contrast, free heme and $Fe^{II+}$ are involved in deleterious pro-oxidative processes, such as lipid peroxidation, protein oxidation, and DNA mutagenesis (Camejo *et al.*, 1998; Jeney *et al.*, 2002; Keyer and Imlay, 1996; Nunoshiba *et al.*, 1999). Both free heme and iron may catalyze the Fenton reaction, which yields the hydroxyl radical, a most potent oxidizing agent among reactive oxygen species (ROS), from hydrogen peroxide. Thus, iron or heme overload may initiate iron-mediated programmed cell death called ferroptosis (Ryter*, 2021). Additionally, the heme molecule can also serve as a negative regulator of TFs, such as BACH1 (Hira *et al.*, 2007) or BACH2 (Watanabe-Matsui *et al.*, 2011). Its role in transcriptional regulation will be briefly described in chapter 3.3.2.

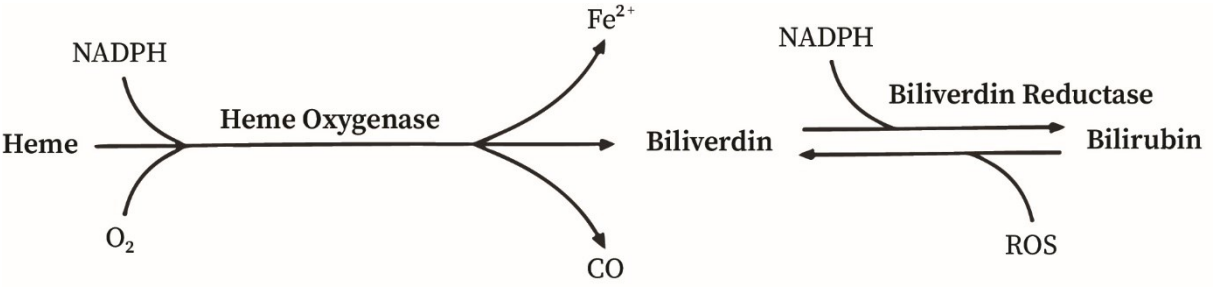


**Figure 7| A scheme of heme degradation cascade**
Heme is degraded into bilirubin in two consecutive reactions catalyzed by Heme Oxygenase and BVR. The scheme additionally shows redox cycling of BV into BR via the catalytic activity of BVR and ROS-mediated oxidation. Adapted from (van Dijk *et al.*, 2017).

### 3.3.1. Biliverdin Reductase A (BVRA)

In the human organism, the BVR is a soluble protein existing in two isoforms, namely BVRA and BVRB, that are encoded within 2 different genomic loci and are sequentially distinc. While the activity of BVRB is limited to broad specificity oxidoreductase (Pereira *et al.*, 2001), BVRA, a major Biliverdin Reductase in an adult human, also displays a dual-specificity (serine-threonine/tyrosine) kinase activity (Lerner-Marmarosh *et al.*, 2005). In addition to these catalytic functions, BVRA facilitates the nuclear transport of heme (Tudor *et al.*, 2008) and can act as a TF (Kravets *et al.*, 2004). Relating the function of TF, BVRA structure was shown to accommodate leucine zipper-like DNA-binding domain and stimulate the expression of HO-1 in response to oxidative stress by binding to AP-1 element located in the HO promoter region (Ahmad *et al.*, 2002; Kravets *et al.*, 2004). Moreover, the overexpression of BVRA upregulates the transcription of a constitutive TF, called activating transcription factor-2 (Kravets *et al.*, 2004), which can interact with other TFs like NF-κB to modulate the expression of genes in the form of heterodimers (Du *et al.*, 1993). As for the kinase activity of BVRA, it has been demonstrated that BVRA is autophosphorylated and that this post-translational modification is required for conversion of BV into BR (Salim *et al.*, 2001). Besides, BVRA can serve as an adaptor protein for other cellular kinases, such as PKC and mitogen-activated protein kinase (MAPK) to stimulate their kinase activities (Lerner-Marmarosh *et al.*, 2005, 2007, 2008). Until recently, there were no described inhibitors of the BVRA catalytic activity. As of 2017, DSF and Montelukast became the first reported inhibitors of BVRA (van Dijk *et al.*, 2017). In conclusion, BVRA pleiotropy appears to be implicated in multiple cellular functions, including cell growth, apoptosis, oxidative response, and gene expression.

### 3.3.2. BTB Domain And CNC Homolog 2 (BACH2)

The BACH2 protein is a heme-regulated transcription repressor involved in the B- and T-cell differentiation (Watanabe-Matsui *et al.*, 2011). It belongs to the family of Cap'n'collar (CNC) TFs along with its homolog Bach1, p45 Nuclear Factor Erythroid-derived 2 (NF-E2), and the NF-E2-related factors (Nrf), namely Nrf1, Nrf2, and Nrf3. All members of the CNC family contain C-terminal basic leucine zipper domain (Sykiotis* and Bohmann, 2010) and BACH proteins also accommodate the BTB (Broad complex–Tramtrack–Bric-a-brac) domain at N-termini (Oyake *et al.*, 1996). To exert their regulatory function, CNC TFs associate with small

musculoaponeurotic fibrosarcoma proteins and bind NF-E2 sites on DNA in the form of heterodimers (Oyake *et al.*, 1996; Toki *et al.*, 1997). The Nrfs and NF-E2 are generally characterized as transactivators of transcription, whereas BACH proteins act almost exclusively as transcription repressors (Sykiotis* and Bohmann, 2010). Regarding heme metabolism and redox homeostasis, the Nrf2 axis promotes cell survival by transcriptional activation of antioxidant response element (ARE), stimulating the expression of phase II detoxifying enzymes, such as HO-1, NAD(P)H:quinine Oxidoreductase 1, and Glutathione S-transferase in response to oxidative stress (Hong *et al.*, 2010; Itoh *et al.*, 1997). Contrarily, BACH2 was described as a negative regulator of HO-1 promoter (Watanabe-Matsui *et al.*, 2011; Yoshida *et al.*, 2007) and a driver of cellular apoptosis during the oxidative challenge (Muto *et al.*, 2002). Besides of its prominent function in B-cell lineage, where it controls differentiation and antibody class switching (Muto *et al.*, 1998, 2004; Watanabe-Matsui *et al.*, 2011), BACH2 may be fundamentally involved in the regulation of T-cell maturation and quiescence. In fact, BACH2 was found to repress the expression of maturation factors in CD4+ T-cells, arresting them in a naïve state (Tsukumo *et al.*, 2013). The regulation of BACH2 stems from its cellular localization, post-translational modifications, and heme-responsiveness. The retention of BACH2 in cytoplasm is determined by the presence of a phosphorylation marker at Serin residue 521 (Yoshida *et al.*, 2007) and mobilization to the nucleus by oxidation of cysteine residues, C820 and C827, at the C-terminal domain of the protein (Hoshino *et al.*, 2000). The C-terminal cysteines are oxidized upon increased oxidative stress (Hoshino *et al.*, 2000), thus the activity of the protein is directly influenced by the redox homeostasis in the intracellular milieu. The heme, on the other hand, regulates BACH2 allosterically as its binding induces a conformational change of the protein, restricting the DNA-binding capabilities and increasing turnover rate (Watanabe-Matsui *et al.*, 2011, 2015). Current literature seems to neglect the role of BACH2 in HIV-1 infected cells, although it is evidently involved in crucial cellular processes that also influence HIV-1 expression.

# 4. Materials and methods

## 4.1. Materials

This chapter contains a detailed list of chemicals, solutions, culture media, cell lines, plasmids, and commercial kits used throughout the experimental work. Overview of used chemicals is enclosed in table 1.

### 4.1.1. Chemicals

**Table 1| List of chemicals used**

| Chemical | Manufacturer | Abbreviation |
|---|---|---|
| Absolute ethanol | Penta | *Et*OH |
| Agar | Sigma | - |
| Agarose | Amresco | - |
| Agua pro injectione | Ardeapharma | - |
| Amonium Acetate | Sigma | - |
| Bromophenolblue | Sigma | - |
| Chloroform | Penta | - |
| Dimethyl sulfoxide | Sigma | DMSO |
| Disulfiram | TCI | DSF |
| Ethylenediamine tetraacetic acid | Fermentas | EDTA |
| Ethidium bromide | Sigma | *Et*Br |
| Normosang (Heme arginate) | Orphan Europe | HA |
| Hydrochloric acid | Penta | - |
| Isopropyl alcohol | Penta | IP |
| Kaseine hydrolysate | Sigma | - |
| Phorbol 12-myristate 13-acetate | Sigma | PMA |
| qPCR primers | IGN | - |
| Propidium Iodide | Sigma | PI |
| RNAse A | Fermentas | - |
| RNAse free water | Sigma | - |
| Sucrose | Penta | - |
| Triton X-100 | Sigma | - |
| Trizma® base | Sigma | Tris |
| Trypan blue | Sigma | - |
| Yeast extract | Fluka | - |
| Roswell Park Memorial Institute | Lonza | RPMI |
| 4-(2-hydroxyethyl)-1-piperazineethanesulfonic acid | Serana | HEPES |
| β-mercaptoethanol | Sigma | BME |
| Fetal bovine serum | Gibco | FBS |

### 4.1.2. Solutions

Solutions used for work with tissue cultures and in most molecular biological methods were prepared with apyrogenic Agua pro injectione and subsequently sterilized by autoclaving or filtration through a 0.22 μM filter. Solutions used in assays for detection and/or quantification of nucleic acids were prepared with DNAse/RNAse free water. Solutions employed in biochemical methods were prepared in non-sterile Milli-Q water (25 °C, 18.2 Ω). Overview of used solutions is enclosed in the table 2.

**Table 2| List of solutions used**

| Solution | Composition | Full name |
|---|---|---|
| **TE buffer** | 10 mM Tris pH 8.0, 1mM EDTA | Tris-EDTA buffer |
| **Bacteria lysis buffer** | 0.05M Tris pH 8.0, 0.05M EDTA, Sucrose 8%, Triton X-100 | Zippy buffer |
| **10x concentrated TBE** | 0.89M Tris 0.89M pH 7.6, $H_3BO_3$, 0.04M EDTA $2Na^+ \cdot 2H_2O$ | Tris-borate-EDTA buffer |
| **10x concentrated PBS** | 1.38M NaCl, 2.7mM KCl; 1.1mM $KH_2PO_4$, 8.1mM $Na_2HPO_4$, pH 7.4 | Phosphate buffer saline |
| **10x concentrated Blue juice** | 25% ficol, 0.1M Tris pH 7.4, 1mM EDTA, 0.25% bromophenol blue | DNA loading buffer |
| **P3 electroporation buffer** | 5mM KCl, 15mM $MgCl_2$, 90mM NaCl, 10mM Glucose, 0.4mM $Ca(NO_3)_2$, 40mM $Na_2HPO_4/NaH_2PO_4$, pH 7.2 | - |
| **Cell extraction buffer** | HEPES 25 mM ; EDTA 1mM, glycerol 10% | - |
| **BVRA activity assay buffer** | 50 mM Tris pH 6.75; BSA 400 μg/ml, biliverdin 10 μM | - |

### 4.1.3. Bacterial growth media and supplements

Bacterial cultures were grown in liquid LB (Luria Broth) medium containing 0.5% yeast extract, 1% casein hydrolysate, 0.17M NaCl, 1mM NaOH or were cultured on solid LB agar composed of 0.5% yeast extract, 1% casein hydrolysate, 1.5% agar, 0.17M NaCl, and 1mM NaOH. Transformed bacterial strains were cultured on/in the corresponding media with the addition of Ampicillin 100 mg/mL or Kanamycin 50 mg/mL.

### 4.1.4. Tissue culture growth media and supplements

Jurkat clone A2 and A3.01 cell culture cell lines were grown in 10% FBS–RPMI medium.

- FBS –inactivated for 30 minutes at 56 °C
- RPMI – RPMI 1640 with ultraglutamine 1 supplemented with HEPES 12.5 mM, Penicillin ($1 \cdot 10^5$ U/l; Sigma); Streptomycin (100 mg/ml; Sigma)

### 4.1.5. Bacteria and plasmids

The following plasmids were transformed into and multiplied in transformation competent *E. coli* strain DH5α (kindly provided by Dr. Mělková). Plasmids used in this work are listed bellow (schematic plasmid maps are provided in figure 8):

- pDsRed2–N1 (Clontech)
- pcDNA3.1 + C-DYK– BVRA (Genscript; pcDNA3.1-BVRA)
- pcDNA3.1 + C-DYK– BACH2 (Genscript; pcDNA3.1-BACH2)
- pcDNA3–LUC (received from Dr. Mělková, Addgene)

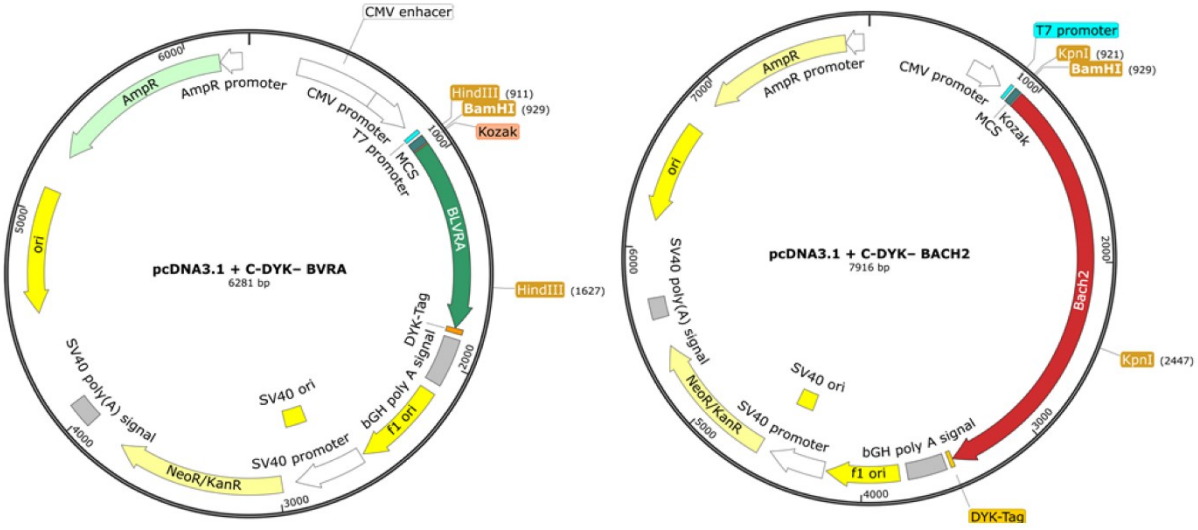

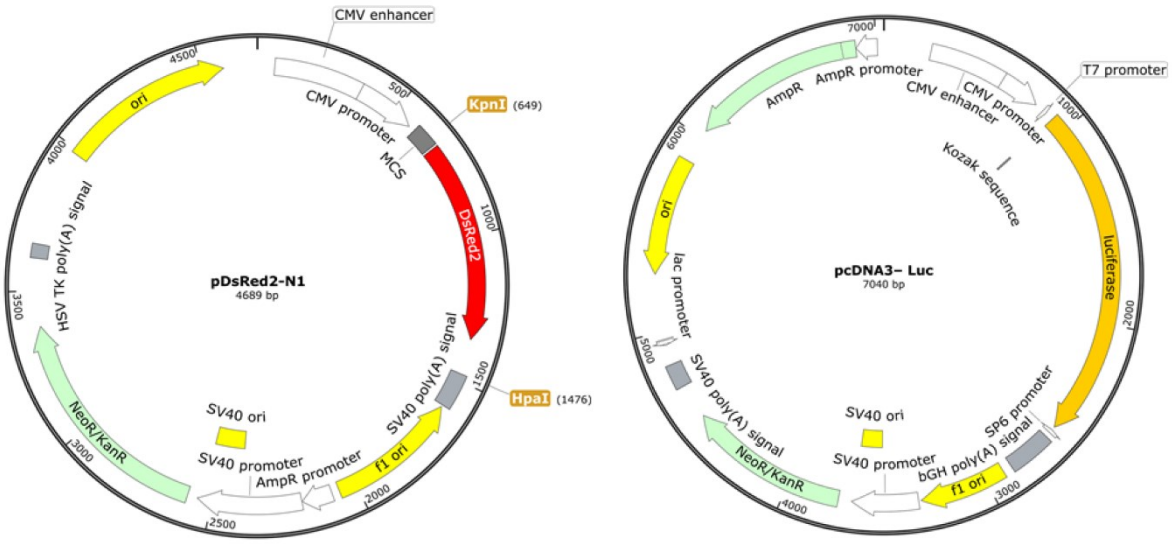


**Figure 8| Schematic representation of plasmids**
Diagrams illustrate the circular structure and sequence features of pcDNA3.1 + C-DYK-BVRA and BACH2, pcDNA3-LUC, and pDsRed2-N1 plasmids. The locations of restriction sites selected for plasmid digestion in restriction analysis are highlighted in orange. Plasmid diagrams were constructed via GeneSnap® software.

### 4.1.6. Tissue culture cell lines

In this work, *in* vitro experiments involving tissue cultures were conducted using human suspension T-cell lines A3.01 and clone A2 of Jurkat cells. The clone A2 of Jurkat cells harboring integrated, replication-incompetent HIV-1 "*mini-virus*" (LTR-Tat-IRES-EGFP-LTR)(Jordan, 2001) and A2 clone derived cells expressing specific cDNAs (see 4.1.5) have been used throughout the experiments. Tissue culture cell lines were grown in 10% FBS-RPMI in a $CO_2$ incubator for tissue cultures (37°C/ 5% $CO_2$/ 95% humidity) at all times.

### 4.1.7. Commercial kits

- Amaxa® Cell Line Nucleofector® kit V (Lonza)
- Ambion ® TURBO DNA-*free*™ (Invitrogen)
- Qiagen® plasmid midi-prep kit (Qiagen)
- SensiFAST SYBR® Hi-ROX One-Step Kit (Bio-Line)
- TP SYBR® 2x Master Mix (Top-Bio)

### 4.1.8. Computer programmes used for research and data analysis

- GraphPad® Prism®
- Figma®
- Biorender®
- Microsoft® Excel®
- SnapGene®
- BD FACSDiva™ software version 6
- Mendeley©

## 4.2. Methods

This chapter provides a detailed description of the methods used throughout the experimental work. Experiments were conducted under the supervision of Dr. Mělková at the laboratory certified for work with genetically modified organisms at biological safety levels 1 and 2 (GMO/BSL-1 and 2) at the Department of Immunology and Microbiology and BIOCEV, 1st Faculty of Medicine, Charles University.

### 4.2.1. *In vitro* methods

#### 4.2.1.1. Handling of tissue cultures

##### 4.2.1.1.1. Cultivation and passaging

Suspension cell lines were grown in tissue cultures flask (25 $cm^2$; TP25; Sarstedt) in 8 mL of 10% FBS-RPMI and were passed 2-3 times a week (every 3 days) in a volume ratio 1:7 (cell suspension to fresh media). Prior to the cell passage, the cells were resuspended by repeated pipetting, and 1 mL of this culture was brought to 8 mL with a pre-warmed 10% FBS-RPMI. The remaining cells were either discarded or used for seeding at bacterial Petri dish (see section 4.1.1.1.2.). Provided that a larger quantity of cells was required for upcoming experiments, the cell suspension was cultured in double volume and passed in an equal ratio.

Stably transfected Jurkat A2 clones (see section 4.2.1.9) were cultured in 10% FBS-RPMI supplemented with Geneticin sulfate (G418) and β-mercaptoethanol (BME) at final concentrations 1 mg/mL and 0.05 mM, respectively. These cell lines were passaged every 3 days in volume ratio 1:3 at a final volume of 8 or 16 mL.

#### 4.2.1.1.2. Cell seeding and harvesting

Prior to every experiment with tissue culture cell lines, cells were seeded from the culture flasks onto a non-adherent, bacterial Petri dish(es)(90 mm; P-Lab), diluted 1:1 with fresh 10% FBS-RPMI and incubated in a $CO_2$ incubator for approximately 24 hours. The next day, a cultured cell suspension was resuspended, harvested into a 50 mL conical tube, and a 100 µL aliquot of the cell suspension was transferred into a new 1.5 mL Eppendorf tube for cell counting (see section 4.1.1.1.3). After determination of the cell density, a required volume of the harvested cell suspension was transferred into a new 15 or 50 mL conical tube, the suspension was centrifuged on Eppendorf centrifuge 5810 R (90g/ 10 min/ 25°C), and the supernatant was discarded. Unless stated otherwise, pelleted cells were resuspended in a pre-warmed 10% FBS-RPMI at final concentration $0.5 \cdot 10^6$ cells/mL and seeded onto tissue culture treated 96-well plate (JETBioFil®) or 96-well plate with U-shaped base (Corning™ Costar™) at 100 µL/well.

#### 4.2.1.1.3. Cell counting

The density of living cells was determined in aliquots of harvested cell suspensions. To this end, 2 x 40 µL of cell suspension were pipetted into two separate 1.5 mL Eppendorf tubes and diluted 1:1 with 40 µL of 0.1% trypan blue in 1x concentrated PBS solution. Subsequently, 10 µL from each stained cell suspension were pipetted and counted on the Neubauer chamber. The number of viable cells was determined by counting transparent cells in 8 large $1mm^2$ fields. Given the heigh of the chamber of 0.1 mm the number of cell was determined according to this formula:

$$\text{Cell concentration } (10^6/mL) = ((\#\text{ of counted cells} / 8) * 2 / 100$$

#### 4.2.1.1.4. Cryopreservation of cell lines

Cell suspensions in culture flasks were diluted 1:1 with 10% FBS-RPMI and incubated in a $CO_2$ incubator for 24 hours. The following day, the cells were collected into 15 mL conical tubes, the cell suspensions were centrifuged (400g/ 5 min/ 25°C), and the supernatants were discarded. Pelleted cells were resuspended in 1 mL of freezing medium (20% FBS-RPMI + 10% DMSO), and these suspensions were transferred into cryogenic tubes (1,2 mL; T311 Simport Cryovial®). The tubes were first held on ice for 30 minutes, and then they were placed in a freezer (-20°C) for additional 30 minutes. Thereafter, the tubes were kept in a deep freeze

(-80°C) for approximately 24 hours. The following day, vials were was transferred into liquid nitrogen.

#### 4.2.1.1.5. Thawing of the frozen cell lines

A vial with frozen cells was removed from liquid nitrogen storage and quickly thawed in a water bath at 37 °C. Once thawed, 1 mL of cell suspension was transferred from a cryogenic tube into a 15 mL conical tube containing 10 mL of fresh, pre-warmed 10% FBS-RPMI, and the suspension was centrifuged (400g/ 5 min/ 25°C). The supernatant was removed, and pelleted cells were resuspended in 2 mL of 10% FBS-RPMI. The cell suspension was then transferred into a tissue culture flask and incubated $CO_2$ incubator for 24 hours. The following day, the volume in the flask was adjusted to 8 ml with 10% FBS-RPMI. From this point on, cells were cultured and passaged as described in section 4.2.1.1.1.

### 4.2.1.2. PMA titration assay

The A2 cells were seeded onto 96-well plate at 100 µL/well and treated with PMA at final concentrations 0.5 ng/mL, 0.4 ng/mL, 0.3 ng/mL, 0.2 ng/mL, 0.1 ng/mL, 0.05 ng/mL, and 0.025 ng/mL. Dilutions of PMA for treatment of the cells were freshly prepared in DMSO from PMA stock solution (1 µg/mL in DMSO) at 2000x working concentration (e. g. 1 µg/mL; 0.8 µg/mL; *etc.*). PMA stock solution was left to thaw at RT for approximately 15 seconds, and sequential dilution in DMSO immediately followed. Each prepared aliquot was promptly put onto a freezing block, and after completion of the dilution series, aliquots were transferred from the freezing block to a freezer (-20°C) to avoid degradation of PMA. One at the time, PMA aliquots were taken out of the freezer and diluted 100x with fresh 10% FBS-RPMI to 20x working concentration (e. g. 10 ng/mL; 8 ng/mL; *etc.*). Freshly diluted PMA solution was then distributed to wells containing 100 µL of cell suspension at 5 µL/well to the final concentration specified above. Mock-treated wells were treated with 5 µL of 10% FBS-RPMI. The cells were incubated in a $CO_2$ incubator for 24h.

### 4.2.1.3. Treatment assays

On the day of treatment, the A2 cells were harvested and seeded onto a 96-well plate with a U-shaped base as described in section 4.1.1.1.2. Cells were then treated with DSF (final concentrations 5 µM; 2.5 µM; 1 µM ) or HA (2.5 µL/mL; 1.25 µL/mL), or a combination of these agents and subsequently stimulated with PMA (final concentration 0.5 ng/mL). Aliquots of DSF and PMA for treatment were prepared at 20x working concentration with fresh 10% FBS-

RPMI from stock solutions (DSF 10 mM in DMSO; PMA 1 µg/mL in DMSO; stored at -20°C) and added at 5 µL/well to final concentration specified in each experiment. The HA (Normosang 25 mg/mL; stored at 4°C ) was added at final concentration of 2.5 µL/mL or 1.25 µL/mL per well. Volume in wells with mock-treated samples or samples treated by a single agent was adjusted with 10% FBS-RPMI to match the volume in wells treated with multiple compounds. The cells were incubated in a $CO_2$ incubator for 24h.

#### 4.2.1.4. Measurement of BVRA kinetic activity

The A3.01 cells were split 1:1 and cultured on 2 non-adherent bacterial Petri dishes as described in section 4.1.1.1.2. After 24 hours of cultivation, A3.01 cells were harvested, centrifuged (300g/ 10 min/ 25°C), and the supernatant was discarded. Pelleted cells were resuspended in 1 mL of hypotonic extraction buffer (HEPES 25 mM; EDTA 1mM, glycerol 10%) and subsequently held on ice for 15 minutes. Following the incubation on ice, the cell lysate was centrifuged (14 000g/ 10 min/ 4°C), and the supernatant containing the extracted cytosol was aliquoted at 150 µL per 1.5 mL centrifugation tube. One of the aliquots was kept on ice until employed in the assay, and the rest were stored at deep freeze (-80°C). The BVRA activity assay buffer (50 mM Tris pH 6.75; BSA 400 µg/ml, biliverdin 10 µM) was pipetted to designated wells in 96-format at 180 µl/well, and the plate was pre-incubated for 5 minutes at 37 °C. Then, 10 µL of cytosolic extract (containing approximately 5 µg of protein) and 5 µL of DSF at final concentrations of 20 µM or 10 µM were added. Biliverdin Reductase activity assay was initiated by the addition of 5 µL of NADH at a final concentration of 100 µM. The rate of conversion of biliverdin to bilirubin was determined by measuring absorbance at wavelengths 450 nm, 660 nm every 2 minutes for 1 hour at 37°C using the Perkin Elmer spectrofluorometer.

#### 4.2.1.5. Plasmids preparation

##### 4.2.1.5.1. Transformation of DH5α *E.coli* strain by heat shock

An aliquot of competent DH5α *E.coli* cells was taken out from the deep freezer (-80°C) and left to thaw on ice for approximately 20 minutes. In the meantime, lyophilized pcDNA3.1 plasmids (10 µg) were reconstituted in 20 µL of TE buffer and were left to incubate at room temperature for 5 minutes. Subsequently, 1 µL of each plasmid was transferred to 1.5 mL tubes containing 100 µL of the bacterial suspension, and the tubes were next incubated on ice for 30 min. Following the incubation, tubes were transferred to 42°C water bath for 45 seconds

and put back on the ice for 2 minutes. A 200 µL of pre-warmed LB liquid medium was added to both bacterial suspensions, and the tubes were placed in the thermostat for bacterial cultures for 1 hour at 37°C. Thereafter, 10 µL, 50 µL, and 150 µL from each suspension were inoculated and spread on separate bacterial Petri dishes (90 mm) containing LB agar supplemented with ampicillin (100 µg/mL). The Petri dish was incubated in a bacteriological incubator at 37°C. Transformation of competent bacteria by pDsRed2-N1 was performed accordingly, but cell suspensions were inoculated on Petri dishes containing LB agar with the addition of kanamycin (50 µg/mL).

#### 4.2.1.5.2. Plasmid isolation and purification

Approximately 24 hours after the inoculation of Petri dishes (see section 4.2.1.5.1), individual colonies transformed with different plasmids were picked up using a disposable bacterial loop and transferred into a 15 mL tube containing 5 mL of LB medium supplemented and corresponding antibiotic. Bacterial colonies were resuspended in the medium by gentle stirring, and an aliquot of each suspension was inoculated on a new Petri dish with LB agar and appropriate antibiotic. The inoculated Petri dishes were cultured for approximately 24h and then stored in a refrigerator at 4°C. Bacterial suspensions in 15 mL tubes were left to incubate for 24 hours on the heated Schoeller ISS 40705R (Schoeller instruments) shaker at 220 rpm and 37°C. The next day, the bacterial suspensions were centrifuged (1200g/10 min/ 4°C), supernatants were discarded, and the tubes were placed on ice. Bacterial pellets in 15 mL tube were resuspended in 0.7 mL of bacterial lysis buffer (Zippy buffer), the suspension was transferred to a 1.5 mL centrifuge tube, and 50 µL of lysozyme (10 mg/mL) was added. Lysed cultures in 1.5 mL tubes were thoroughly mixed by pipetting and boiled twice in boiling water on or on a heat block for 30-45s. Following a centrifugation (21 000g/ 10min/ 4°C), the precipitated material from the bottom of the tube was gently picked out by a toothpick and discarded. Then 0.75 mL of pre-cooled isopropanol was added, the solution was mixed and kept at -80°C for 5 min. Samples were then centrifuged (21 000g/ 10min/ 4°C), supernatants were slowly discarded, and pellets containing precipitated nucleic acids were left to dry on air. Pellets were resuspended in 150 µL of TE buffer, and 350 µL of 7,5M $NH_4Ac$, and DNA precipitated with 1 mL of absolute ethanol. The solution was again left in -80°C for 5 min and centrifuged in the same way. The supernatants were discarded, and the pellets containing the precipitated DNA were washed with 1mL of 70% EtOH and centrifuged again (21 000g/5 min/ 4°C). This step was repeated twice. The remaining solvent was discarded, and DNA was left to

dry on air for 5-10 minutes and resuspended in 50 µL of TE buffer. The isolated DNA was stored in a freezer (-20°C).

#### 4.2.1.5.3.Plasmid amplification and isolation by the Qiagen Midi prep kit

A positive bacterial clone, in which the successful transformation and presence of plasmid DNA was previously confirmed by restriction analysis, was inoculated into a 100 mL Erlenmeyer flask containing 25 mL of fresh LB medium supplemented with the appropriate antibiotic. The inoculated flask was incubated for approximately 16 hours in a heated bacterial shaker (220 rpm/ 37°C). The next day, 250 µL of this culture was taken for preparation of glycerol stock (see section 4.2.1.6). The rest of the culture was used for plasmid midi-prep isolation performed by Qiagen® plasmid midi-prep kit according to the protocol provided by the manufacturer.

The overnight culture grown in Erlenmeyer flask was harvested into a 50 mL conical tube, centrifuged (6000g/ 15 min/ 4°C), and the supernatant was discarded. Pellet was resuspended in 4 ml of buffer P1 (containing RNase A; c= 100 µg/ml), 4 ml of buffer P2 were added, and the tube was mixed by repeated inverting (4-6 times). The solution in the tube was incubated for 5 minutes at room temperature, and 4 ml of a pre-cooled buffer P3 were added. The suspension was put on ice for 15 min and then centrifuged (15 000g / 30 min/ 4°C). In the meantime, the QIAGEN-tip 100 was equilibrated by 4 ml of buffer QBT. After the centrifugation, the supernatant was applied on the QIAGEN-tip, the column was allowed to empty by gravity flow, and it was washed twice by 5 ml of QC buffer. DNA retained on the column was then eluted into a new 15 mL conical tube with 5 ml of QF buffer. DNA was precipitated by the addition of 3.5 mL of isopropanol, and the solution was centrifuged (15 000g/ 30 min/ 4°C). The supernatant was discarded, and precipitated DNA was washed with 1 ml of 70% ethanol, transferred to a 1.5 mL centrifuge tube, and the suspension was centrifuged (15 000g/ 10 min/ 4°C). The supernatant was discarded again, and the pellet was left to dry on air for 5-10 min. Precipitated DNA was resuspended in 50 µl of TE buffer and stored in a freezer (-20°C). The quality of isolated plasmid DNA was checked by restriction analysis, and the DNA concentration and purity were determined using spectrophotometry by measuring absorbance at 260/280 nm on a NanoDrop ND-1000 (Nanodrop Technologies).

### 4.2.1.6. Glycerol stock preparation

A 250 µL of the overnight bacterial culture (see section 4.2.1.5.3) were combined with 250 µl of 40% glycerol. Bacterial suspension in glycerol solution at a final concentration of 20% was then stored in a deep freezer (-80°C).

### 4.2.1.7. Plasmid DNA restriction analysis

Isolated plasmid DNA was digested by restriction endonucleases, and digested products were resolved on agarose gel electrophoresis. Each restriction reaction was performed in a 20 µL solution containing 15 µL of sterile $H_2O$, 2 µL of 10x concentrated buffer, 2 µL of DNA, and 1 µL of the restriction enzyme. All the components were held on ice with the exception of the restriction enzyme, which was held in a freezing block (-20°C). Individual reagents were added to the reaction solution in the order listed above, and after the addition of the restriction enzyme, the solution was mixed and incubated for 1 hour at 37°C. The enzymes and buffers used for digestion of particular pDNA are summarized in the table 3. Following the incubation, the samples were transferred back on the ice, and 2.2 µL of 10x blue juice (DNA loading buffer) and 1 µL of RNAse A at a final concentration of 0.5 mg/mL were added to each sample. Ten µL of each restriction digest and 5 µL of a molecular ladder (1kbp ladder; Fermentas) were then loaded onto 1x TBE 1% agarose gel with ethidium bromide (0.5 µg/mL). The electrophoresis was performed at 80 V initially for 15-30 minutes to resolve short fragments and then for about 1 hr or more, depending on the expected length of digested DNA product. The gel was then visualized by AzureBiosystems c600 (Azure Biosystems).

**Table 3| Overview of restriction enzymes, buffers and digested plasmids**

| Enzyme | Buffer | Manufacturer | Digested plasmid |
|---|---|---|---|
| BamHI | React® 3 | Invitrogen | pcDNA3.1 - BVRA; pcDNA3.1- BACH2 |
| KpnI | React® 4 | Invitrogen | pcDNA3.1- BACH2; pDsRed2–N1 |
| HindIII | R | Fermentas | pcDNA3.1 - BVRA |
| HpaI | React® 4 | Invitrogen | pDsRed2–N1 |

### 4.2.1.8. Transfection of the A2 clone of Jurkat cells

The A2 cells used in transfection experiments were cultured and collected from Petri dishas described in section 4.1.1.1.2. The amount of plasmid DNA and the number of cells used in each transfection method were selected with respect to the highest viability/transfection efficiency ratio observed in previous optimization assays. Transient expression of a gene of interest was evaluated by flow cytometry approximately 24h after the

transfection. Alternatively, the cells were treated and cultured as described in section 4.2.1.3. When employed in treatment assays, the transient expression and the effect of treatment were assessed 48 h after the transfection.

#### 4.2.1.8.1. Cell electroporation using "*in house*" prepared buffer

For each electroporation reaction, $2.5 \cdot 10^6$ cells were harvested and centrifuged (90g /10 min/ 25°C). The supernatant was discarded, and pelleted cells were resuspended in 100 µL of P3 electroporation buffer, which was prepared according to Chicabayan *et al.* (2013). The cell suspension was then transferred into a 1.5 mL centrifuge tube containing 0.3 µg of desired plasmid DNA (0.15 µg of pDsRed2-N1 + 0.15 µg of pDNA containing cDNA insert). The transfection mixture was mixed, transferred into an electroporation cuvette, and immediately electroporated using Amaxa™ nucleofector™ II device and the program X-001 (high-viability). The cell suspension in the cuvette was then incubated for 10 minutes at room temperature. In the meantime, designated wells in a 12-well plate (JETBiofil®) were filled with 750 µL of 10% FBS-RPMI, and the plate was placed in a $CO_2$ incubator to pre-equilibrate the pH and the temperature. After the incubation, 500 µL of 10% FBS-RPMI were combined with cell suspension, which was subsequently transferred from the cuvette was onto a 12-well plate using a 2 mL Pasteur pipette. Control cells were treated accordingly but were not electroporated. Following the transfer of all samples, the plate was placed in a $CO_2$ incubator, and the cells were incubated for approximately 24 hours.

#### 4.2.1.8.2. Cell electroporation using Amaxa® Cell Line Nucleofector® kit V

For each electroporation reaction, $1 \cdot 10^6$ cells were centrifuged (90g /10 min/ 25°C), the supernatant was discarded, and the cells were resuspended in 100 µL of the electroporation buffer, which was prepared by combining 82 µL of the Nucleofector solution® with 12 µL of supplement. The cell suspension was transferred into a 1.5 mL centrifugation tube containing 1 µg of total plasmid DNA ( 0.5 µg of pDsRedN1 + 0.5 µg of pDNA containing cDNA insert), and the suspension was thoroughly mixed by repeated pipetting. Next, the transfection mix was transferred into an electroporation cuvette, and electroporation was performed on the Amaxa™ nucleofector™ II device using the X-001 program. After 10 minutes of incubation at room temperature, 500 µL of the pre-warmed 10% FBS-RPMI were added to the cells in an electroporation cuvette, and the suspension was transferred onto a pre-equilibrated 12-well plate containing 1 mL of 10% FBS-RPMI. Cells in the plate were then incubated in a $CO_2$ incubator for approximately 24 hours.

#### 4.2.1.9. Transfection and selection of transfected A2 clones of Jurkat cells

Transfection of A2 cells by pcDNA3.1-BVRA, pcDNA3.1-BACH2, and pcDNA3-Luc plasmids was performed by Amaxa® Cell Line Nucleofector® kit V as described in section 4.2.1.8.2. Generation of A2 clone-derived cell lines expressing a gene of interest was accomplished by a positive selection of G418-resistant clones in a pool, which is described in section 4.2.1.9.2. The selective concentration of G418 was determined in the antibiotic kill curve assay as described in section 4.2.1.9.1.

##### 4.2.1.9.1. Antibiotic kill curve assay

The A2 cells were seeded onto a 96-well plate with U-shaped base at 300 µL/well at a final concentration of $0.25 \cdot 10^6$ cells/mL Cells were challenged with 14 different concentrations of G418 ranging from 0.2 mg/mL to 2.8 mg/mL. Growth of the cultures was evaluated every day by light microscopy, and a culture medium supplemented with the corresponding concentration of G418 was replaced every 3 days. Cell viability was determined by flow cytometry on the $6^{th}$ and $11^{th}$ days of culture.

##### 4.2.1.9.2. Positive selection of transfected clones

Transfected cells were cultured on a 12-well plate in 10% FBS-RPMI for approximately 24 hours, and then the culture medium was replaced with 4 mL of fresh 10% FBS-RPMI supplemented with G418 and BME at final concentrations 1.6 mg/mL and 0.05 mM, respectively. The selection medium was changed every 3 days, and from day 11 after the transfection, the concentration of G418 in media was reduced to 1 mg/mL. At the day 20 after the transfection, first G418-resistant colonies started to appear, and the cell suspensions were transferred into tissue culture flasks. Cell suspensions have reached an optimal concentration of 0.5~1/ml approximately 30 days after the transfection. Stably transfected cell lines were then regularly passaged as described in section 4.2.1.1.1.

##### 4.2.1.9.3. Determination of growth in stably transfected cells

The A2 cells and A2-derived cell lines expressing genes of interest were cultured and harvested from Petri dishes as described in section 4.1.1.1.2. Cells were then resuspended in fresh 10% FBS-RPMI at final concentration $0.1 \cdot 10^6$ cells/mL and seeded onto 24-WP at 500 µL/well. The number of cells was assessed at 0h, 24h, 48h, and 72h after seeding by flow cytometry.

#### 4.2.1.10. Preparation of tissue culture samples

##### 4.2.1.10.1. Collection of samples for flow cytometric analysis

Samples from PMA titration and treatment assays (4.2.1.2. and 4.2.1.3., respectively) were collected from 96-well plates approximately 24 hours after the treatment. When not stated otherwise, cell suspensions cultured on 96-well plates were harvested at 100 µL/sample into 5 mL FACS tubes (Falcon® 5 mL Round Bottom Polystyrene Test Tube; Corning®) containing 200 µL of 10% FBS-RPMI supplemented with Propidium iodide (PI) at final concentration of 1 µg/µL. If not employed in treatment assays, samples from transfection experiments (4.2.1.8) cultured in 12-well plates were collected 24h post-transfection at 500 µL/well into 5 mL FACS tubes.

Samples from antibiotic kill curve assay (4.2.1.9.1) cultured on 96-well plates with U-shaped base were collected at 100 µL/well into FACS tubes containing 100 µL of 10% FBS-RPMI supplemented with PI at a final concentration of 1 µg/µL.

##### 4.2.1.10.2. Samples for quantitative polymerase chain reaction

Stably transfected cells were harvested at $1 \cdot 10^6$ cells/sample, centrifuged (400g /10 min/ 25°C), and the supernatant thoroughly discarded. Pelleted cells were then lysed in 25 µL of DEP-25 START solution (Top-Bio) and incubated at 95°C for 10 minutes. Next, tubes containing the samples were left to cool down at room temperature for 2 minutes, and 25 µL of DEP-25 STOP solution were added. Samples were stored at -80 °C.

##### 4.2.1.10.3. Samples for RNA isolation

Stably transfected cells were harvested at $1 \cdot 10^6$ cells/sample and centrifuged (400g /10 min/ 25°C). The supernatant was discarded, and samples were lysed at 0.8 mL of RNA blue solution (Top-Bio). The suspension was mixed by pipetting and stored at -80 °C.

### 4.2.2. Analytical methods

#### 4.2.2.1. Quantitative polymerase chain reaction (qPCR)

##### 4.2.2.1.1. Primer design

Primers were designed manually using ApE plasmid editor and SnapGene® software. The NCBI Primer-BLAST tool was used as a reference database to prevent unspecific

annealing of primers. The primer sets for detection pcDNA3.1-BVRA and pcDNA3.1-BACH2 were designed to overlap vector sequences downstream of the canonical stop codon, allowing for specific detection of genes of interest (see figure 9). The primer set for Luc was designed by the Primer-BLAST tool to meet the annealing conditions of other primer sets and to avoid the detection of endogenous off-targets. Primers were synthesized by the Integrated DNA Technologies (IDT) company, and the primer sets for detection of reference house-keeping gene, Glyceraldehyde-3-phosphate dehydrogenase (GAPDH), was kindly provided by MUDr. Mělková, PhD. Oligonucleotide sequences of primers employed in qPCR are enclosed in table 4.

**Table 4| Overview of primer sets employed in qPCR experiments.**

| Target gene | Forward primer | Reverse primer |
|---|---|---|
| pcDNA3.1 BVRA | TGCTGAAAAGAAACGCATCCTG | AGCGGGTTTATCACTTATCGTCG |
| pcDNA3.1 BACH2 | CCAAACAGTGACCGTGGACT | AGCGGGTTTATCACTTATCGTCG |
| pcDNA3 LUC | ATGAAGAGATACGCCCTGGTTC | TTCATAGCTTCTGCCAACCGA |
| GAPDH | CCCCACACACATGCACTTACC | CCTAGTCCCAGGGCTTTGATT |

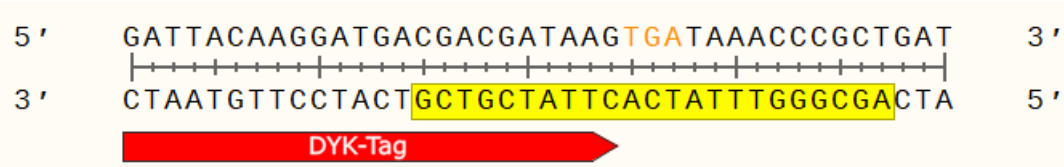


**Figure 9| Oligonucleotide sequence and annealing of the reverse primer for detection of pcDNA3.1-encoded transgenes.**
The reverse primer was designed to hybridize with pcDNA3.1 specific sequence features. The reverse primer sequence is highlighted in yellow color (shown in 3'-5' orientation). The TGA stop codon flanking pcDNA3.1-encoded DYK-Tag is displayed in orange color. Sequence encoding DYK-Tag in pcDNA3.1 + C-DYK vectors is located downstream of the canonical 3' coding termini of cDNA.

#### 4.2.2.1.2. qPCR-based detection of transgenes in stably transfected cell lines

The qPCR method was employed in this work to confirm the presence of individual cDNAs stably transfected cells, using the lysates in DEP-25. The qPCR was performed with the TP SYBR 2x Master Mix (Top-Bio; TP SYBR 2x MM) at a final volume of 20 µL/well on Light cycler® 480 (Roche). The reaction mix composition and qPCR conditions are summarized in tables 5 and 6, respectively. Prepared reaction premix containing a specific set of primers was distributed to designated wells on PCR strips at 18 µL/well, and samples were added at 2 µL/well. The reaction mix and PCR strips were held on freeze block at all times. PCR strips were briefly spun before the initiation of the reaction.

**Table 5| qPCR mix composition (1 reaction).**

| Reagent | Final concentration | Volume (µL) |
|---|---|---|
| PCR Ultra $H_2O$ | - | 7.20 |
| TP SYBR 2x | 1x | 10.00 |
| Forward | 0.4 µM | 0.40 |
| Reverse primer | 0.4 µM | 0.40 |

**Table 6| qPCR program.**

| Step | Temperature °C | Time (mm:ss) | Repetition |
|---|---|---|---|
| Initial denaturation | 95 | 10:00 | 1 |
| Denaturation | 95 | 0:15 | 55 |
| Annealing | 60 | 0:45 | |
| Extension | 72 | 0:45 | |
| Terminal extension | 72 | 10:00 | 1 |
| Melting curve | 95 | 0:15 | 1 |
| | 65 | | |
| | 97 (continuous) | ramp rate (0.11 °C/s) | |

### 4.2.2.2. Reverse transcription qPCR (RT-qPCR)

#### 4.2.2.2.1. RNA isolation

Total cellular RNA isolation was performed by acid guanidinium thiocyanate-phenol-chloroform extraction (Chomczynski and Sacchi, 1987) with RNA blue solution (Top-Bio). Cell lysates prepared in 0.8 mL of RNA blue solution (4.2.1.10.3) were taken out of the deep freeze (-80 °C) and thawed at room temperature. After the thawing, 160 µL of $CHCl_3$ were added, tubes were shaken vigorously for 15 seconds, and left incubating for 10 minutes at room temperature. Samples were centrifuged (12 000g/ 10 min/ 4°C), and the aqueous phase containing the cellular RNA fraction was transferred to a new 1.5 mL centrifugation tube. The aqueous phase was combined with 0.4 mL of isopropanol, and samples were incubated for 10 minutes at room temperature and centrifuged (12 000g/10 min/4°C). The supernatant was discarded, and the precipitated RNA was washed with 1 mL of 75% *Et*OH. Following the centrifugation (12 000g/10 min/4°C), the ethanol supernatant was discarded, and the RNA pellet was left to dry on air for 5 minutes. The isolated RNA was dissolved in 50 µL of RNAse-free $H_2O$ and stored in deep freeze (-80 °C). The purity and concentration of RNA was determined in aliquots diluted 1:1 with RNAse-free $H_2O$ by measuring absorbance at wavelengths 260 nm and 280nm using NanoDrop ND-1000.

#### 4.2.2.2.2. Treatment of RNA samples with DNAse

Isolated RNA samples were subjected to DNAse treatment by Ambion® TURBO DNA-*free*™ Kit. This method utilizes engineered DNAse I and DNAse inactivating beads to remove contaminating genomic DNA in a two-step reaction. The reaction mixture was prepared in a 0.5 mL centrifugation tube in a final volume of 30 µL and incubated in a heat block (10 min/ 37°C). The composition of the reaction mixture is summarized in table 7. After the DNAse treatment, 3.3 µL of the DNAse inactivating reagent was added and the suspension was mixed. The sample was incubated at room temperature for 5 minutes and occasionally mixed. Next, the a aqueous phase was transferred into a new 1.5 mL centrifugation tube, and the sample was stored in a deep freeze (-80 °C).

**Table 7| Reaction mixture for DNAse treatment of RNA samples using TURBO DNA-*free*™ Kit.**

| Reagent | Stock concentration | Volume (µL) |
|---|---|---|
| RNA sample | *100 ng/µL | 26 |
| TURBO DNase buffer | 10x | 3 |
| TURBO DNase | 2 U/µL | 1 |

*The concentration of RNA in individual isolates varied (90 – 130 ng/ µL)

#### 4.2.2.2.3. RT-qPCR-based assessment of transgene expression in stably transfected cell lines

The active transcription of transgenes in RNA samples prepared from stably transfected tissue cultures has been evaluated by one-step quantitative reverse transcription PCR (RT-qPCR). Primers used for selective reverse transcription and subsequent amplification of exogenous cDNAs are listed in table 4 (see section 4.2.2.1.2). The primer set used for the detection of *house-keeping* gene, GAPDH mRNA, is provided in table 8. The RT-qPCR was performed with SensiFAST SYBR® Hi-ROX One-Step Kit (Bio-Line) in the final volume of 10 µL on Light cycler® 480. The reaction mixture was prepared according to table 9, and reaction conditions are specified in table 10. RT-qPCR mix was distributed to designed wells in PCR strip at 8 µL/well, and RNA samples were added at 2 µL/well. Samples, reagents, and PCR strips were held at a cooling block all the time. Strips were briefly spun-down before the start of RT-qPCR.

**Tab 8| Primer set used for detection of endogenous GAPDH in RT-qPCR experiments.**

| Target gene | Forward primer | Reverse primer |
|---|---|---|
| GAPDH | AAGATCATCAGCAATGCCTCCT | CATGAGTCCTTCCACGATACCA |

**Tab 9| RT-qPCR mix composition (1 reaction)**

| Reagent | Final concentration | Volume (µL) |
|---|---|---|
| *DEPC-$H_2O$ | - | 2.30 |
| 2x SensiFAST SYBR® Hi-ROX One-Step | 1x | 5.00 |
| RiboSafe RNase Inhibitor | 1 | 0.20 |
| Reverse transcriptase | 1 | 0.10 |
| Forward primer (µM) | 0.4 µM | 0.20 |
| Reverse primer (µM) | 0.4 µM | 0.20 |

**Tab 10| RT-qPCR program.**

| Step | Temperature °C | Time (mm:ss) | Repetition |
|---|---|---|---|
| Reverse transcription | 45 | 20:00 | **1** |
| Polymerase activation | 95 | 5:00 | **1** |
| Denaturation | 95 | 0:15 | **55** |
| Annealing | 60 | 0:45 | |
| Extension | 72 | 0:45 | |
| Terminal extension | 72 | 10:00 | **1** |
| Melting curve | 95 | 0:15 | **1** |
| | 65 | | |
| | 97 (continuous) | ramp rate (0.11 °C/s) | |

*Thermo Scientific® deionized, diethylpyrocarbonate (DEPC) treated and 0.22 µm membrane-filtered water

### 4.2.3. Statistical analysis

Graph design and statistical analysis were performed in GraphPad Prism® (version 8) and Microsoft Excel® softwares. The statistical significance was determined using two-tailed, unpaired t-test with Welch's correction. The p-values are indicated in graphs as follows: *$p < 0.05$; **$p < 0.01$; ***$p < 0.001$; ****$p < 0.0001$.

### 4.2.4. Flow cytometric analysis

Flow cytometric analysis of tissue culture samples was performed using BD FACSCanto™ II (Becton Dickinson) flow cytometer equipped with 3 lasers emitting at 405, 488, 633 nm, and 8 detectors. Data obtained from all measurements were analyzed using BD FACSDiva™ software version 6 (Becton Dickinson). Ten thousand of living cells were collected from each specimen and analyzed as described in each experiment. The cell viability was assessed based on the size and granulosity, which was analyzed by the distribution of cells on the FSC x SSC dot and contour plots (see figure 10) and/or by using PI staining. When employing PI staining, the apoptotic cell population was distinguished by measuring fluorescence intensity in FL-3 (detecting at 670 nm). The green fluorescence, conferred by the EGFP expression, was detected by flow cytometry in FL-1 (detecting at 515–545 nm). The level of EGFP expression was calculated by multiplying the arithmetic mean of fluorescence intensity of EGFP-positive (EGFP+) cells after subtracting the background (arithmetic mean of fluorescence intensity of the EGFP-negative population in FL-1) with the percentage of EGFP+ cells (Shankaran, 2016; Shankaran *et al.*, 2011). The fluorescence of DsRed2 protein expressed in transfected cells was characterized by flow cytometry analysis in FL-3.

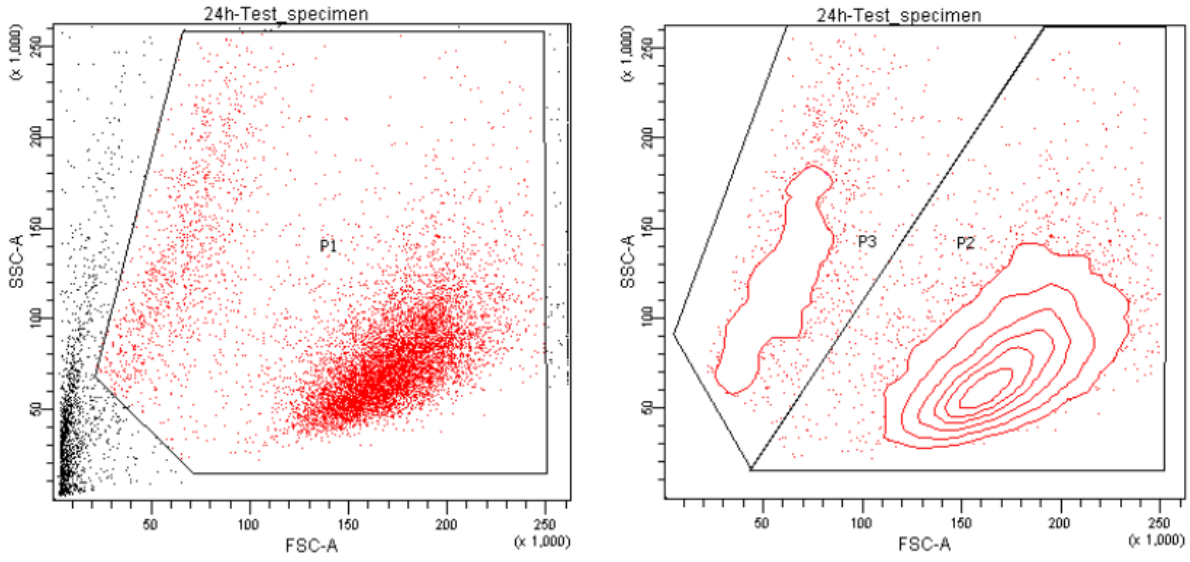


**Figure 10| Representative examples of the flow cytometric analysis.**
FSC x SSC dot plot (left) and contour plot (right) shows the distribution of cell populations based on their size and granulosity. P1 gate shown in dot plot represents a population of cells selected for further analysis. Living and apoptotic cell populations were distinguished by P2 and P3 gating in the contour plot. Events outside of the parent P1 gate were not included in P2 and P3 gates.

# 5. Results

## 5.1. DSF-mediated inhibition of BVRA

The ability of DSF to inhibit BVRA was examined spectrophotometrically in a pre-cleared lysate of A3.01 cells that was treated with 15 µM or 30 µM of DSF. BV conversion into BR in the lysate samples was characterized in time by measuring absorbance at wavelengths 660 nm and 450 nm, respectively, at 37°C for 1 hour using spectrofluorometer. The BVRA activity was determined in a kinetic assay according to previously published protocol (van Dijk *et al.*, 2017) with certain modifications. The inhibition of the enzymatic reaction by DSF was evaluated based on a reduced rate of substrate conversion in DSF treated samples. Time-dependent changes of the absorbance are shown in figure 11. A relative decrease of BVRA activity in DSF-treated samples compared to DMSO-treated control was expressed as the ratio of slopes in percentage calculated for the linear part of trendlines. Representative results of the BVRA activity assay are shown in figure 12. These results indicate that DSF inhibits BVRA activity at both concentrations used and that the treatment decreases the conversion rate of BV in a dose-dependent manner. Additional experiments confirming the inhibitory effect of DSF were performed by Dr. Mělková and Ing. Madleňáková. DSF specificity was also confirmed using a purified BVRA enzyme (Mělková, personal communication).

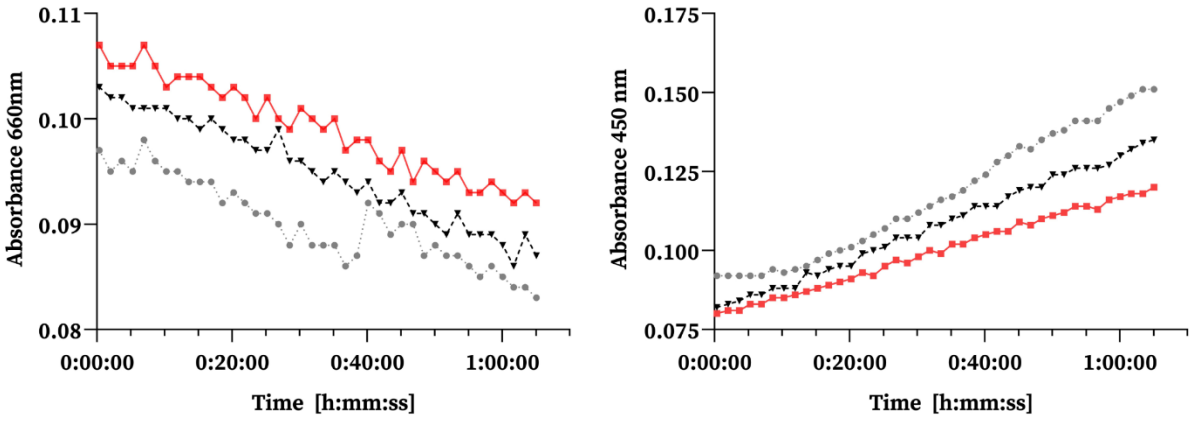


**Figure 11| Spectrophotometric analysis of the enzymatic conversion of BV to BR.**
Graphs illustrate a progressive decrease or increase of absorbances measured at wavelengths 660 nm (BV) and 450 nm (BR), respectively, in A3.01 cellular lysate treated with control DMSO (2000x diluted; control; grey), 15 µM (black), or 30 µM DSF (red). The measurement of absorbance was performed in technical duplicates every 90 seconds for 65 minutes at 37°C. The enzymatic reaction was initiated by the addition of 5 µL of NADH at a final concentration of 100 µM.

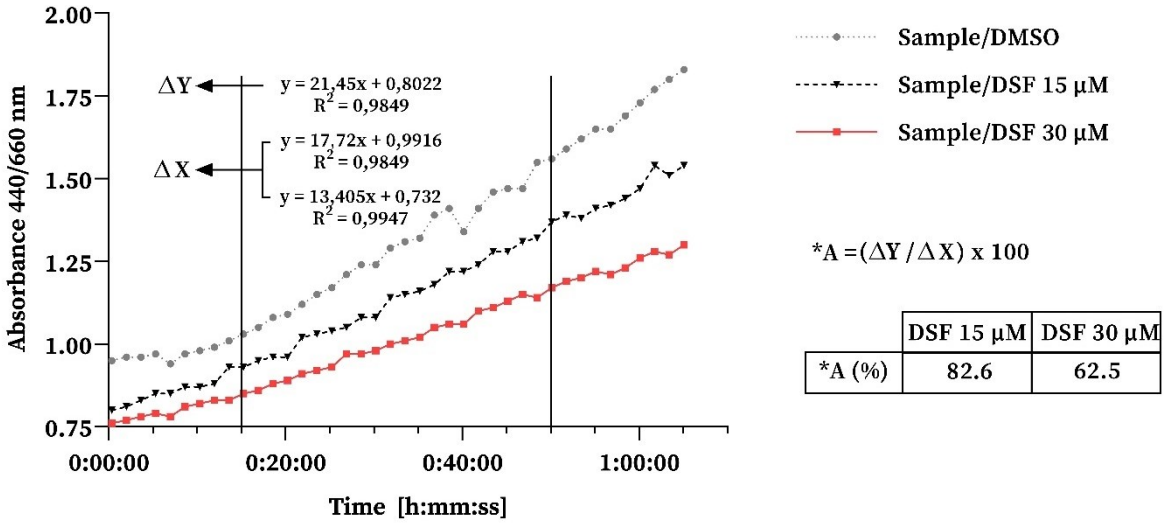


**Figure 12| Representative result of the BVRA activity assay.**
Inhibition of the enzymatic conversion of BV to BR expressed as A440/660 nm ratio. The indicated formulas characterize the trendlines for the linear part of the curves obtained using a linear regression (from top = DMSO; DSF 15 µM; DSF 30 µM). *Residual activity of BVRA in DSF-challenged A3.01 cell lysates was determined according to the provided formula.

## 5.2. Induction of HIV-1 *"mini-virus"* expression by PMA, HA, DSF, and a combined treatment in the A2 cells

The capacity of PMA, HA, and DSF to revert HIV-1 latency was examined in an HIV-1 latency model using A2 clone of Jurkat cells harboring integrated, replication-incompetent HIV-1 *"mini-virus"* (LTR-Tat-IRES-EGFP-LTR)(Jordan, 2001). In this model, latency reversal is characterized by EGFP fluorescence using flow cytometry analysis. The extent of EGFP expression in particular treatment conditions was assessed as described in 4.2.4.

The optimal concentrations of PMA (0.5 ng/mL) and HA (1.25 or 2.5 µL/mL) used in combination with DSF were chosen based on previously published experimental results (Shankaran, 2016; Shankaran *et al.*, 2011) and PMA titration assay performed in this work (Figure 13). Challenging the A2 cells with increasing concentrations of PMA (ranging from 0.025 – 0.5 ng/mL) for 24 hours demonstrated a dose-dependent relationship on the HIV-1 *"mini-virus"* expression. Cell viability correlated inversely with the increase in the EGFP expression. Untreated cells and cells treated with DMSO at 2000x dilution served as controls in these experiments. Since the treatment of cells with 0.5 ng/mL of PMA proved most efficient in terms of the *"mini-virus"* reactivation while causing only a minor decrease in cellular viability, it was selected for further experimental work.

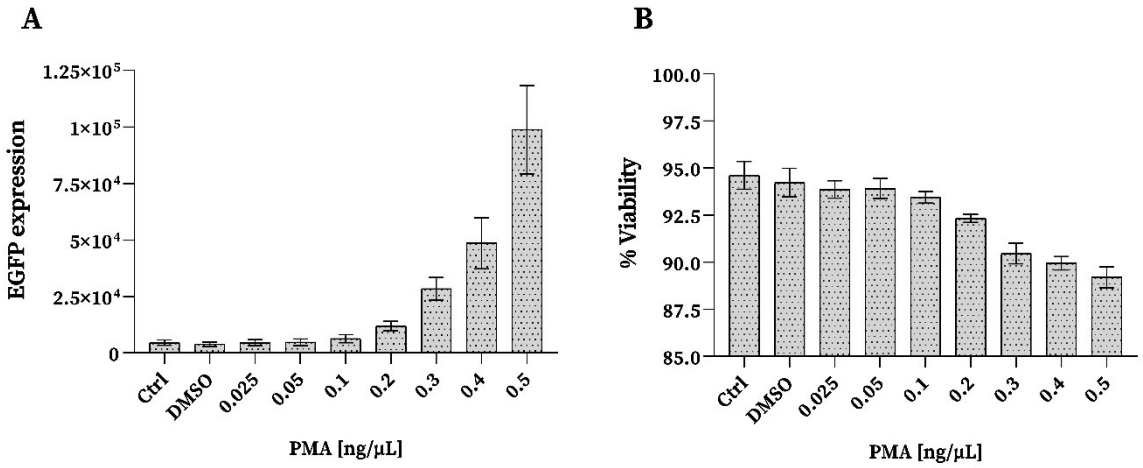


**Figure 13| PMA-mediated stimulation of the HIV-1 *"mini-virus"* expression and the impact on cellular viability.**

A2 cells treated with increasing concentrations of PMA (0.025 – 0.5 ng/mL) for 24h. Graphs show arithmetic mean of 2 independent experiments performed in biological triplicates ± SEM. Ctrl and DMSO bars represent the untreated control and a control-treated with DMSO (2000x diluted in 10% FBS-RPMI), respectively. **(A)** Shows EGFP expression **(B)** Depicts impact of PMA treatment on cellular viability.

The effect of DSF on the *"mini-virus"* reactivation and cellular viability was examined in treatment assays, where A2 cells was treated with increasing concentrations of DSF (1 µM; 2.5 µM; or 5 µM) alone, or in combination with HA (2.5 µL/mL), PMA (0.5 ng/mL), or both (Figure 14). The administration of DSF alone did not lead to any significant increase in EGFP expression in none of the selected DSF concentrations, but the concomitant treatment of cells with DSF and HA, PMA, or both, increased the EGFP expression profoundly. When compared to cells treated PMA or HA alone, the combined use of PMA + DSF or HA + DSF significantly increased the expression of EGFP. The levels of EGFP expression were highest in samples treated with all three compounds, however, when compared to PMA + HA treatment, the addition of DSF did not increase the EGFP expression. The EGFP expression was comparable in HA + DSF and PMA+ DSF treated samples. When comparing the combined treatments to DSF-only treated specimens, combined use of PMA or HA and PMA + HA with DSF led to a 50-90-fold and 250-600-fold increase in the EGFP expression, respectively, depending on the DSF concentration. The cell viability was not substantially decreased in any of the selected DSF concentration.

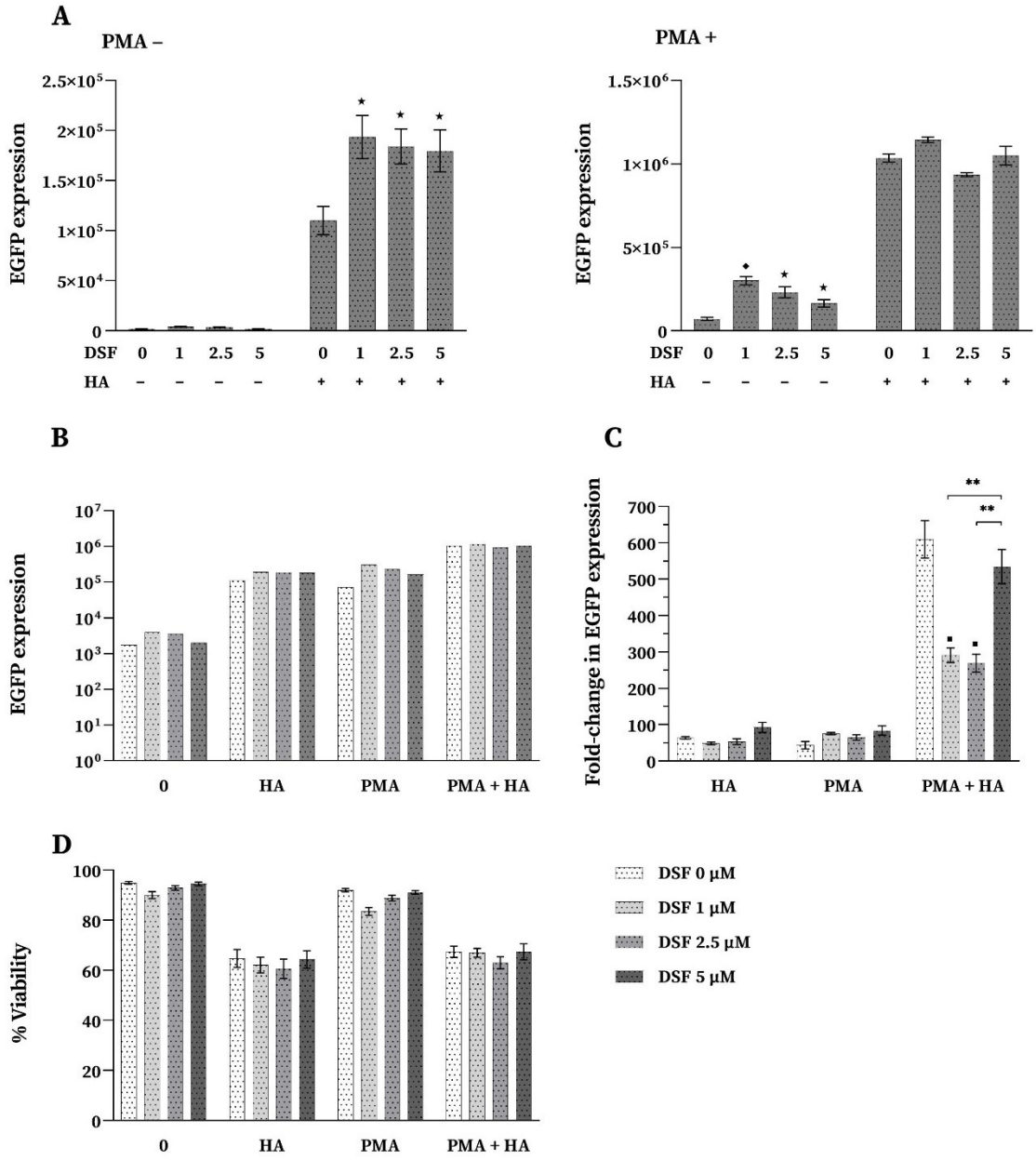


**Figure 14| Effect of the combinational treatment on the HIV-1 *"mini-virus"* reactivation and cell viability.**

A2 cells treated with 0, 1, 2.5, 5 µM DSF; 2.5 µL/mL HA; 0.5 ng/mL PMA; and both HA + PMA for 24h. Graphs represent arithmetic means of 4 independent experiments performed in biological triplicates ± SEM. ◆,■,* denote p-values (*p < 0.05; **p < 0.01; ***p< 0.001) when comparing DSF treatments to mock-treated control (DSF 0 µM) in each treatment conditions. **(A)** shows changes in EGFP expression when administering DSF alone or in combination with HA, PMA, or both. The EGFP expression was significantly increased in PMA + HA treatment when compated to 0, HA, and PMA treatments in all DSF concentrations used (***p < 0.001). When compared to 0 treatment, the EGFP expression was significantly increased in HA and PMA treatments in all DSF concentrations used (**p < 0.01). **(B)** Illustrates changes in EGFP expression on a logarithmic scale. **(C)** Shows relative fold-increase in EGFP expression in samples treated with a combination of compounds compared 0 treatment. **(D)** Depicts % of cell viability upon different treatment challenges. Cellular viability has been significantly decreased when comparing 0 or PMA versus HA or HA+PMA treatments in all DSF concentrations (*p < 0.05).

## 5.3. Role of BVRA and BACH2 overexpression on HIV-1 "*mini-virus*" reactivation

To evaluate the role of BVRA and BACH2 genes in the reactivation of HIV-1, recombinant pcDNA3.1 plasmids encoding cDNA of the corresponding genes or control pcDNA3 plasmid encoding cDNA for LUC, and pDsRed2–N1 plasmids were transfected into the A2 cells. The quality of plasmid vectors containing cDNA of provided genes was assessed based on the restriction analysis, which is shown in figure 15. The impact of BVRA and BACH2 overexpression in transiently and stably transfected cell lines will be discussed in detail in sections 5.3.1 and 5.3.2, respectively.

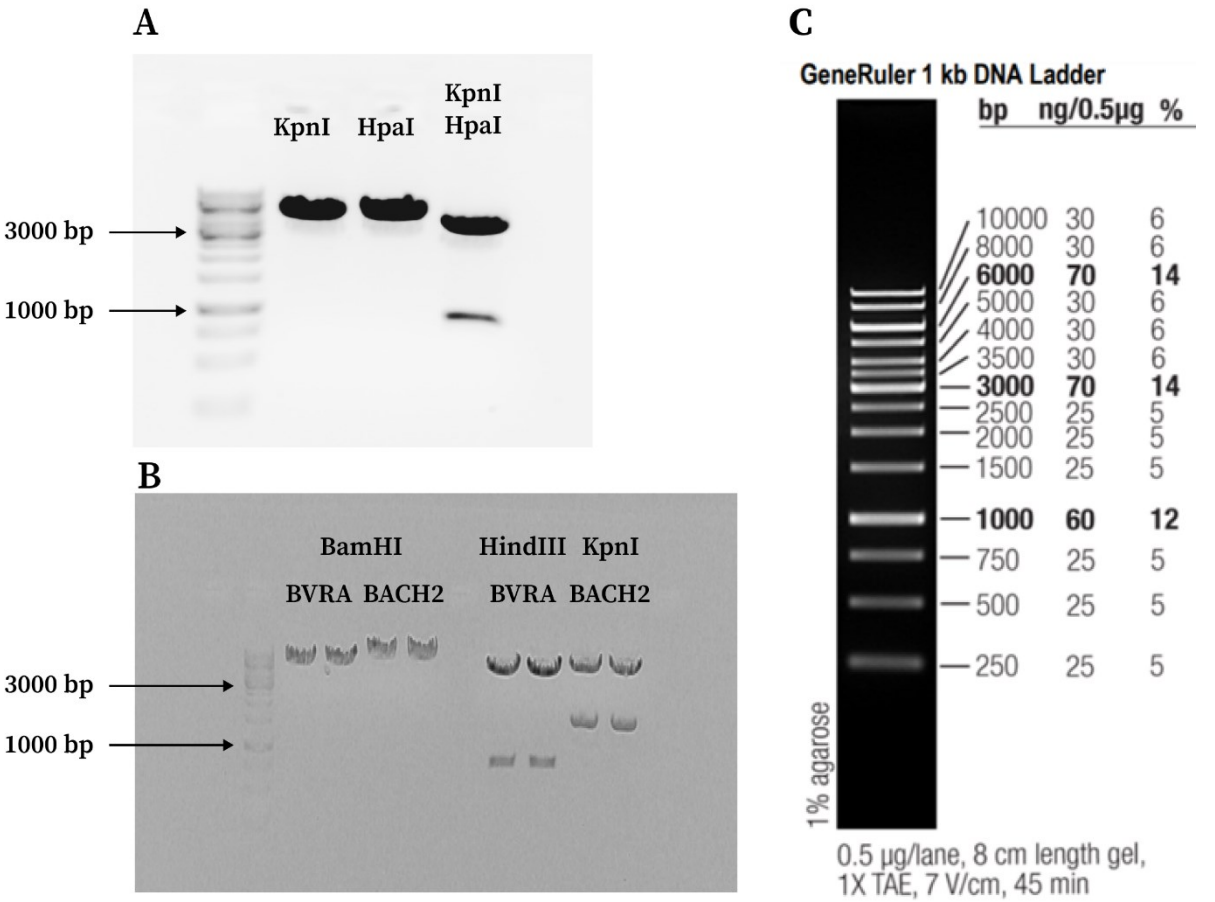


**Figure 15| Restriction digestion and analysis of pDsRed-N1 and pcDNA3.1 plasmids**.
**(A)** Restriction digestion of pDsRed-N1 with restriction enzymes KpnI and HpaI. Expected lenght of restriction products: KpnI, HpaI = 4689 bp (single digest); KpnI + HpaI = 3862 bp + 829 bp (double digest). **(B)** Restriction digestion of pcDNA3.1 plasmids encoding BVRA and BACH2, with BamHI, HindIII, and KpnI. Expected lenght of restriction products: pcDNA3.1-BVRA with BamHI = 6281 bp (single digest) and HindIII= 5565 bp + 716 bp (single digest, 2 products); pcDNA3.1-BACH2 with BamHI= 7716 bp (single digest) and KpnI= 6390 bp +1526 bp (single digest, 2 products). **(C)** Representative picture of a molecular ladder provided by the manufacturer (Fermentas). Schematic plasmid maps are shown in figure 8 (see section 4.1.5) Agarose gels were visualized and captured by AzureBiosystems c600.

### 5.3.1. Reactivation of the HIV-1 *"mini-virus"* in transiently transfected cells treated with HA and PMA

The effect of BVRA and BACH2 overexpression was first evaluated in the transiently transfected A2 cells. To this end, the A2 cells were electroporated with either BVRA, BACH2, or LUC-encoding plasmids and pDsRed2-N1. Twenty four hours after the electroporation, the cells were treated with HA (2.5 µL/mL), PMA (0.5 ng/mL), or both, and the effect of the treatment on transiently transfected cells overexpressing genes of interest was assessed after an additional 24h of incubation (48h after the electroporation). The gating of the transfected population was based on red fluorescence, conferred by the expression of DsRed2 protein. A viable double-positive cell population expressing both DsRed2 and EGFP proteins was selected to examine the phenotype of short-term BVRA and BACH2 overexpression (P2; shown in figure 16). Cells co-transfected with pcDNA3-LUC and pDsRed2-N1 served as transfection control in these experiments.

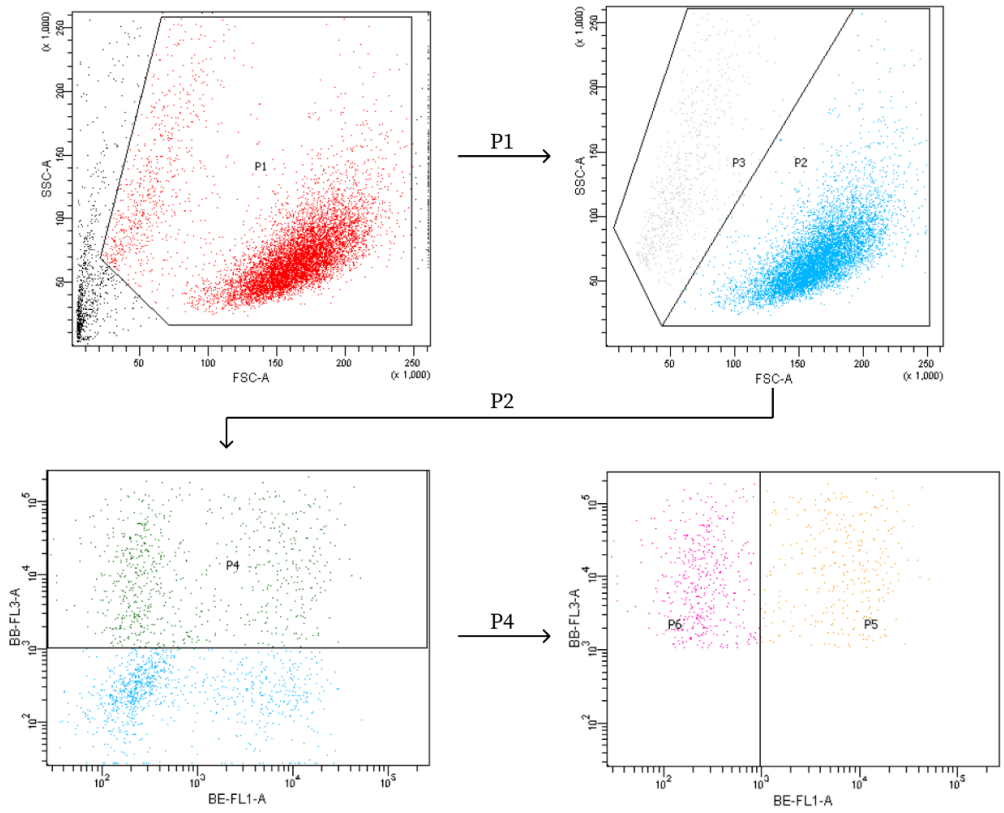


**Figure 16| Representative example of flow cytometry analysis of transiently transfected cells.** FSC x SSC dot plots (top) demonstrate representative gating on live cells (P2). The pDsRed2-N1 positive population (P4) was gated from parent P2 on FL-3 x FL-1 dot plot. The population of double-positive cells (pDsRed2-N1+ EGFP+; P5) and single positive red cells (pDsRed2-N1+; P6) were selected from the parent P4 population and used to assess the phenotype of co-transfected cells. EGFP expression was assessed in P5 (FL-1) after the substraction of fluorescence in P6 as a background.

Gene transfer into the A2 cells was essentially performed by cell electroporation, according to modified Chicaybam *et al.* (2013) protocol, using Amaxa™ nucleofector™ II device and *in-house* prepared electroporation buffer (P3 buffer)(Chicaybam *et al.*, 2013). While these experiments produced preliminary results, the method failed to deliver reproducible results after several attempts for optimization. Nevertheless, tendencies observed in the initial electroporation experiments performed in this work suggested that BVRA and BACH2 overexpression might influence the LTR-driven expression of EGFP and cellular viability under the particular stimulatory settings. The representative result of one of these experiments is shown in figure 17.

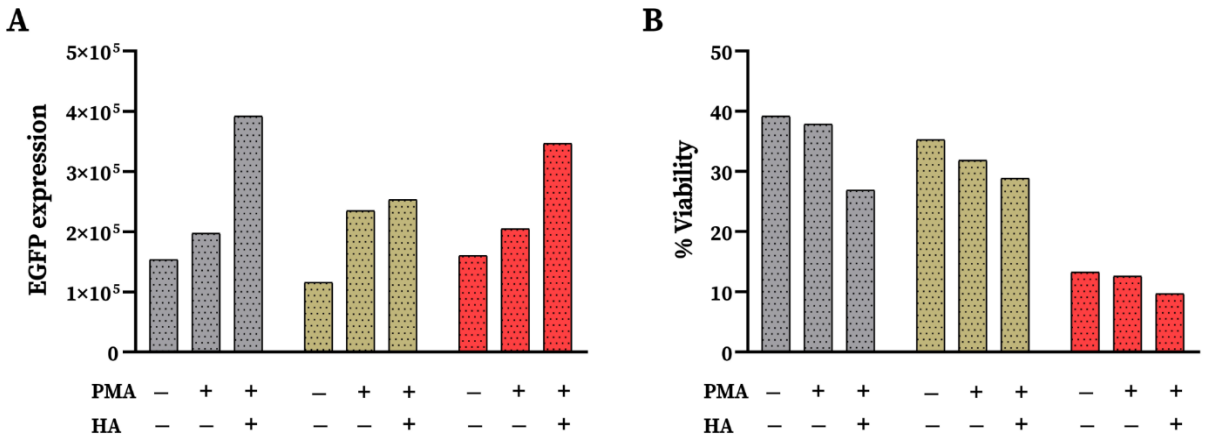


**Figure 17| Representative results of the transfection experiment using *in-house* prepared electroporation buffer.**
A2 cells electroporated simultaneously with either BVRA, BACH2, or LUC-encoding plasmids and pDsRed2-N1 plasmid in P3 buffer using Amaxa™ nucleofector™ II device. Tissue cultures transiently expressing exogenous LUC (grey), BVRA (green), and BACH2 (red) treated with 2.5 µL/mL HA and/or 0.5 ng/mL PMA for 24h. Graphs show the arithmetic means of one experiment performed in technical duplicates. **(A)** Depicts magnitude of EGFP expression. **(B)** Shows the percentage of viable cells.

Next, transfection of the A2 cells was performed with the Amaxa® Cell Line Nucleofector® kit V. Experiments using different amounts of pDsRed2-N1 plasmid were performed to optimize transfection efficiency and cellular viability in electroporated samples. The optimal concentration of plasmid DNA employed in the following experiments was selected with regard to the highest transfection efficiency observed in the optimization assays, which was evaluated based on the level of DsRed2 protein expression and cellular viability. Representative images from one of these experiments captured 24 hours after the transfection on Leice DMi8 (Leica microsystems) are shown in figure 18.

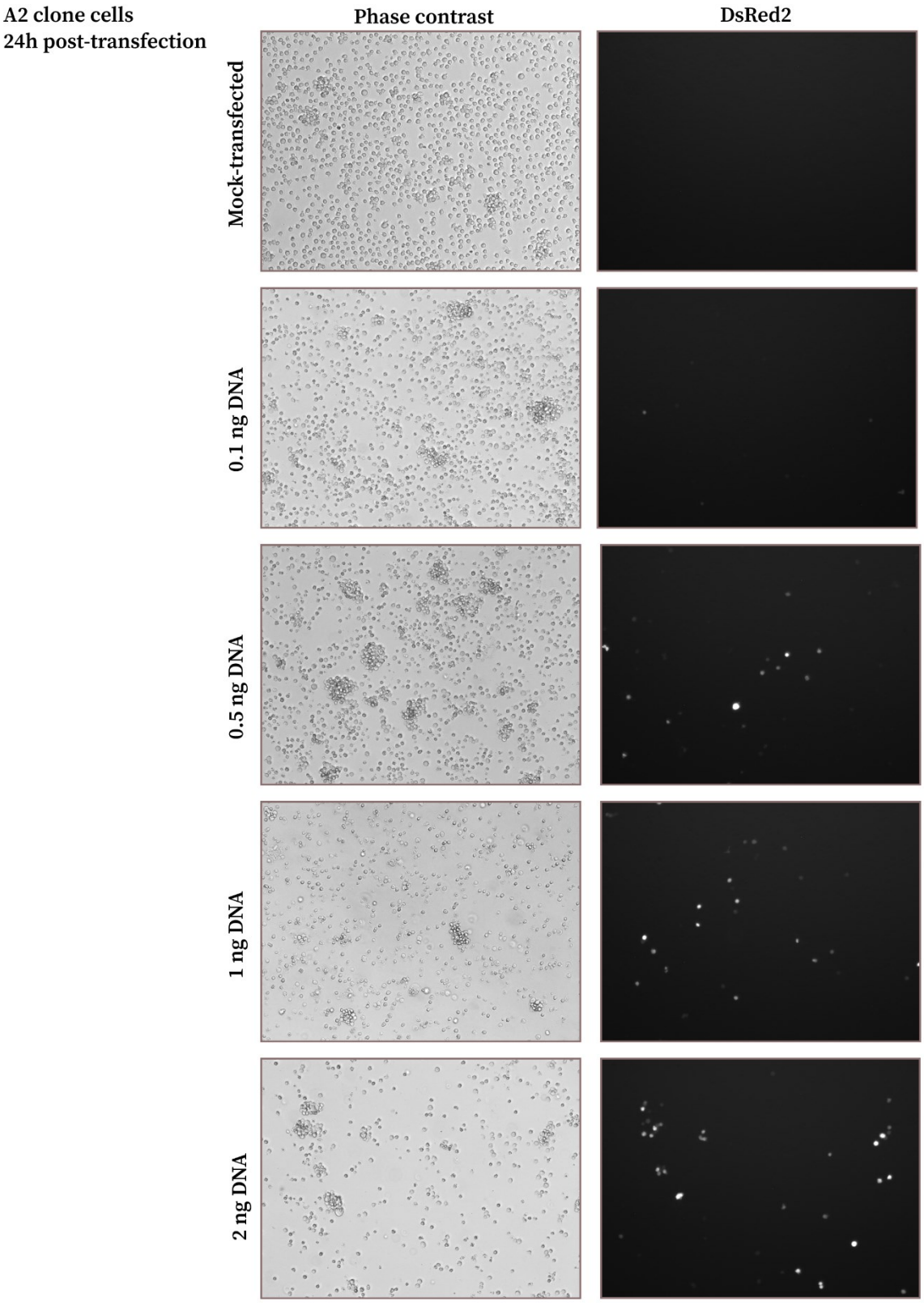


**Figure 18| Captured images of the A2 cells transfected with pDsRed2-N1 DNA.**
Pictures represent images of the A2 cell cells electroporated with pDsRed2-N1 plasmid using Amaxa® Cell Line Nucleofector® kit V captured 24h after the transfection. Phase contrast (left) and DsRed2 (right). From top: mock-transfected cells, pDsRed2-N1 transfected cells (0.1 ng; 0.5 ng; 1 ng; 2 ng). Pictures were captured on fluorescent microscope Leica DMi8. Original magnification 40x.

Employing the same approach but a commercial electroporation buffer, Amaxa® Cell Line Nucleofector® kit V, transfection of the A2 cells was more reproducible. Cell cytotoxicity and transfection efficiency followed a common trend among individual experiments, which allowed for a more in-depth analysis of effects of the studied treatment. Similarly as before, 24h after the electroporation, the cells were treated with HA (1.25 µL/mL) or HA (1.25 µL/mL) + PMA (0.5 ng/ µL), cultured for additional 24 hours, and analyzed by flow cytometry. The results of 4 experiments (see figure 19) shows that transient expression of BVRA and BACH2 mildly decreased the expression of EGFP in samples treated with HA or PMA + HA compared to control cells expressing LUC. While this particular trend was observed in each of the performed experiments, the decrease in EGFP expression was statistically insignificant, probably due to large variability of the absolute values. On the other hand, when evaluating fold-change in EGFP expression in cells simultaneously treated with PMA + HA, the highest increase was observed in specimens transfected with the plasmid encoding cDNA for BVRA.

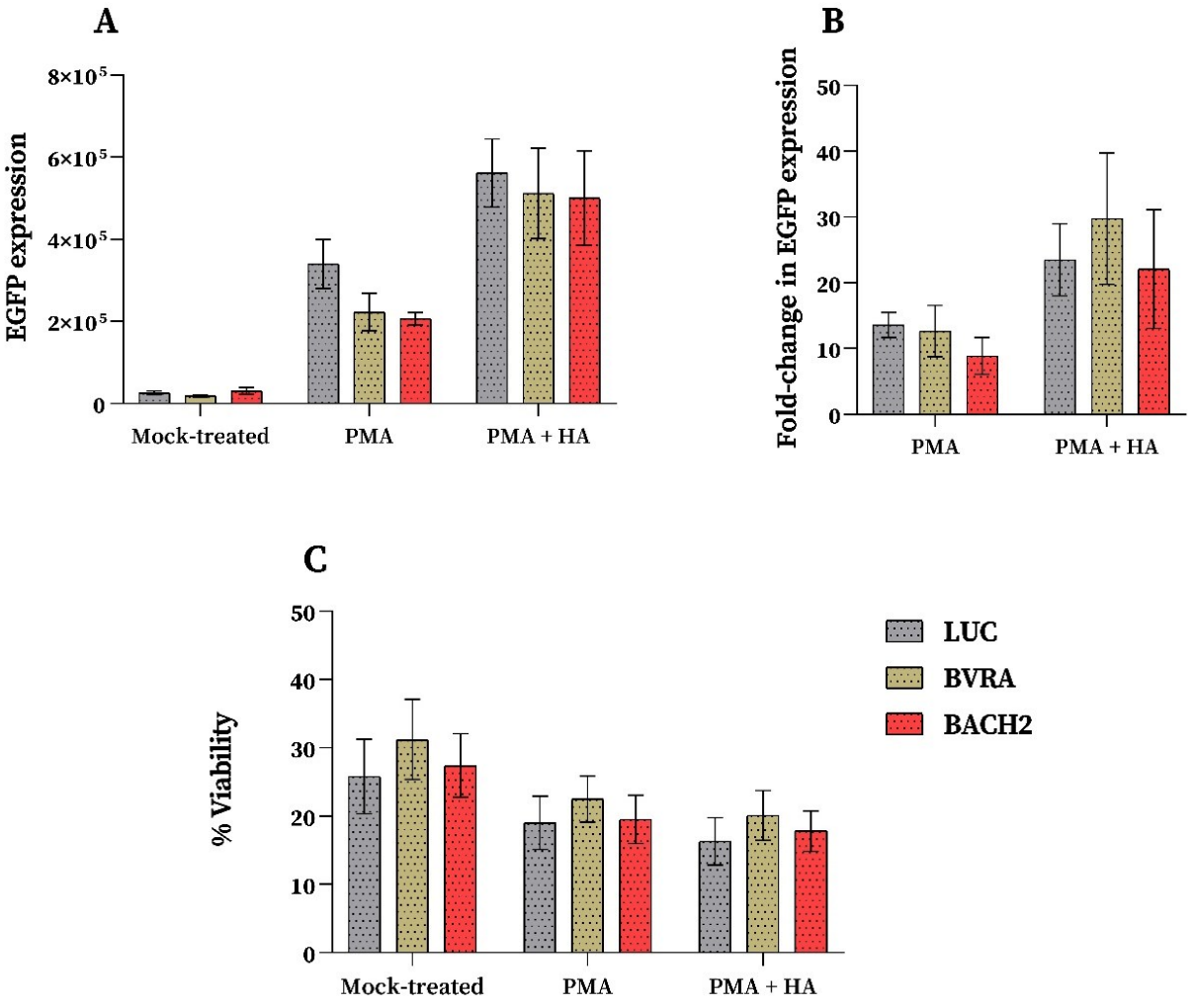

**Figure 19| Reactivation of the HIV-1 *"mini-virus"* and cell viability upon HA and PMA stimulation in transiently transfected cells**
A2 cells electroporated simultaneously with either BVRA, BACH, or LUC plasmids and pDsRed2-N1 plasmid. Transfected tissue culture samples overexpressing LUC (grey), BVRA (green), BACH2 (red), and DsRed2 treated with 1,25 µL/mL HA and/or 0.5 ng/mL PMA for 24h. Graphs show the arithmetic means of 4 individual experiments performed in technical duplicates ± SEM. **(A)** Shows EGFP expression in double-positive cell populations under different stimulatory conditions. The level of EGFP expression was significantly increased when comparing PMA and PMA + HA treated cells to mock-treated ones (*$p < 0.05$). Variations in the EGFP expression among transfected groups in particular treatment conditions were not significant. **(B)** Shows fold-change in EGFP expression in treated specimens compared to basal EGFP expression in mock-treated cells. **(C)** Shows % of viable cells. Variations of cell viability have been non-significant both in between particular treatments in each transfected group and among them.

### 5.3.2. Effects of HA, PMA, and DSF treatment on the HIV-1 *"mini-virus"* reactivation in stably transfected cells

The effect of combined treatments and BVRA or BACH2 overexpression was finally investigated in stably transfected cells derived from parental A2 clone of Jurkat cell line. Stably transfected cell lines overexpressing the individual genes were prepared by cell electroporation using Amaxa® Cell Line Nucleofector® kit V and a subsequent selection of positive cell population with antibiotic G418. The selective outgrowth of the positive cell populations has been conferred by the expression of the antibiotic resistance gene (NeoR) from the backbone of pcDNA3 and pcDNA3.1 plasmids.

The appropriate G418 concentration for positive screening of transfectants was determined in antibiotic kill curve experiments, where the A2 cells were treated with increasing concentrations of G418, ranging from 0.2 mg/mL to 2.8 mg/mL. These experiments have demonstrated that G418 at concentrations of 1.6 mg/ml and higher induced a progressive death of the cells within 11 days. Results of the antibiotic kill curve assays are shown in figure 20.

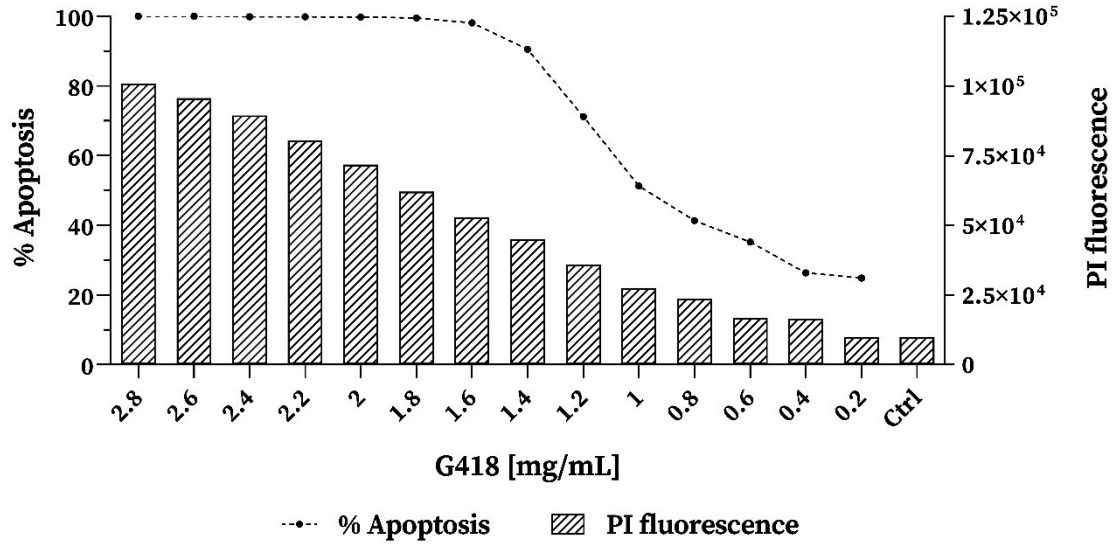


**Figure 20| Results of the antibiotic kill curve assays.**
A2 cells treated for 11 days with 14 increasing concentrations of G418 (0.2 – 2.8 mg/mL). The graph shows the results of 2 independent experiments performed in biological triplicates. The dotted line depicts % of apoptotic cells (P3; FSC x SSC dot plot). The right Y-axis and stripped bars represent calculated PI fluorescence measured in FL-3 in an apoptotic cell population upon PI staining (1 µg/µL).

Cells transfected with pcDNA3 or pcDNA3.1 plasmids were therefore treated and selected with 1.6 mg/mL of G418. Additionally, the cells were treated also with 0.05 M of BME to reduce a redox stress and to promote the growth. After the selection, the cells were cultured at 1 mg/mL of G418 and 0.05 M of BME. Selected tissue cultures reached an optimal handling density of $0.5 \cdot 10^6$ cells/mL in approximately 30 days after the electroporation. Consequently, the growth rate of the selected cell lines was determined (shown in figure 21). Results of 2 independent experiments performed in triplicates demonstrated that the growth rates of the A2, LUC, and BVRA cells were comparable. On the other hand, the growth of BACH2 cells was mildly decreased compared to A2 clone of Jurkat cells.

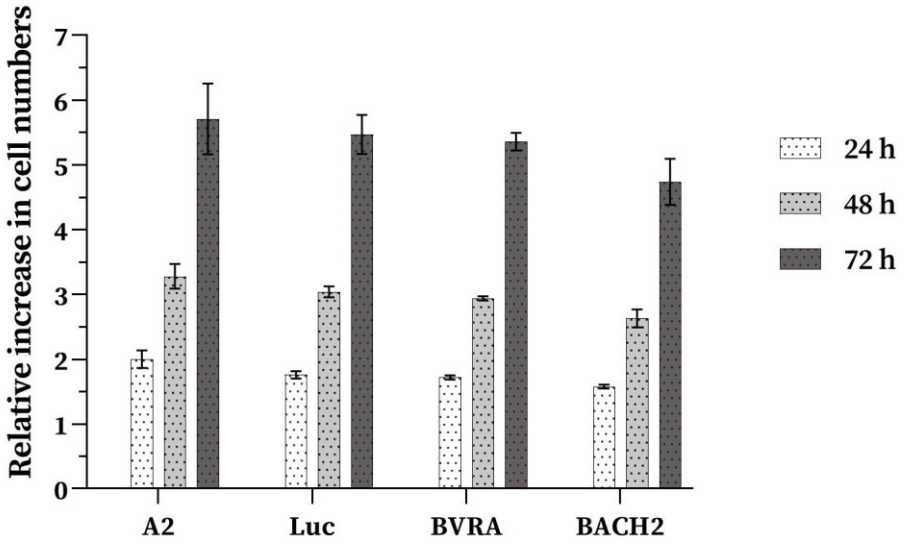


**Figure 21| Growth curve of Jurkat A2 clone and derived cell lines**
A2, LUC, BVRA, and BACH2 cells cultured for 3 days in 10% FBS-RPMI. The number of living cells was determined by flow cytometry. The quantity of living cells in tissue culture samples was measured at the time of seeding and 24h (white), 48h (light grey), and 72h (dark grey) of culture. The cellular growth rate was evaluated in 2 independent experiments performed in biological triplicates. The graph shows a relative fold increase in cell numbers at each time point compared to the number of cells at the time of seeding ± SEM (n=6).

The insertion of transgenes in the genome and their copy number in each stably transfected cell line was characterized using qPCR with primers specific for inserted cDNA and for GAPDH as a reference endogenous gene. The amplification of exogenous DNA products was performed in lysates of the individual selected cell lines and of the parental Jurkat clone A2. The Cp values and melting peaks of qPCR products are shown in figure 22. Unspecific qPCR products observed in the parental A2 cells and in $H_2O$ controls were distinguished from the specific products by melting curve analysis. Given the results of qPCR experiments, it was rationalized that exogenous sequences encoding cDNAs for BVRA, BACH2, and LUC were present specifically in the samples collected from corresponding transfected tissue cultures and that plasmid DNA was successfully integrated into the genomes. Cp values for BACH2 and LUC products were similar to the Cp for the reference endogene GAPDH. In contrast, Cp values for the BVRA were approximately 10 cycles higher than GAPDH. This finding was observed twice in 2 distinct experiments. Thus, the results of qPCR experiments suggest that LUC and BACH2 transgenes were present in a similar copy number than GAPDH reference, while the BVRA transgene was represented in lower copy number per cell.

A

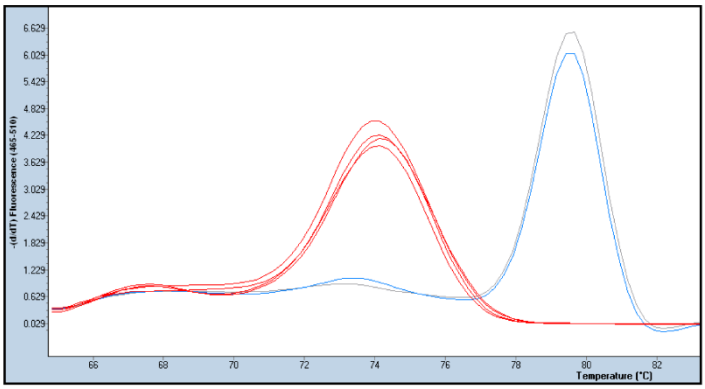


| | Target | | | |
|---|---|---|---|---|
| | Exogenous cDNA | | GAPDH | |
| **LUC** | 24.79 | 27.72 | 27.61 | 25.93 |
| **A2** | 37.87 | 36.63 | 26.27 | 26.34 |
| **$H_20$** | 36.79 | 35.42 | 37.56 | 40.34 |

B

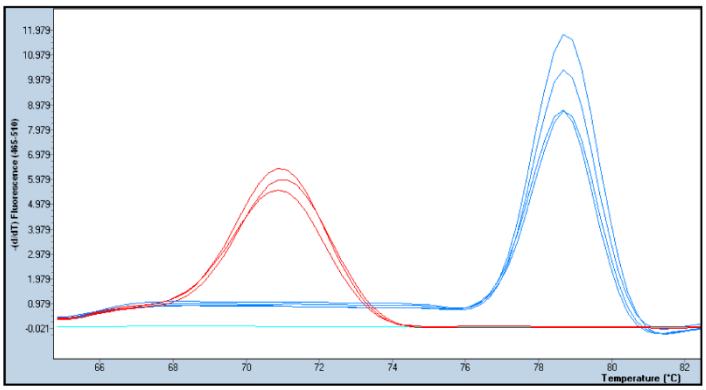


| | Target | | | |
|---|---|---|---|---|
| | Exogenous cDNA | | GAPDH | |
| **BVRA** | 38.28 | 38.66 | 28.25 | 26.37 |
| **A2** | ND | 42.92 | 25.31 | 25.71 |
| **$H_20$** | 41.34 | 42.91 | 37.56 | ND |
| **pDNA*** | 6.00 | 8.99 | | |

C

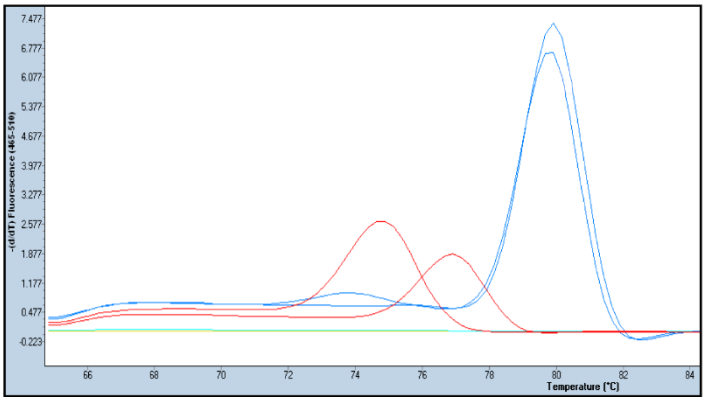


| | Target | | | |
|---|---|---|---|---|
| | Exogenous cDNA | | GAPDH | |
| **BACH2** | 28.23 | 31.32 | 28.2 | 27.84 |
| **A2** | ND | >50 | 26.27 | 26.34 |
| **$H_20$** | ND | >50 | 37.56 | 40.34 |

**Figure 22| Schematic illustration and results of qPCR experiments**
Graphs show melting curves of the selected products of qPCR performed with cell lysate of stably transfected cells LUC (A), BVRA (B), BACH2 (C), and parental A2 cells. Adjacent tables show the resulting Cp values of all detected products, including products amplified with GAPDH-specific set of primers in samples from each transfected cell line and from Jurkat clone A2 cell line. **ND** ~ No product. The qPCR experiments were performed in technical duplicates. Cp values in blue ~ specific products, in red ~ unspecific products. Melting curves in blue ~ specific products, in red ~ unspecific products detected in A2 cells and in $H_2O$ negative controls. Melting curve analysis of BVRA samples also include melting curves of positive plasmid DNA controls (10x and 100x diluted; original concentration= 2.738 µg/mL)

Next, the expression of transgenes was characterized by RT-qPCR in DNAse-treated total RNA purified from stably transfected cell lines. Owing to the design of primers, the selective reverse transcription of messenger RNAs (mRNA) of interest in DNA-free samples was performed with the exogene-specific primers that were previously used for the detection of exogenous cDNA sequences. The levels of exogenous BVRA, BACH2, and LUC mRNA are expressed relative to the expression of the *house-keeping* GAPDH. The Cp values of RT-qPCR products and melting curves are shown in figure 23. The RT-qPCR-based detection of selected mRNAs was performed in technical duplicates. Results of RT-qPCR experiments show that in selected cell lines, LUC and BACH2 mRNA levels were approximately 1,000 times lower than GAPDH, while BVRA mRNA levels were approximately 1,000,000 times lower. Based on the RT-qPCR results it was concluded that stably transfected cells were actively expressing the transgene-encoded mRNAs.

A

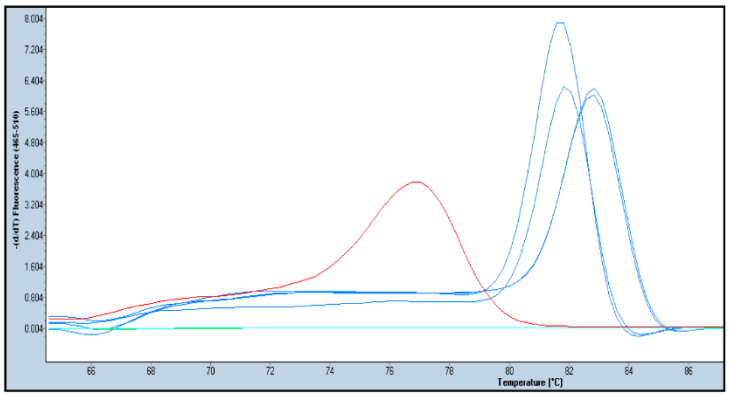


| | Target | | | |
|---|---|---|---|---|
| | Exogenous cDNA | | GAPDH | |
| **LUC** | **31.34** | **29.52** | **21.58** | **20.75** |
| **A2** | **43.95** | ND | 17.57 | 17.25 |
| **$H_20$** | ND | | ND | |

B

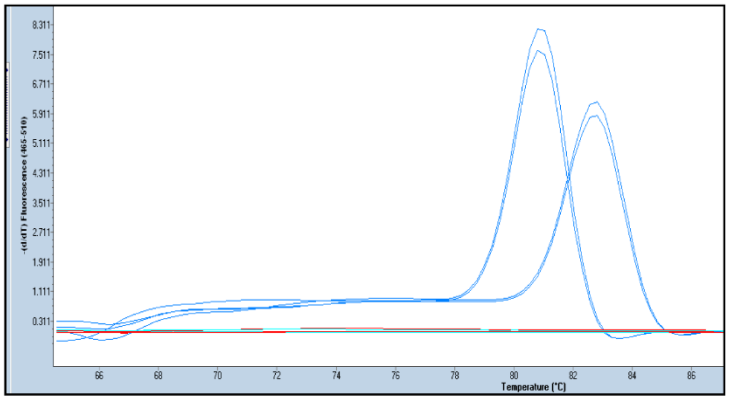


| | Target | | | |
|---|---|---|---|---|
| | Exogenous cDNA | | GAPDH | |
| **BVRA** | **33.91** | **32.08** | **15.96** | **16.10** |
| **A2** | ND | ND | 16.84 | 16.89 |
| **$H_20$** | ND | | ND | |

C

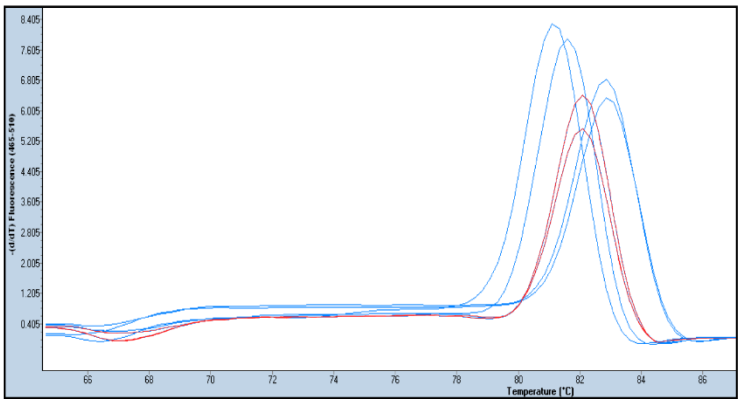


| | Target | | | |
|---|---|---|---|---|
| | Exogenous cDNA | | GAPDH | |
| **BACH2** | **25.93** | **26.78** | **16.54** | **16.33** |
| **A2** | **35.06** | **33.65** | 15.61 | 15.96 |
| **$H_20$** | ND | | ND | |

**Figure 23| Schematic illustration of RT-qPCR experiments**
Graphs show melting curves of selected products of RT-qPCR experiments in total RNA isolated from stably transfected LUC (A), BVRA (B), BACH2 (C), and parental A2 cells. The adjacent tables indicate calculated Cp values for each reaction product, including products amplified with GAPDH-specific set of primers in samples from each transfected cell line and from Jurkat clone A2 cell line. RT-qPCR experiments have been performed in technical duplicates. **ND** ~ No product.. Cp values in blue ~ specific products, in red ~ unspecific products. Melting curves in blue ~ specific products, in red ~ unspecific targets detected in A2 cells and in $H_2O$ negative controls.

Finally, the effect of the combined treatment with PMA (0.5 ng/m), HA (1.25 µL/mL), and DSF (1 µM) on *"mini-virus"* reactivation was investigated in stably transfected cells derived from the parental Jurkat clone A2, in which the presence and expression of selected transgenes were previously verified by qPCR and RT-qPCR, respectively. The EGFP expression in LUC, BVRA, BACH2, and in the A2 cells was characterized in viable EGFP+ population after 24 hours of treatment. The results of 5 independent experiments are shown in figure 24. The basal LTR-driven EGFP expression was increased in all transfected cell lines, but the highest increase in basal EGFP expression was observed in the BACH2 cell line. The expression of EGFP in PMA-stimulated cells was significantly decreased in BVRA cells when compared to control LUC cells. The *"mini-virus"* reactivation was comparable in LUC and BACH2 tissue culture samples in these treatment conditions. The highest increase in stimulated EGPF expression was observed in BACH2 tissue culture samples treated with the combination of PMA, HA, and DSF. In contrast, cells expressing BVRA revealed a reduced EGFP expression under these stimulatory settings. Results of these experiments imply that a stable expression of BACH2 upregulates while BVRA downregulates the *"mini-virus"* expression in cells stimulated with combination of PMA, HA, and DSF.

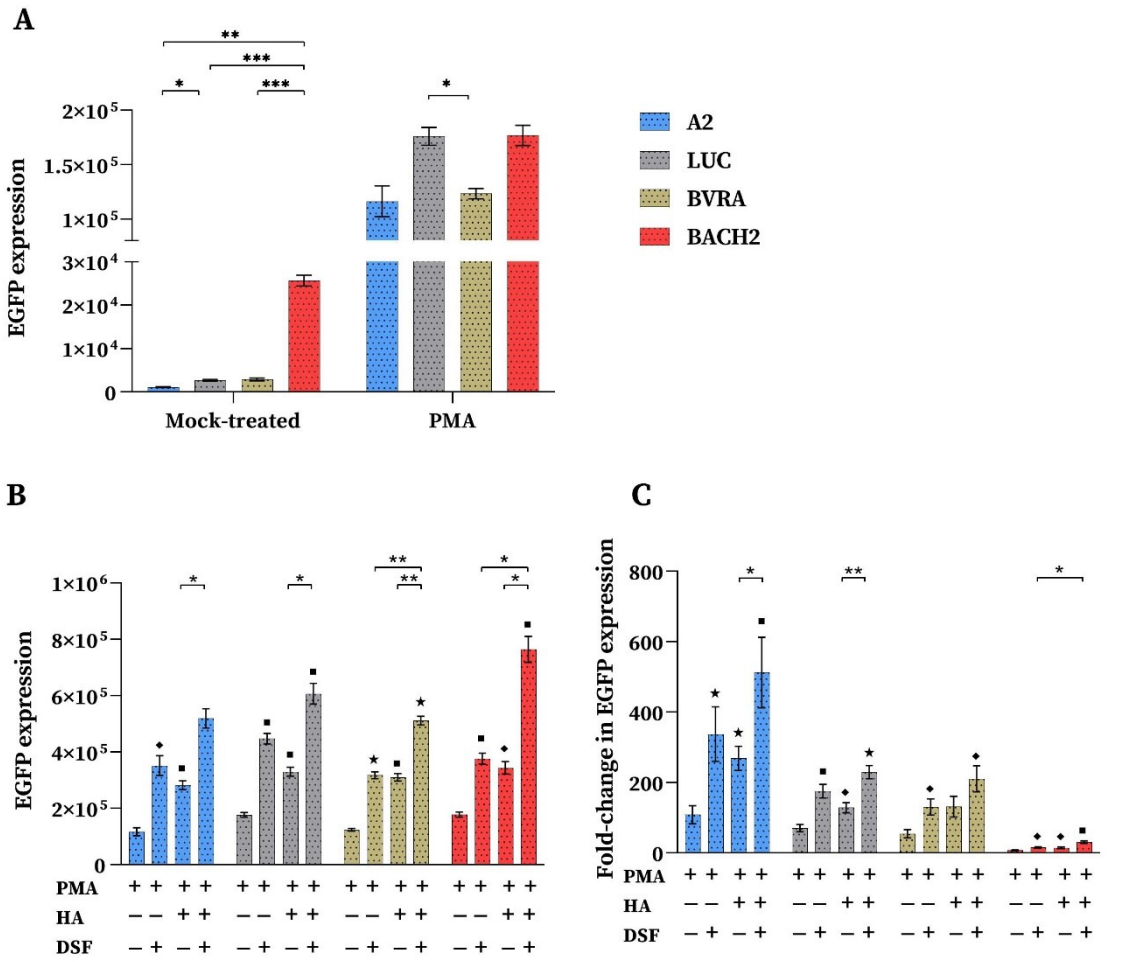


**Figure 24| Effect of the combined treatment with PMA, HA, and DSF on HIV-1 LTR-driven expression of EGFP in stably transfected cell lines.**
The parental Jurkat clone A2 (blue) and stably transfected cell lines LUC (grey), BVRA (green), and BACH2 (red) treated with PMA (0.5 ng/mL), HA (1.25 µL/mL), and DSF (1 µM). Graphs represent arithmetic means of 5 independent experiments performed in biological duplicates ± SEM (4 in the case of A2 cells). (**A)** Shows basal and stimulated EGFP expression in mock-treated and PMA-treated cells, respectively. The PMA treatment has significantly increased the EGFP expression in all treatment conditions (**p<0.01). **(B)** Depicts levels of EGFP expression in samples treated with PMA or with a combination of agents in each cell line. The expression of EGFP has been significantly decreased in BVRA cells in PMA and PMA + DSF treatments when compared to LUC cells (p*<0.05). **(C)** Shows relative fold-changes in EGFP expression when comparing basal vs stimulated expression of EGFP in mock-treated and treated cells, respectively. The fold-change in the EGFP expression has been significantly decreased in BACH2 cells in all treatment conditions when compared to A2 (*p< 0.05), LUC (**p< 0.01), or BVRA (*p< 0.05) cells. The EGFP expression fold-change was also significantly decreased in PMA + HA treated samples when comparing LUC and BVRA to A2 cells (*p< 0.05). ◆,■,* denote p-values (*p < 0.05; **p< 0.01; and ***p< 0.001) when comparing EGFP expression or EGFP fold-change of PMA-treated specimens to samples treated with a combination of agents in each cell line.

# 6. Discussion

Latency reversal followed by a subsequent clearance of the reservoir cells, or "shock and kill" strategy, today represents one of the actively approaches towards HIV-1 sterilizing cure. Previous LRA studies were, however, largely conducted in the *in vitro* and *ex* vivo platforms (Wei *et al.*, 2014), and their investigation in clinical settings faces several issues, such as safety and tolerability profile, transmission risk concerns, and availability of subjects. Additionally, to successfully achieve the objective of „shock and kill" strategy, the effects of LRA should be more thoroughly studied not only in common target cells, but also in cellular reservoirs that are usually neglected, such as HIV-1 permissive non-lymphoid cells (Kula *et al.*, 2019). Latest proof-of-concept clinical trials on cART-adherent patients treated with single LRA have independently reported a successful reactivation of latent HIV-1 characterized by an increase in cell-associated unspliced (CA-US) HIV-1 RNA in CD4+ T-cells and in some cases also in blood plasma. The LRA-induced reactivation of the virus in treated HIV+ patients was achieved upon administration of HDACi, like romidepsin (Søgaard *et al.*, 2015), vorinostat (Archin *et al.*, 2012), panobinostat (Rasmussen *et al.*, 2014), and DSF (Elliott *et al.*, 2015; Spivak *et al.*, 2014). On the other hand, a pilot clinical study assessing the safety of PKC inducer bryostatin-1, administered in two-single doses at 10 or 20 mg/m$^2$, had no effect on latent HIV-1 transcription. However, its administration in higher therapeutic doses or in combination with other drugs might still induce latency reversal (Gutiérrez *et al.*, 2016). While all of these trials failed to deliver a desirable decrease in numbers of HIV-1 specific T-cells, it should be noted that they were performed in small patient cohorts (5-40 subjects tested), LRAs were generally well-tolerated, and their effect on the HIV-1 reservoir size in patients was evaluated only during short-term administrations.

The limited potential of described LRA to reactivate and purge reservoir cells *in vivo* underlines the need for development of more efficient latency-reversing interventions with a broader spectrum of effect. Historically, the combined use of mechanistically distinct LRAs was mostly analyzed in the *in vitro* and *ex vivo* systems (Laird *et al.*, 2015) or in humanized BLT mice (Marsden *et al.*, 2017). A synergy between particular classes of LRAs in HIV+ patients thus remains to be characterized in future clinical trials. Current literature on the "shock and kill" strategy also reveals that this sterilizing HIV-1 cure approach is further complicated by the heterogeneity of cellular reservoirs (Kula *et al.*, 2019). Recent studies on HIV-1 reactivation patterns among different CD4+ $T_M$ cell subsets (Pardons *et al.*, 2019) and in between resting CD4+ T-cells isolated from different anatomical compartments (Telwatte *et*

*al.*, 2020) shows that the extent of latent provirus reactivation varies with regard to the infected cell type and a class of LRA administered. However, the mechanisms underlying these observations are not fully understood. Additionally, novel curative strategies might include combinations of various other approaches, such as gene therapy and/or gene editing, stem cell transplantation or the "block and lock" strategy (Ahlenstiel* *et al.*, 2020).

Previous studies of Dr. Melkova's research group revealed that HA, a human blood derived preparation of hemine approved for clinical use, has a unique set of anti-HIV-1 properties, acting repressively on acute HIV-1 infection and stimulatory on the provirus reactivation in latently infected cells. The HIV-1 latency reversal by HA was demonstrated in HIV-1 latency model cell lines, including human T-cell lines ACH-2, H12, and A2 clones of Jurkat, as well as *ex vivo* in PBMCs isolated from treated HIV+ patients (Shankaran *et al.*, 2011, 2017). In addition, the latency-reversing capacity of HA is currently being investigated in a pilot clinal study (Melkova *et al.*, unpublished data). In the experimental systems, HA acted alone or in synergy with PMA, TNFα, or other agents to reactivate latent HIV-1 provirus (Shankaran *et al.*, 2011). Since the degradation of heme leads to a release of pro-oxidative $Fe^{2+}$ (Ryter*, 2021), and the TNFα (Dong *et al.*, 2000; Westendorp *et al.*, 1995) and oxidative stress were shown to activate HIV-1 LTR via redox-sensitive NF-κB axis (Pyo *et al.*, 2008), the effect of HA treatment on HIV-1 reactivation was also investigated in the presence of redox modulators, iron chelators, and heme degradation products, such as N-acetyl cysteine (NAC) or ascorbate, Desferrioxamine (DFO), and bilirubin, $CO_2$, and $Fe^{2+}$, respectively. When NAC or DFO were employed in combination with HA and/or PMA, the stimulatory effects on HIV-1 reactivation were inhibited. Based on these experiments it has been suggested that the latency-reversing ability of HA may be closely related to free-iron turnover and/or oxidative stress (Shankaran *et al.*, 2011, 2017). In light of these findings, HA was proposed as a novel candidate LRA.

The earlier hopes for broad latency-reversing capacity of DSF raised by the successful reactivation of HIV-1 in the Bcl-2-immortalized primary CD4+ T-cell model of latent HIV-1 infection (Xing *et al.*, 2011) and several monocyte-derived cell lines, were diminished when DSF failed to reactivate HIV-1 in other models of latent HIV-1 infection of lymphoid origin (Doyon *et al.*, 2013; Kula *et al.*, 2019). The disappointment from newly described LRA that was already approved for use in humans to treat alcohol dependence, was further entrenched by a pilot clinical study, where administration of DSF to HIV+ patients on suppressive cART for 14 days at a clinically established concentration (500 mg/mL) failed to significantly reduce latent reservoir size, although a transient increase in HIV-1 expression was observed (Spivak

*et al.*, 2014). A more recent clinical study on DSF, using the same or higher doses of DSF (500, 1000, and 2000 mg/mL) for 3 consecutive days, revealed that a higher exposure to DSF was accompanied by a more robust increase in CA-US HIV-1 RNA in CD4+ T-cells. Levels of plasma HIV-1 RNA were found increased exclusively in the 2000 mg/mL dosing group, 31 days after the DSF administration (Elliott *et al.*, 2015; Lee *et al.*, 2019). *Ex vivo* research on patient-derived PBMCs also indicates that DSF can potentiate the latent HIV-1 expression in resting CD4+ T-cells in combination with PKC inducer Bryostatin-1 (Laird *et al.*, 2015). Thus, it is possible that DSF may exert stronger latency-reversing effects in combination with other mechanistically distinct LRAs, namely with PCK inducers. The authors, investigating the mode of action of DSF, have provided the *in vitro* evidence, suggesting that DSF-mediated latency reversal occurs via an NF-κB-dependent mechanism (Doyon *et al.*, 2013). Additionally, DSF was recently characterized as a novel inhibitor of BVRA (van Dijk *et al.*, 2017). Since the oxidation of BR into BV by free radicals and a subsequent recycling of BV into BR by the action of BVRA represents an essential antioxidant mechanism regulating cellular redox homeostasis (Jansen *et al.*, 2010; Sedlak *et al.*, 2009), these findings together suggest that the effect of DSF on latent HIV-1 reactivation may be tightly associated with the redox state of the infected cell. The inhibitory activity of DSF was also addressed in this work. Based on the spectrofotometrical analysis of BVRA substrate and catabolite in A3.01 cell lysate treated with different doses of DSF, it has been concluded that the enzymatic activity of BVRA is, indeed, inhibited in the presence of DSF. The determination of BVRA activity in the presence of DSF was further confirmed in the experiments performed by Dr. Melkova, both in the same experimental settings and in assays involving a purified BVRA enzyme (data not shown).

As a logical consequence of the previously described studies and the earlier research of Dr. Melkova's group, this work has been set to examine the latency-reversing capacity of HA, DSF, and their combination in unstimulated and PMA-stimulated clone A2 of Jurkat cells. Unlike HA, DSF alone did not revert latency of the HIV-1 "*mini-virus"* in the unstimulated cells. The lack of DSF-mediated reactivation of latent HIV-1 in Jurkat cell lines was previously addressed by Doyon and colleagues, who have hypothesized that this is due to the absence of the endogenous PTEN expression in Jurkat cells (Doyon *et al.*, 2013). Similarly, DSF alone did not induce reactivation of latent HIV-1 in untreated ACH-2 cells (Melkova and Shankaran, unpublished data). In this work, consistent with previously published results (Shankaran *et al.*, 2011), HA increased the expression of the "*mini-virus*" in the A2 cells alone and in combination with PMA. Of note, DSF synergized with both HA and PMA and stimulated reactivation of the "*mini-virus"*. No increase in LTR-driven expression of EGPF was revealed

in the combination treatment with PMA + HA + DSF when compared to treatment with PMA + HA. Inconsistent effects of treatments on EGFP expression in specimens simultaneously treated with PMA, HA, and DSF at different concentrations were attributed to experimental deviations and fluctuations in cellular redox balance. The relative fold-change of EGFP expression in the combination treatment PMA + HA treatment was highest in DSF mock-treated control (DSF 0 μM) and DSF 5 μM samples. The EGFP expression fold-change in PMA + HA + DSF treated cells was significantly reduced when DSF was administrated at concentrations 2.5 μM and 1 μM compared to DSF 0 and DSF 5 μM. The decreased EGFP-expression fold-change in samples treated with DSF at concentrations 2.5 μM and 1 μM stems from the observed inverse dose-dependent effect of DSF on the *"mini-virus"* reactivation.

PMA is a potent LRA, however, its administration to HIV+ patients is clinically irrelevant due to its tumorigenic potential (Melkova* *et al.*, 2017). In independent experiments using Bcl-2-immortalized primary CD4+ T-cells as a model HIV-1 latency cell line, the administration of DSF did not cause undesirable large-scale T-cell activation (Xing *et al.*, 2011). HA alone or in combination with PMA did not affect expression of CD69 activation marker in A3.01 T-cell line nor in PBMCs *ex vivo* (Shankaran *et al.*, 2011; Melkova and Shankaran, unpublished data). Thus, it would be interesting to investigate the expression of T-cell activation markers in A2 cells treated with the combination of HA and DSF or PMA (or a clinically relevant PKC inducer) and DSF. When considering the cytotoxicity of individual treatment combinations, the combined use of HA and DSF profoundly reduced the viability of treated cells. The decrease in cell viability could be probably solely attributable to HA as the viability was not reduced in samples treated with DSF only or with PMA + DSF, implying that DSF was generally well-tolerated at all selected concentrations. On the other hand, the reduction in cell viability was comparable in all HA-treated samples, including the combined treatments. In summary, these experiments show that the gene expression uder control of HIV-1 LTR is positively regulated by the combined administration of HA and DSF in an HIV-1 latency model cell line derived from the Jurkat lineage. DSF alone did not increase the LTR-driven expression of the HIV-1 *"mini-virus"* in Jurkat clone A2, but it synergized with both HA and PMA.

Since BVRA (Ahmad *et al.*, 2002; Tudor *et al.*, 2008; Jansen *et al.*, 2010) and BACH2 are directly involved in heme metabolism and redox homeostasis, this work has next aimed to investigate phenotype of the A2 cells overexpressing the genes of interest under specific treatment conditions. Effects of various treatment conditions, including combinations of HA, PMA, or both, on reactivation of the latent HIV-1, were first evaluated in the A2 cells

transiently expressing cDNAs for BVRA and BACH2. The HIV-1 "*mini-virus"* reactivation patterns were initially assessed in cells transfected with plasmids containing cDNA of respective genes using a low-cost electroporation method described by Chicaybam and colleagues (Chicaybam *et al.*, 2013). While the authors of this article reported an efficient gene transfer into Jurkat cells, the electroporation method did not reveal reproducible transfection rates. Thus, commercially available transfection kit from Lonza was used. Even though the cell viability and efficiency of electroporation improved, the results of electroporation experiments performed with the transfection kit suggest that the electroporation itself (Jakstys *et al.*, 2020), transduction of foreign DNA (Semenova *et al.*, 2019) and its expression as well as the subsequent treatment of transfected cells profoundly decreased the viability and/or expression of HIV-1 *„mini-virus"* in samples treated with PMA or PMA + HA. Due to a high variation among the individual experiments, it is hard to interpret the effects of BVRA and BACH2 expression on the reactivation of the "mini-virus" upon individual treatments and combinations. When considering means of the absolute values, there was a slight, albeit insignificant, increase in the basal LTR-driven expression of EGFP in the mock-treated cells transiently overexpressing BACH2, and a general decrease in the PMA and PMA+HA treated cells expressing BVRA or BACH2. On the other hand, when considering data normalized to the basal LTR-driven expression of EGFP in the mock-treated cells, there was a visible fold-increase in EGFP expression observed in PMA + HA-treated cells overexpressing BVRA, while there was a fold-decrease in EGFP expression in PMA-treated cells overexpressing BACH2. Hovewever, there were relatively big differencies among individual experiments. These results thus may stem from deviations introduced by the experimental design rather than from the direct effect of BVRA or BACH2 overexpression. Slight variations have been also noticed in cell viability, but again, these were statistically insignificant. The conclusions were made based on the differences in EGFP expression and viability in tissue culture samples transfected with plasmids encoding cDNA for genes of interest and control cells transfected with the plasmid encoding cDNA for LUC. The expression of LUC itself should not directly affect the regulation of HIV-1 LTR promoter or interfere with canonical endogenous processes. To stress some of the other important aspects of this approach, it should be noted that in some samples, the cell population gated within the investigated P5 region consisted of 20-30 cells. Thus, such a low number of cells may not be representative of the observed phenotype. Also, whilst the gating on double-positive cell population allowed for discrimination of transfected cells, this gating approach operated with a presumption that all double-positive cells were co-transfected with pDsRed2-N1 and pcDNA3.1 or pcDNA3

plasmids. Treatment of electroporated cells with DSF or its combination with other agents was not included in these experiments, because of the low numbers of live cells in the tissue cultures 24 hours after the electroporation.

Due to the mentioned limitations of the transient transfection approaches used, the effect of various treatment combinations on the *"mini-virus"* reactivation in cells overexpressing BVRA and BACH2 were finally addressed in stably transfected cell lines. Polyclonal cell lines overexpressing genes of interest, derived from the parental Jurkat clone A2, were established by a positive selection of cells expressing the plasmid-encoded gene for Neomycin resistance under the selective pressure of G418. As demonstrated in the results of antibiotic kill curve assays, the originally selected concentration of G418 (e.g. 1.6 mg/mL) for the positive selection of transfected cells was too stringent for the subsequent culture of the positive clones. Consequently, the concentration of G418 in culture medium was reduced to 1 mg/mL to maintain the selection pressure and to promote the growth of transfected cells. The presence and expression of transgenes in the resulting cell lines were validated in qPCR and RT-qPCR experiments, respectively, using an exogene-specific set of primers. The growth of tissue cultures expressing transgenes for LUC, BVRA, and BACH2 and the parental Jurkat clone A2 was determined in growth curve assays. The growth rate of stably transfected cell lines was comparable to the Jurkat clone A2 cell line in the case of BVRA and LUC transfected tissue cultures. The growth of cells expressing BACH2 transgene was slightly decreased. The observed decrease in BACH2 cell line growth was very mild and could stem from experimental deviations

The transgene copy number per cell was characterized based on the ΔCp between qPCR products amplified with exogene- and GAPDH-specific sets of primers. Using this approach, it was estimated that the transgenes encoding LUC and BACH2 were present in the corresponding cell lines in numbers as the endogenous GAPDH target, which was reported to be present in the human genome in a single copy (Ercolanis *et al.*, 1988). Unexpectedly, the detection of the qPCR product of BVRA transgene was delayed by approximately 10 cycles when compared to the reference endogene, suggesting that the transgene for BVRA was not present in each cell at the time of sample collection. This result could possibly stem from the ongoing adaptation and the selection processes induced by the initially excessive production of BVRA and it could also affect the results of the experiments performed with this cell line.

In RT-qPCR experiments, it has been demonstrated that, even at a lower rate than a GAPDH endogene, transgenes were actively expressed from the Cytomegalovirus (CMV) promoter included in the plasmid. The quantification of the transgene mRNA levels was

performed relatively to the levels of the endogenous GAPDH mRNA. The results of RT-qPCR experiments show that the levels of transgene mRNAs were much lower than the levels of the *house-keeping* GAPDH mRNA. Consistent with the results of qPCR experiments, levels of LUC and BACH2 mRNAs were similar, whilst the BVRA mRNA in corresponding tissue culture was evidently lower. The observed discrepancies in the detection threshold values for GAPDH mRNA among samples from different tissue cultures were attributed to the different RNA input (concentrations ranging from 90 to 130 ng/μL) and could have been also caused by low volume pipetting errors in the RT-qPCR working protocol. It should be stressed here that the results are rather qualitative than quantitative - qPCR and RT-qPCR experiments were performed in technical duplicates, they were not repeated in independent experiments, and they did not include calibration curves. Also, although the expression of transgenes was validated in RT-qPCR experiments, the actual overexpression of BVRA and BACH2 on the protein level was not characterized. Notwithstanding, since phenotypic differences among transfected groups in individual treatment experiments were consistent, the phenotype observed in treated, stably transfected tissue cultures was attributed directly to the combined effect of treatment and transgene expression. The western blot analyses of proteins of interest were originally outlined as a part of this work, however, they were not performed due to time limitations.

The degree of *"mini-virus"* reactivation in transfected cells stably expressing transgenes of interest was evaluated 24 hours after treatment with PMA or combined treatment with DSF + PMA, HA + PMA, and DSF + HA + PMA. In accordance with the original hypothesis, it has been demonstrated that overexpression of BVRA decreased the expression of EGFP from the canonical HIV-1 LTR promoter. A significant decrease in EGFP expression compared to control LUC transfected cells was found only in samples stimulated with PMA or PMA + HA, but the decreasing trend on the EGFP expression was also seen in PMA + HA + DSF treated samples. It could be reasoned that the observed decrease in the stimulated HIV-1 *"mini-virus"* reactivation in BVRA overexpressing cells was mediated directly by its antioxidative properties, as it has been previously shown that PMA or PMA + HA stimulated reactivation of the *"mini-virus"* can be weakened by concomitant administration of the antioxidant NAC (Shankaran *et al.*, 2011). Besides, BVRA is reportedly a TF that binds to the AP-1 binding site in response to oxidative stress, activating the expression of HO-1 (Ahmad *et al.*, 2002). Hence, if the reactivation of the "*mini-virus"* upon treatment was truly caused by a shift in cell redox balance, the effect of BVRA overexpression could have been also exerted indirectly. Moreover, because the AP-1 site is located within the HIV-1 LTR promoter region

and the AP-1 protein was shown to coordinate the expression of latent HIV-1 together with NF-kB (Hokello *et al.*, 2021), it would be interesting to examine, whether BVRA binds to the HIV-1 promoter itself. As follows from RT-qPCR experiments, the expression of BVRA transgene was decreased relative to the expression of transgenes in LUC and BACH2 transfected tissue cultures. Thus, the observed decrease in LTR-driven expression of EGFP may be underrated.

On the other hand, the treatment of cells overexpressing BACH2 with the combination of PMA + HA + DSF apparently induced a higher reactivation of the *"mini-virus"* when compared to LUC expressing cells. Strikingly, the combined administration of PMA + HA + DSF significantly increased the EGFP expression in all stably transfected cell lines and in A2 cells when compared to PMA + HA treated specimens in each cell line. The synergism between these three compounds was not observed in the earlier treatment experiments performed on the parental A2 cells with increasing DSF concentrations. Contrarily to BVRA, BACH2 was previously described as a negative regulator of HO-1 promoter (Watanabe-Matsui *et al.*, 2011) and a driver of cellular apoptosis during the oxidative stress (Muto *et al.*, 2002). Therefore, it seems reasonable to assume that the EGFP expression from the HIV-1 promotor was potentiated as a result of the increased oxidative challenge caused by the combined effect of treatment and stable expression of BACH2.

Regarding the mode of action of BACH2, it was initially hypothesized that BACH2 might upregulate the expression of the *"mini-virus"* through the modulations of the cellular redox milieu or possibly downregulate it through its putative binding to HIV-1 LTR. Using the transient expression, the cells were not adapted to the effects of BACH2, but the two different electroporation conditions yielded inconsistent results. On the othe hand, use of constitutive, stable expression led to the adaptation of the cells to BACH2 overexpression, resulting in the modification of EGFP expression levels. Unlike in the unstimulated LUC and BVRA cells, the basal EGFP expression was significantly increased in BACH2 cells, possibly due to an increased redox stress. Consequently, fold-increases in EGFP expression upon individual treatments were severely reduced, possibly suggesting BACH2-mediated inhibitory effects on the induced HIV-1 expression.

DSF + PMA treatment did not cause any significant changes in EGFP expression in BVRA or BACH2 cells when compared to LUC control. Since DSF did not affect the expression of *"mini-virus"* in A2 cells probably due to the unavailability of PTEN (Doyon *et al.*, 2013), its latency-reversing ability in the context of BVRA and BACH2 overexpression should be investigated in tissue cultures of different cellular origin. Moreover, the activity of BACH2 is

directly regulated by heme binding (Watanabe-Matsui *et al.*, 2015) and BVRA is a nuclear transporter of heme (Tudor *et al.*, 2008), thus their role in HIV-1 reactivation should be also examined in an experimental system overexpressing both proteins.

While these and previous findings strongly suggest that the effect of selected treatments is mediated via fluctuations in the fine-tuned cell redox balance, this work was unable to thoroughly investigate the production of ROS in the generated stably transfected cell lines overexpressing genes of interest. Nevertheless, preliminary experiments using 2′,7′-Dichlorofluorescin diacetate as a cell membrane-permeable ROS probe have revealed that production of ROS in stably transfected cell lines is, indeed, variable. A more in-depth analysis of ROS production in these cell lines will be addresed in the future.

To summarize, this work provides the very first *in vitro* evidence for the synergistic effect of DSF and HA, both FDA-approved substances for use in humans, on latent HIV-1 reactivation in the model A2 clone of Jurkat cells. Moreover, it has examined the role of the major enzyme of heme metabolism, BVRA (Kravets *et al.*, 2004; Tenhunen *et al.*, 1969), and of the heme-regulated transcription factor crucial for B- and T-cells differentiation and maturation, BACH2 (Tsukumo *et al.*, 2013; Watanabe-Matsui *et al.*, 2011), in A2 cells and A2-derived cells overexpressing genes of interest in multiple experimental systems. The effect of BVRA and BACH2 overexpression was investigated in both unstimulated cells and cells stimulated with DSF, HA, and PMA or their combinations. While the mechanisms behind the effects of DSF and HA on HIV-1 reactivation remain examined and characterized, the combined administration of these drugs should be considered in future clinical trials.

# 7. Conclusion

Aims of this thesis were to examine the role of BVRA and BACH2 genes products in the *in vitro* model of HIV-1 latency and to evaluate the effects of DSF, HA, and PMA or their combinations on HIV-1 reactivation. This work has demonstrated:

- Inhibition of BVRA catalytic activity by DSF in the cell lysate of A3.01 cells

- Synergism between DSF, HA, and PMA on expression of the HIV-1 *"mini-virus"* from the canonical HIV-1 promoter in a model of HIV-1 latency, A2 clone of Jurkat cells

- Inverse dose-dependency of DSF at selected concentration on the HIV-1 reactivation in A2 clone of Jurkat cells when administered in combination with HA or PMA

- Antagonistic effect of BVRA and BACH2 overexpression on the reactivation of HIV-1 in stably transfected cells derived from A2 clone of Jurkat cells

# 8. References


Abdi, B., Nguyen, T., Brouillet, S., Desire, N., Sayon, S., Wirden, M., Jary, A., Achaz, G., Assoumou, L., Palich, R., *et al.* (2020). No HIV-1 molecular evolution on long-term antiretroviral therapy initiated during primary HIV-1 infection. AIDS (London, England) *34*, 1745–1753.

Agbottah, E., Deng, L., Dannenberg, L.O., Pumfery, A., and Kashanchi, F. (2006). Effect of SWI/SNF chromatin remodeling complex on HIV-1 Tat activated transcription. Retrovirology *3*, 48.

Aghokeng, A.F., Ayouba, A., Mpoudi-Ngole, E., Loul, S., Liegeois, F., Delaporte, E., and Peeters, M. (2010). Extensive survey on the prevalence and genetic diversity of SIVs in primate bushmeat provides insights into risks for potential new cross-species transmissions. Infection, Genetics and Evolution *10*, 386–396.

Agosto, L.M., Herring, M.B., Mothes, W., and Henderson, A.J. (2018). HIV-1-Infected CD4+ T Cells Facilitate Latent Infection of Resting CD4+ T Cells through Cell-Cell Contact. Cell Reports *24*, 2088–2100.

Ahlenstiel*, C.L., Symonds, G., Kent, S.J., and Kelleher, A.D. (2020). Block and Lock HIV Cure Strategies to Control the Latent Reservoir. Frontiers in Cellular and Infection Microbiology *10*.

Ahmad, Z., Salim, M., and Maines, M.D. (2002). Human Biliverdin Reductase Is a Leucine Zipper-like DNA-binding Protein and Functions in Transcriptional Activation of Heme Oxygenase-1 by Oxidative Stress. Journal of Biological Chemistry *277*, 9226–9232.

Anton, P.A., Elliott, J., Poles, M.A., McGowan, I.M., Matud, J., Hultin, L.E., Grovit-Ferbas, K., Mackay, C.R., Chen, I.S.Y., and Giorgi, J. v. (2000). Enhanced levels of functional HIV-1 co-receptors on human mucosal T cells demonstrated using intestinal biopsy tissue. AIDS *14*, 1761–1765.

Archin, N.M., Keedy, K.S., Espeseth, A., Dang, H., Hazuda, D.J., and Margolis, D.M. (2009). Expression of latent human immunodeficiency type 1 is induced by novel and selective histone deacetylase inhibitors. AIDS *23*, 1799–1806.

Archin, N.M., Cheema, M., Parker, D., Wiegand, A., Bosch, R.J., Coffin, J.M., Eron, J., Cohen, M., and Margolis, D.M. (2010). Antiretroviral intensification and valproic acid lack sustained effect on residual HIV-1 viremia or resting CD4+ cell infection. PloS One *5*, e9390.

Archin, N.M., Liberty, A.L., Kashuba, A.D., Choudhary, S.K., Kuruc, J.D., Crooks, A.M., Parker, D.C., Anderson, E.M., Kearney, M.F., Strain, M.C., *et al.* (2012). Administration of vorinostat disrupts HIV-1 latency in patients on antiretroviral therapy. Nature *487*, 482–485.

Archin, N.M., Bateson, R., Tripathy, M.K., Crooks, A.M., Yang, K.-H., Dahl, N.P., Kearney, M.F., Anderson, E.M., Coffin, J.M., Strain, M.C., *et al.* (2014). HIV-1 Expression Within

Resting CD4+ T Cells After Multiple Doses of Vorinostat. The Journal of Infectious Diseases *210*, 728.

Bailey, J.R., Sedaghat, A.R., Kieffer, T., Brennan, T., Lee, P.K., Wind-Rotolo, M., Haggerty, C.M., Kamireddi, A.R., Liu, Y., Lee, J., *et al.* (2006). Residual human immunodeficiency virus type 1 viremia in some patients on antiretroviral therapy is dominated by a small number of invariant clones rarely found in circulating CD4+ T cells. Journal of Virology *80*, 6441–6457.

Ballweber, L., Robinson, B., Kreger, A., Fialkow, M., Lentz, G., McElrath, M.J., and Hladik, F. (2011). Vaginal Langerhans Cells Nonproductively Transporting HIV-1 Mediate Infection of T Cells. Journal of Virology *85*, 13443–13447.

Barañano, D.E., Rao, M., Ferris, C.D., and Snyder, S.H. (2002). Biliverdin reductase: A major physiologic cytoprotectant. Proceedings of the National Academy of Sciences of the United States of America *99*, 16093.

Barboric, M., Yik, J.H.N., Czudnochowski, N., Yang, Z., Chen, R., Contreras, X., Geyer, M., Peterlin, M.B., and Zhou, Q. (2007). Tat competes with HEXIM1 to increase the active pool of P-TEFb for HIV-1 transcription. Nucleic Acids Research *35*, 2003–2012.

Battivelli, E., Dahabieh, M.S., Abdel-Mohsen, M., Svensson, J.P., da Silva, I.T., Cohn, L.B., Gramatica, A., Deeks, S., Greene, W.C., Pillai, S.K., *et al.* (2018). Distinct chromatin functional states correlate with HIV latency reactivation in infected primary CD4+ T cells. ELife *7*.

Baxter, A.E., Niessl, J., Fromentin, R., Richard, J., Porichis, F., Charlebois, R., Massanella, M., Brassard, N., Alsahafi, N., Delgado, G.G., *et al.* (2016). Single-Cell Characterization of Viral Translation-Competent Reservoirs in HIV-Infected Individuals. Cell Host and Microbe *20*, 368–380.

Beans, E.J., Fournogerakis, D., Gauntlett, C., Heumann, L. v., Kramer, R., Marsden, M.D., Murray, D., Chun, T.-W., Zack, J.A., and Wender, P.A. (2013). Highly potent, synthetically accessible prostratin analogs induce latent HIV expression in vitro and ex vivo. Proceedings of the National Academy of Sciences of the United States of America *110*, 11698.

Bebenek, K., Abbottss, J., Roberts, J.D., Wilson$, S.H., and Kunkelj, T.A. (1989). Specificity and Mechanism of Error-prone Replication by Human Immunodeficiency Virus-1 Reverse Transcriptase*. Journal of Biological Chemistry *264*, 16948–16956.

Blaak, H., Van't Wout, A.B., Brouwer, M., Hooibrink, B., Hovenkamp, E., and Schuitemaker, H. (2000). In vivo HIV-1 infection of CD45RA+CD4+ T cells is established primarily by syncytium-inducing variants and correlates with the rate of CD4+ T cell decline. Proceedings of the National Academy of Sciences of the United States of America *97*, 1269–1274.

Blauvelt, A., Glushakova, S., and Margolis, L.B. (2000). HIV-infected human Langerhans cells transmit infection to human lymphoid tissue ex vivo. AIDS *14*, 647–651.

Blazkova, J., Trejbalova, K., Gondois-Rey, F., Halfon, P., Philibert, P., Guiguen, A., Verdin, E., Olive, D., van Lint, C., Hejnar, J., *et al.* (2009). CpG Methylation Controls Reactivation of HIV from Latency. PLoS Pathogens *5*, e1000554.

Bleul, C.C., Wu, L., Hoxie, J.A., Springer, T.A., and Mackay, C.R. (1997). The HIV coreceptors CXCR4 and CCR5 are differentially expressed and regulated on human T lymphocytes. Proceedings of the National Academy of Sciences *94*, 1925–1930.

Boehm, D., Jeng, M., Camus, G., Gramatica, A., Schwarzer, R., Johnson, J.R., Hull, P.A., Montano, M., Sakane, N., Pagans, S., *et al.* (2017). SMYD2-Mediated Histone Methylation Contributes to HIV-1 Latency. Cell Host & Microbe *21*, 569-579.e6.

Boily, M.C., Baggaley, R.F., Wang, L., Masse, B., White, R.G., Hayes, R.J., and Alary, M. (2009). Heterosexual risk of HIV-1 infection per sexual act: systematic review and meta-analysis of observational studies. The Lancet Infectious Diseases *9*, 118–129.

Borrow, P., Lewicki, H., Wei, X., Horwitz, M.S., Peffer, N., Meyers, H., Nelson, J.A., Gairin, J.E., Hahn, B.H., Oldstone, M.B.A., *et al.* (1997). Antiviral pressure exerted by HIV-1-specific cytotoxic T lymphocytes (CTLs) during primary infection demonstrated by rapid selection of CTL escape virus. Nature Medicine *3*, 205–211.

Bouchat, S., Gatot, J.S., Kabeya, K., Cardona, C., Colin, L., Herbein, G., de Wit, S., Clumeck, N., Lambotte, O., Rouzioux, C., *et al.* (2012). Histone methyltransferase inhibitors induce HIV-1 recovery in resting CD4+ T cells from HIV-1-infected HAART-treated patients. AIDS *26*, 1473–1482.

Bouchat, S., Delacourt, N., Kula, A., Darcis, G., Driessche, B. van, Corazza, F., Gatot, J.-S., Melard, A., Vanhulle, C., Kabeya, K., *et al.* (2016). Sequential treatment with 5-aza-2′-deoxycytidine and deacetylase inhibitors reactivates HIV-1. EMBO Molecular Medicine *8*, 117–138.

Brady, T., Agosto, L.M., Malani, N., Berry, C.C., O'Doherty, U., and Bushman, F. (2009). HIV integration site distributions in resting and activated CD4+ T cells infected in culture. AIDS (London, England) *23*, 1461.

Brenchley, J.M., Hill, B.J., Ambrozak, D.R., Price, D.A., Guenaga, F.J., Casazza, J.P., Kuruppu, J., Yazdani, J., Migueles, S.A., Connors, M., *et al.* (2004). T-Cell Subsets That Harbor Human Immunodeficiency Virus (HIV) In Vivo: Implications for HIV Pathogenesis. Journal of Virology *78*, 1160.

Briggs, J.A.G., Wilk, T., Welker, R., Kräusslich, H.G., and Fuller, S.D. (2003). Structural organization of authentic, mature HIV-1 virions and cores. EMBO Journal *22*, 1707–1715.

Briggs, J.A.G., Grünewald, K., Glass, B., Förster, F., Kräusslich, H.G., and Fuller, S.D. (2006). The mechanism of HIV-1 core assembly: Insights from three-dimensional reconstructions of authentic virions. Structure *14*, 15–20.

Brooks, G.D., Kitchen, G.S., Kitchen, M.R.C., Scripture-Adams, D.D., and Zack, A.J. (2001). Generation of HIV latency during thymopoiesis. Nature Medicine *7*, 459–464.

Bruner, K.M., Murray, A.J., Pollack, R.A., Soliman, M.G., Laskey, S.B., Capoferri, A.A., Lai, J., Strain, M.C., Lada, S.M., Hoh, R., *et al.* (2016). Defective proviruses rapidly accumulate during acute HIV-1 infection. Nature Medicine *22*, 1043.

Bunnik, E.M., Swenson, L.C., Edo-Matas, D., Huang, W., Dong, W., Frantzell, A., Petropoulos, C.J., Coakley, E., Schuitemaker, H., Harrigan, P.R., *et al.* (2011). Detection of inferred CCR5- and CXCR4-using HIV-1 variants and evolutionary intermediates using ultra-deep pyrosequencing. PLoS Pathogens *7*.

Burleigh, L., Lozach, P.-Y., Schiffer, C., Staropoli, I., Pezo, V., Porrot, F., Canque, B., Virelizier, J.-L., Arenzana-Seisdedos, F., and Amara, A. (2006). Infection of Dendritic Cells (DCs), Not DC-SIGN-Mediated Internalization of Human Immunodeficiency Virus, Is Required for Long-Term Transfer of Virus to T Cells. Journal of Virology *80*, 2949–2957.

Camejo, G., Halberg, C., Manschik-Lundin, A., Hurt-Camejo, E., Rosengren, B., Olsson, H., Hansson, G.I., Forsberg, G.B., and Ylhen, B. (1998). Hemin binding and oxidation of lipoproteins in serum: mechanisms and effect on the interaction of LDL with human macrophages. Journal of Lipid Research *39*, 755–766.

Campbell, J.J., Murphy, K.E., Kunkel, E.J., Brightling, C.E., Soler, D., Shen, Z., Boisvert, J., Greenberg, H.B., Vierra, M.A., Goodman, S.B., *et al.* (2001). CCR7 Expression and Memory T Cell Diversity in Humans. The Journal of Immunology *166*, 877–884.

Carias*, A.M., and Hope, T.J. (2019). Barriers of Mucosal Entry of HIV/SIV. Current Immunology Reviews *15*, 4–13.

Cavrois, M., Neidleman, J., Kreisberg, J.F., and Greene, W.C. (2007). In vitro derived dendritic cells trans-infect CD4 T cells primarily with surface-bound HIV-1 virions. PLoS Pathogens *3*, 0038–0045.

Cesana, D., Santoni de Sio, F.R., Rudilosso, L., Gallina, P., Calabria, A., Beretta, S., Merelli, I., Bruzzesi, E., Passerini, L., Nozza, S., *et al.* (2017). HIV-1-mediated insertional activation of STAT5B and BACH2 trigger viral reservoir in T regulatory cells. Nature Communications 2017 8:1 *8*, 1–11.

Charpentier, C., Nora, T., Tenaillon, O., Clavel, F., and Hance, A.J. (2006). Extensive Recombination among Human Immunodeficiency Virus Type 1 Quasispecies Makes an Important Contribution to Viral Diversity in Individual Patients. Journal of Virology *80*, 2472–2482.

Chavez, L., Calvanese, V., and Verdin, E. (2015). HIV Latency Is Established Directly and Early in Both Resting and Activated Primary CD4 T Cells. PLoS Pathogens *11*.

Chen, W.T., Shiu, C.S., Yang, J.P., Simoni, J.M., Fredriksen-Goldsen, karen I., Lee, T.S.H., and Zhao, H. (2013). Antiretroviral therapy (ART) side effect impacted on quality of life, and depressive symptomatology: A mixed-method study. Journal of AIDS and Clinical Research *4*, 218.

Chicaybam, L., Sodre, A.L., Curzio, B.A., and Bonamino, M.H. (2013). An Efficient Low Cost Method for Gene Transfer to T Lymphocytes. PLoS ONE *8*, e60298.

Chomczynski, P., and Sacchi, N. (1987). Single-step method of RNA isolation by acid guanidinium thiocyanate-phenol-chloroform extraction. Analytical Biochemistry *162*, 156–159.

Chomont, N., El-Far, M., Ancuta, P., Trautmann, L., Procopio, F.A., Yassine-Diab, B., Boucher, G., Boulassel, M.R., Ghattas, G., Brenchley, J.M., *et al.* (2009). HIV reservoir size and persistence are driven by T cell survival and homeostatic proliferation. Nature Medicine *15*, 893–900.

Chun, T.W., Carruth, L., Finzi, D., Shen, X., DiGiuseppe, J.A., Taylor, H., Hermankova, M., Chadwick, K., Margolick, J., Quinn, T.C., *et al.* (1997). Quantification of latent tissue reservoirs and total body viral load in HIV-1 infection. Nature *387*, 183–188.

Ciuffi, A., Llano, M., Poeschla, E., Hoffmann, C., Leipzig, J., Shinn, P., Ecker, J.R., and Bushman, F. (2005). A role for LEDGF/p75 in targeting HIV DNA integration. Nature Medicine *11*, 1287–1289.

Clayton, F., Snow, G., Reka, S., and Kotler, D.P. (1997). Selective depletion of rectal lamina propria rather than lymphoid aggregate CD4 lymphocytes in HIV infection. Clinical and Experimental Immunology *107*, 288–292.

Connor, R.I., Sheridan, K.E., Ceradini, D., Choe, S., and Landau, N.R. (1997). Change in coreceptor use correlates with disease progression in HIV-1- infected individuals. Journal of Experimental Medicine *185*, 621–628.

Coplan, P.M., Gortmaker, S., Hernandez-Avila, M., Spiegelman, D., Uribe-Zuñiga, P., and Mueller, N.E. (1996). Human immunodeficiency virus infection in Mexico City: Rectal bleeding and anal warts as risk factors among men reporting sex with men. American Journal of Epidemiology *144*, 817–827.

Daar, E.S., Kesler, K.L., Petropoulos, C.J., Huang, W., Bates, M., Lail, A.E., Coakley, E.P., Gomperts, E.D., and Donfield, S.M. (2007). Baseline HIV type 1 coreceptor tropism predicts disease progression. Clinical Infectious Diseases *45*, 643–649.

Dai, J., Agosto, L.M., Baytop, C., Yu, J.J., Pace, M.J., Liszewski, M.K., and O'Doherty, U. (2009). Human Immunodeficiency Virus Integrates Directly into Naïve Resting CD4+ T Cells but Enters Naïve Cells Less Efficiently than Memory Cells. Journal of Virology *83*, 4528.

Dampier, W., Nonnemacher, M.R., Mell, J., Earl, J., Ehrlich, G.D., Pirrone, V., Aiamkitsumrit, B., Zhong, W., Kercher, K., Passic, S., *et al.* (2016). HIV-1 genetic variation resulting in the development of new quasispecies continues to be encountered in the peripheral blood of well-suppressed patients. PLoS ONE *11*, 155382.

Davy-Mendez, T., Napravnik, S., Zakharova, O., Kuruc, J., Gay, C., Hicks, C.B., McGee, K.S., and Eron, J.J. (2018). Acute HIV infection and CD4/CD8 ratio normalization after antiretroviral therapy initiation. Journal of Acquired Immune Deficiency Syndromes *79*, 510–518.

Deeks*, S.G. (2012). HIV: Shock and kill. Nature *487*, 439–440.

Deeks, S.G., Wrin, T., Liegler, T., Hoh, R., Hayden, M., Barbour, J.D., Hellmann, N.S., Petropoulos, C.J., McCune, J.M., Hellerstein, M.K., *et al.* (2001). Virologic and immunologic consequences of discontinuing combination antiretroviral-drug therapy in HIV-infected patients with detectable viremia. New England Journal of Medicine *344*, 472–480.

Díaz, L., Martínez-Bonet, M., Sánchez, J., Fernández-Pineda, A., Jiménez, J.L., Muñoz, E., Moreno, S., Álvarez, S., and Muñoz-Fernández, M.Á. (2015). Bryostatin activates HIV-1 latent expression in human astrocytes through a PKC and NF-κB-dependent mechanism. Scientific Reports *5*.

van Dijk, R., Aronson, S.J., de Waart, D.R., van de Graaf, S.F., Duijst, S., Seppen, J., Elferink, R.O., Beuers, U., and Bosma, P.J. (2017). Biliverdin Reductase inhibitors did not improve severe unconjugated hyperbilirubinemia in vivo. Scientific Reports *7*, 1–9.

Divsalar, D.N., Simoben, C.V., Schonhofer, C., Richard, K., Sippl, W., Ntie-Kang, F., and Tietjen, I. (2020). Novel Histone Deacetylase Inhibitors and HIV-1 Latency-Reversing Agents Identified by Large-Scale Virtual Screening. Frontiers in Pharmacology *0*, 905.

Donahue*, D.A., and Wainberg, M.A. (2013). Cellular and molecular mechanisms involved in the establishment of HIV-1 latency. Retrovirology *10*, 1–11.

Dong, Q., Kelkar, S., Xiao, Y., Joshi-Barve, S., McClain, C.J., and Barve, S.S. (2000). Ethanol enhances TNF-α-inducible NFκB activation and HIV-1-LTR transcription in CD4+ Jurkat T lymphocytes. Journal of Laboratory and Clinical Medicine *136*, 333–343.

Doranz, B.J., Rucker, J., Yi, Y., Smyth, R.J., Samson, M., Peiper, S.C., Parmentier, M., Collman, R.G., and Doms, R.W. (1996). A dual-tropic primary HIV-1 isolate that uses fusin and the β-chemokine receptors CKR-5, CKR-3, and CKR-2b as fusion cofactors. Cell *85*, 1149–1158.

Doré, S., Takahashi, M., Ferris, C.D., Hester, L.D., Guastella, D., and Snyder, S.H. (1999). Bilirubin, formed by activation of heme oxygenase-2, protects neurons against oxidative stress injury. Proceedings of the National Academy of Sciences *96*, 2445–2450.

Dornadula, G., Zhang, H., VanUitert, B., Stern, J., Livornese, L., Ingerman, M.J., Witek, J., Kedanis, R.J., Natkin, J., DeSimone, J., *et al.* (1999). Residual HIV-1 RNA in blood plasma of patients taking suppressive highly active antiretroviral therapy. Journal of the American Medical Association *282*, 1627–1632.

Doyon, G., Zerbato, J., Mellors, J.W., and Sluis-Cremer, N. (2013). Disulfiram reactivates latent HIV-1 expression through depletion of the phosphatase and tensin homolog. AIDS *27*.

Du, W., Thanos, D., and Maniatis, T. (1993). Mechanisms of Transcriptional Synergism between Distinct Virus-Inducible Enhancer Elements. Cell *74*, 887–898.

Duverger, A., Jones, J., May, J., Bibollet-Ruche, F., Wagner, F.A., Cron, R.Q., and Kutsch, O. (2009). Determinants of the Establishment of Human Immunodeficiency Virus Type 1 Latency. Journal of Virology *83*, 3078.

Eckstein, D.A., Penn, M.L., Korin, Y.D., Scripture-Adams, D.D., Zack, J.A., Kreisberg, J.F., Roederer, M., Sherman, M.P., Chin, P.S., and Goldsmith, M.A. (2001). HIV-1 Actively Replicates in Naive CD4+ T Cells Residing within Human Lymphoid Tissues. Immunity *15*, 671–682.

Elliott, J.H., McMahon, J.H., Chang, C.C., Lee, S.A., Hartogensis, W., Bumpus, N., Savic, R., Roney, J., Hoh, R., Solomon, A., *et al.* (2015). Short-term administration of disulfiram for reversal of latent HIV infection: a phase 2 dose-escalation study. The Lancet HIV *2*, e520–e529.

Ercolanis, L., Florence, B., Denaro, M., Alexander, M., Alexander, M., and Curtis, G. (1988). Isolation and Complete Sequence of a Functional Human Glyceraldehyde-3-phosphate Dehydrogenase Gene . J. Biol. Chem *263*, 15335–15341.

Faria, N.R., Rambaut, A., Suchard, M.A., Baele, G., Bedford, T., Ward, M.J., Tatem, A.J., Sousa, J.D., Arinaminpathy, N., Pépin, J., *et al.* (2014). The early spread and epidemic ignition of HIV-1 in human populations. Science *346*, 56–61.

Fiebig, E.W., Wright, D.J., Rawal, B.D., Garrett, P.E., Schumacher, R.T., Peddada, L., Heldebrant, C., Smith, R., Conrad, A., Kleinman, S.H., *et al.* (2003). Dynamics of HIV viremia and antibody seroconversion in plasma donors: Implications for diagnosis and staging of primary HIV infection. AIDS *17*, 1871–1879.

Finzi, D., Blankson, J., Siliciano, J.D., Margolick, J.B., Chadwick, K., Pierson, T., Smith, K., Lisziewicz, J., Lori, F., Flexner, C., *et al.* (1999). Latent infection of CD4+ T cells provides a mechanism for lifelong persistence of HIV-1, even in patients on effective combination therapy. Nature Medicine *5*, 512–517.

Fisher, A.G., Ensoli, B., Looney, D., Rose, A., Gallo, R.C., Saag, M.S., Shaw, G.M., Hahn, B.H., and Wong-Staal, F. (1988). Biologically diverse molecular variants within a single HIV-1 isolate. Nature *334*, 444–447.

Folks, T., Powell, M.D., Lightfoot, M.M., Benn, S., Martin, A.M., and Fauci, A.S. (1986). Induction of HTLV-III/LAV from a nonvirus-producing T-cell line: implications for latency. Science (New York, N.Y.) *231*, 600–602.

Frankel*, A.D., and Young, J.A.T. (1998). HIV-1: Fifteen Proteins and an RNA. Annual Review of Biochemistry *67*, 1–25.

Fritsch, R.D., Shen, X., Sims, G.P., Hathcock, K.S., Hodes, R.J., and Lipsky, P.E. (2005). Stepwise Differentiation of CD4 Memory T Cells Defined by Expression of CCR7 and CD27. The Journal of Immunology *175*, 6489–6497.

Gao, F., Balles, E., Robertson, D.L., Chen, Y., Rodenburg, C.M., Michael, S.F., Cummins, L.B., Arthur, L.O., Peeters, M., Shaw, G.M., *et al.* (1999). Origin of HIV-1 in the chimpanzee Pan troglodytes troglodytes. Nature *397*, 436–441.

Garber, M.E., Mayall, T.P., Suess, E.M., Meisenhelder, J., Thompson, N.E., and Jones, K.A. (2000). CDK9 Autophosphorylation Regulates High-Affinity Binding of the Human

Immunodeficiency Virus Type 1 Tat-P-TEFb Complex to TAR RNA. MOLECULAR AND CELLULAR BIOLOGY *20*, 6958–6969.

Geijtenbeek, T.B.H., Kwon, D.S., Torensma, R., van Vliet, S.J., van Duijnhoven, G.C.F., Middel, J., Cornelissen, I.L.M.H.A., Nottet, H.S.L.M., KewalRamani, V.N., Littman, D.R., *et al.* (2000). DC-SIGN, a dendritic cell-specific HIV-1-binding protein that enhances trans-infection of T cells. Cell *100*, 587–597.

Gilbert, M.T.P., Rambaut, A., Wlasiuk, G., Spira, T.J., Pitchenik, A.E., and Worobey, M. (2007). The emergence of HIV/AIDS in the Americas and beyond. Proceedings of the National Academy of Sciences of the United States of America *104*, 18566–18570.

Goonetilleke, N., Liu, M.K.P., Salazar-Gonzalez, J.F., Ferrari, G., Giorgi, E., Ganusov, V. v., Keele, B.F., Learn, G.H., Turnbull, E.L., Salazar, M.G., *et al.* (2009). The first T cell response to transmitted/founder virus contributes to the control of acute viremia in HIV-1 infection. Journal of Experimental Medicine *206*, 1253–1272.

Gordon, S.N., Cervasi, B., Odorizzi, P., Silverman, R., Aberra, F., Ginsberg, G., Estes, J.D., Paiardini, M., Frank, I., and Silvestri, G. (2010). Disruption of Intestinal CD4 + T Cell Homeostasis Is a Key Marker of Systemic CD4 + T Cell Activation in HIV-Infected Individuals . The Journal of Immunology *185*, 5169–5179.

Granelli-Piperno, A., Finkel, V., Delgado, E., and Steinman, R.M. (1999). Virus replication begins in dendritic cells during the transmission of HIV-1 from mature dendritic cells to T cells. Current Biology *9*, 21–29.

Grant, L.A., Silverberg, M.J., Palacio, H., Minkoff, H., Anastos, K., Young, M.A., Nowicki, M., Kovacs, A., Cohen, M., and Muñoz, A. (2001). Discontinuation of potent antiretroviral therapy: Predictive value of and impact on CD4 cell counts and HIV RNA levels. AIDS *15*, 2101–2108.

Groot, F., van Capel, T.M., Schuitemaker, J.H., Berkhout, B., and de Jong, E.C. (2006). Differential susceptibility of naïve, central memory and effector memory T cells to dendritic cell-mediated HIV-1 transmission. Retrovirology 2006 3:1 *3*, 1–10.

Gupta, P., Collins, K.B., Ratner, D., Watkins, S., Naus, G.J., Landers, D. v., and Patterson, B.K. (2002). Memory CD4+ T Cells Are the Earliest Detectable Human Immunodeficiency Virus Type 1 (HIV-1)-Infected Cells in the Female Genital Mucosal Tissue during HIV-1 Transmission in an Organ Culture System. Journal of Virology *76*, 9868–9876.

Gutiérrez, C., Serrano-Villar, S., Madrid-Elena, N., Pérez-Eĺas, M.J., Martń, M.E., Barbas, C., Ruipérez, J., Muñoz, E., Muñoz-Fernández, M.A., Castor, T., *et al.* (2016). Bryostatin-1 for latent virus reactivation in HIV-infected patients on antiretroviral therapy. AIDS *30*, 1385–1392.

Hamann, M. v., Ehmele, P., Verdikt, R., Bialek-Waldmann, J.K., Virdi, S., Günther, T., van Lint, C., Grundhoff, A., Hauber, J., and Lange, U.C. (2021). Transcriptional behavior of the HIV-1 promoter in context of the BACH2 prominent proviral integration gene. Virus Research *293*, 198260.

Hemelaar, J., Elangovan, R., Yun, J., Dickson-Tetteh, L., Fleminger, I., Kirtley, S., Williams, B., Gouws-Williams, E., Ghys, P.D., Abimiku, A.G., *et al.* (2019). Global and regional molecular epidemiology of HIV-1, 1990–2015: a systematic review, global survey, and trend analysis. The Lancet Infectious Diseases *19*, 143–155.

Hermankova, M., Siliciano, J.D., Zhou, Y., Monie, D., Chadwick, K., Margolick, J.B., Quinn, T.C., and Siliciano, R.F. (2003). Analysis of Human Immunodeficiency Virus Type 1 Gene Expression in Latently Infected Resting CD4+ T Lymphocytes In Vivo. Journal of Virology *77*, 7383.

Hertoghs, N., Nijmeijer, B.M., van Teijlingen, N.H., Fenton-May, A.E., Kaptein, T.M., van Hamme, J.L., Kappes, J.C., Kootstra, N.A., Hahn, B.H., Borrow, P., *et al.* (2019). Sexually transmitted founder HIV-1 viruses are relatively resistant to Langerhans cell-mediated restriction. PLoS ONE *14*.

Hiener, B., Horsburgh, B.A., Eden, J.S., Barton, K., Schlub, T.E., Lee, E., von Stockenstrom, S., Odevall, L., Milush, J.M., Liegler, T., *et al.* (2017). Identification of Genetically Intact HIV-1 Proviruses in Specific CD4+ T Cells from Effectively Treated Participants. Cell Reports *21*, 813–822.

Hira, S., Tomita, T., Matsui, T., Igarashi, K., and Ikeda-Saito, M. (2007). Bach1, a heme-dependent transcription factor, reveals presence of multiple heme binding sites with distinct coordination structure. IUBMB Life *59*, 542–551.

Hladik, F., Sakchalathorn, P., Ballweber, L., Lentz, G., Fialkow, M., Eschenbach, D., and McElrath, M.J. (2007). Initial Events in Establishing Vaginal Entry and Infection by Human Immunodeficiency Virus Type-1. Immunity *26*, 257–270.

Ho, Y.C., Shan, L., Hosmane, N.N., Wang, J., Laskey, S.B., Rosenbloom, D.I.S., Lai, J., Blankson, J.N., Siliciano, J.D., and Siliciano, R.F. (2013). Replication-Competent Noninduced Proviruses in the Latent Reservoir Increase Barrier to HIV-1 Cure. Cell *155*, 540–551.

Hokello, J., Sharma, A.L., and Tyagi, M. (2021). AP-1 and NF-κB synergize to transcriptionally activate latent HIV upon T-cell receptor activation. FEBS Letters *595*, 577–594.

Hollingsworth, T.D., Anderson, R.M., and Fraser, C. (2008). HIV-1 transmission, by stage of infection. Journal of Infectious Diseases *198*, 687–693.

Hong, Y., Yan, W., Chen, S., Sun, C., and Zhang, J. (2010). The role of Nrf2 signaling in the regulation of antioxidants and detoxifying enzymes after traumatic brain injury in rats and mice. Acta Pharmacologica Sinica *31*, 1421–1430.

Hoshino, H., Kobayashi, A., Yoshida, M., Kudo, N., Oyake, T., Motohashi, H., Hayashi, N., Yamamoto, M., and Igarashi, K. (2000). Oxidative Stress Abolishes Leptomycin B-sensitive Nuclear Export of Transcription Repressor Bach2 That Counteracts Activation of Maf Recognition Element. Journal of Biological Chemistry *275*, 15370–15376.

Huet, T., Cheynier, R., Meyerhans, A., Roelants, G., and Wain-Hobson, S. (1990). Genetic organization of a chimpanzee lentivirus related to HIV-1. Nature *345*, 356–359.

Ikeda, T., Shibata, J., Yoshimura, K., Koito, A., and Matsushita, S. (2007). Recurrent HIV-1 Integration at the BACH2 Locus in Resting CD4+ T Cell Populations during Effective Highly Active Antiretroviral Therapy. The Journal of Infectious Diseases *195*, 716–725.

Imai, K., Togami, H., and Okamoto, T. (2010). Involvement of Histone H3 Lysine 9 (H3K9) Methyltransferase G9a in the Maintenance of HIV-1 Latency and Its Reactivation by BIX01294. The Journal of Biological Chemistry *285*, 16538.

Inderbitzin, A., Kok, Y.L., Jörimann, L., Kelley, A., Neumann, K., Heinzer, D., Cathomen, T., and Metzner, K.J. (2020). HIV-1 promoter is gradually silenced when integrated into BACH2 in Jurkat T-cells. PeerJ *8*.

Isel, C., and Karn, J. (1999). Direct evidence that HIV-1 tat stimulates RNA polymerase II carboxyl-terminal domain hyperphosphorylation during transcriptional elongation. Journal of Molecular Biology *290*, 929–941.

Itoh, K., Chiba, T., Takahashi, S., Ishii, T., Igarashi, K., Katoh, Y., Oyake, T., Hayashi, N., Satoh, K., Hatayama, I., *et al.* (1997). An Nrf2/Small Maf Heterodimer Mediates the Induction of Phase II Detoxifying Enzyme Genes through Antioxidant Response Elements. Biochemical and Biophysical Research Communications *236*, 313–322.

Jaafoura, S., de Goër De Herve, M.G., Hernandez-Vargas, E.A., Hendel-Chavez, H., Abdoh, M., Mateo, M.C., Krzysiek, R., Merad, M., Seng, R., Tardieu, M., *et al.* (2014). Progressive contraction of the latent HIV reservoir around a core of less-differentiated CD4 + memory T cells. Nature Communications *5*.

Jakstys, B., Jakutaviciute, M., Uzdavinyte, D., Satkauskiene, I., and Satkauskas, S. (2020). Correlation between the loss of intracellular molecules and cell viability after cell electroporation. Bioelectrochemistry *135*, 107550.

Jansen, T., Hortmann, M., Oelze, M., Opitz, B., Steven, S., Schell, R., Knorr, M., Karbach, S., Schuhmacher, S., Wenzel, P., *et al.* (2010). Conversion of biliverdin to bilirubin by biliverdin reductase contributes to endothelial cell protection by heme oxygenase-1—evidence for direct and indirect antioxidant actions of bilirubin. Journal of Molecular and Cellular Cardiology *49*, 186–195.

Jeney, V., Balla, J., Yachie, A., Varga, Z., Vercellotti, G.M., Eaton, J.W., and Balla, G. (2002). Pro-oxidant and cytotoxic effects of circulating heme. Blood *100*, 879–887.

Jeong, S.J., Pise-Masison, C.A., Radonovich, M.F., Park, H.U., and Brady, J.N. (2005). Activated AKT regulates NF-κB activation, p53 inhibition and cell survival in HTLV-1-transformed cells. Oncogene 2005 24:44 *24*, 6719–6728.

Jiang, G., Mendes, E.A., Kaiser, P., Wong, D.P., Tang, Y., Cai, I., Fenton, A., Melcher, G.P., Hildreth, J.E.K., Thompson, G.R., *et al.* (2015). Synergistic Reactivation of Latent HIV Expression by Ingenol-3-Angelate, PEP005, Targeted NF-kB Signaling in Combination with JQ1 Induced p-TEFb Activation. PLOS Pathogens *11*, e1005066.

Kacani, L., Frank, I., Spruth, M., Schwendinger, M.G., Müllauer, B., Sprinzl, G.M., Steindl, F., and Dierich, M.P. (1998). Dendritic Cells Transmit Human Immunodeficiency Virus Type 1 to Monocytes and Monocyte-Derived Macrophages. Journal of Virology *72*, 6671–6677.

Kauder, S.E., Bosque, A., Lindqvist, A., Planelles, V., and Verdin, E. (2009). Epigenetic Regulation of HIV-1 Latency by Cytosine Methylation. PLoS Pathogens *5*.

Kawamura, T., Gulden, F.O., Sugaya, M., McNamara, D.T., Borris, D.L., Lederman, M.M., Orenstein, J.M., Zimmerman, P.A., and Blauvelt, A. (2003). R5 HIV productively infects langerhans cells, and infection levels are regulated by compound CCR5 polymorphisms. Proceedings of the National Academy of Sciences of the United States of America *100*, 8401–8406.

Kearney, M., Maldarelli, F., Shao, W., Margolick, J.B., Daar, E.S., Mellors, J.W., Rao, V., Coffin, J.M., and Palmer, S. (2009). Human Immunodeficiency Virus Type 1 Population Genetics and Adaptation in Newly Infected Individuals. Journal of Virology *83*, 2715–2727.

Kedei, N., Lundberg, D.J., Toth, A., Welburn, P., Garfield, S.H., and Blumberg, P.M. (2004). Characterization of the Interaction of Ingenol 3-Angelate with Protein Kinase C. Cancer Research *64*, 3243–3255.

Keele, B.F., van Heuverswyn, F., Li, Y., Bailes, E., Takehisa, J., Santiago, M.L., Bibollet-Ruche, F., Chen, Y., Wain, L. v., Liegeois, F., *et al.* (2006). Chimpanzee reservoirs of pandemic and nonpandemic HIV-1. Science *313*, 523–526.

Keele, B.F., Giorgi, E.E., Salazar-Gonzalez, J.F., Decker, J.M., Pham, K.T., Salazar, M.G., Sun, C., Grayson, T., Wang, S., Li, H., *et al.* (2008). Identification and characterization of transmitted and early founder virus envelopes in primary HIV-1 infection. Proceedings of the National Academy of Sciences of the United States of America *105*, 7552–7557.

Keyer, K., and Imlay, J.A. (1996). Superoxide accelerates DNA damage by elevating free-iron levels. Proc. Natl. Acad. Sci. USA *93*, 13635–13640.

Kinoshita, S., Chen, B.K., Kaneshima, H., and Nolan, G.P. (1998). Host Control of HIV-1 Parasitism in T Cells by the Nuclear Factor of Activated T Cells. Cell *95*, 595–604.

Kint, S., Trypsteen, W., Spiegelaere, W. de, Malatinkova, E., Loes, S.K., Meyer, T. de, Criekinge, W. van, and Vandekerckhove, L. (2020). Underestimated effect of intragenic HIV-1 DNA methylation on viral transcription in infected individuals. Clinical Epigenetics *12*.

Kinter, A., Moorthy, A., Jackson, R., and Fauci, S.F. (2003). Productive HIV infection of resting CD4+ T cells: role of lymphoid tissue microenvironment and effect of immunomodulating agents. AIDS Research and Human Retroviruses *19*, 847–856.

Kok, Y.L., Vongrad, V., Chaudron, S.E., Shilaih, M., Leemann, C., Neumann, K., Kusejko, K., Giallonardo, F. di, Kuster, H., Braun, D.L., *et al.* (2021). HIV-1 integration sites in CD4+ T cells during primary, chronic, and late presentation of HIV-1 infection. JCI Insight *6*.

Koot, M., van Leeuwen, R., de Goede, R.E.Y., Keet, I.P.M., Danner, S., Schattenkerk, J.K.M.E., Reiss, P., Tersmette, M., Lange, J.M.A., and Schuitemaker, H. (1999). Conversion rate towards a syncytium-inducing (SI) phenotype during different stages of human immunodeficiency virus type 1 infection and prognostic value of SI phenotype for survival after AIDS diagnosis. Journal of Infectious Diseases *179*, 254–258.

Kravets, A., Hu, Z., Miralem, T., Torno, M.D., and Maines, M.D. (2004). Biliverdin Reductase, a Novel Regulator for Induction of Activating Transcription Factor-2 and Heme Oxygenase-1 . Journal of Biological Chemistry *279*, 19916–19923.

Kula, A., Delacourt, N., Bouchat, S., Darcis, G., Avettand-Fenoel, V., Verdikt, R., Corazza, F., Necsoi, C., Vanhulle, C., Bendoumou, M., *et al.* (2019). Heterogeneous HIV-1 Reactivation Patterns of Disulfiram and Combined Disulfiram+Romidepsin Treatments. JAIDS Journal of Acquired Immune Deficiency Syndromes *80*, 605–613.

Kulpa, D.A., Talla, A., Brehm, J.H., Ribeiro, S.P., Yuan, S., Bebin-Blackwell, A.-G., Miller, M., Barnard, R., Deeks, S.G., Hazuda, D., *et al.* (2019). Differentiation into an Effector Memory Phenotype Potentiates HIV-1 Latency Reversal in CD4 + T Cells . Journal of Virology *93*, 969–988.

Kwon, D.S., Gregorio, G., Bitton, N., Hendrickson, W.A., and Littman, D.R. (2002). DC-SIGN-mediated internalization of HIV is required for trans-enhancement of T cell infection. Immunity *16*, 135–144.

Laird, G.M., Bullen, C.K., Rosenbloom, D.I.S., Martin, A.R., Hill, A.L., Durand, C.M., Siliciano, J.D., and Siliciano, R.F. (2015). Ex vivo analysis identifies effective HIV-1 latency–reversing drug combinations. The Journal of Clinical Investigation *125*, 1901–1912.

Lalonde, M.S., Lobritz, M.A., Ratcliff, A., Chamanian, M., Athanassiou, Z., Tyagi, M., Wong, J., Robinson, J.A., Karn, J., Varani, G., *et al.* (2011). Inhibition of Both HIV-1 Reverse Transcription and Gene Expression by a Cyclic Peptide that Binds the Tat-Transactivating Response Element (TAR) RNA. PLOS Pathogens *7*, e1002038.

Lee, B., Sharron, M., Montaner, L.J., Weissman, D., and Doms, R.W. (1999). Quantification of CD4, CCR5, and CXCR4 levels on lymphocyte subsets, dendritic cells, and differentially conditioned monocyte-derived macrophages. Proceedings of the National Academy of Sciences of the United States of America *96*, 5215–5220.

Lee, H.Y., Giorgi, E.E., Keele, B.F., Gaschen, B., Athreya, G.S., Salazar-Gonzalez, J.F., Pham, K.T., Goepfert, P.A., Michael Kilby, J., Saag, M.S., *et al.* (2009). Modeling sequence evolution in acute HIV-1 infection. Journal of Theoretical Biology *261*, 341–360.

Lee, S.A., Elliott, J.H., McMahon, J., Hartogenesis, W., Bumpus, N.N., Lifson, J.D., Gorelick, R.J., Bacchetti, P., Deeks, S.G., Lewin, S.R., *et al.* (2019). Population Pharmacokinetics and Pharmacodynamics of Disulfiram on Inducing Latent HIV-1 Transcription in a Phase IIb Trial. Clinical Pharmacology and Therapeutics *105*, 692–702.

Lerner-Marmarosh, N., Shen, J., Torno, M.D., Kravets, A., Hu, Z., and Maines, M.D. (2005). Human biliverdin reductase: A member of the insulin receptor substrate family with

serine/threonine/tyrosine kinase activity. Proceedings of the National Academy of Sciences of the United States of America *102*, 7109.

Lerner-Marmarosh, N., Miralem, T., Gibbs, P.E.M., and Maines, M.D. (2007). Regulation of TNF-α-activated PKC-ζ signaling by the human biliverdin reductase: identification of activating and inhibitory domains of the reductase. The FASEB Journal *21*, 3949–3962.

Lerner-Marmarosh, N., Miralem, T., Gibbs, P.E.M., and Maines, M.D. (2008). Human biliverdin reductase is an ERK activator; hBVR is an ERK nuclear transporter and is required for MAPK signaling. Proceedings of the National Academy of Sciences of the United States of America *105*, 6870.

Li, G., Piampongsant, S., Faria, R.N., Voet, A., Pineda-Peña, A.C., Khouri, R., Lemey, P., Vandamme, A.M., and Theys, K. (2015). An integrated map of HIV genome-wide variation from a population perspective. Retrovirology *12*, 18.

Li, Q., Dua, L., Estes, J.D., Ma, Z.M., Rourke, T., Wang, Y., Reilly, C., Carlis, J., Miller, C.J., and Haase, A.T. (2005). Peak SIV replication in resting memory CD4+ T cells depletes gut lamina propria CD4+ T cells. Nature *434*, 1148–1152.

Li, S., Juarez, J., Alali, M., Dwyer, D., Collman, R., Cunningham, A., and Naif, H.M. (1999). Persistent CCR5 Utilization and Enhanced Macrophage Tropism by Primary Blood Human Immunodeficiency Virus Type 1 Isolates from Advanced Stages of Disease and Comparison to Tissue-Derived Isolates. Journal of Virology *73*, 9741–9755.

Lin, J., Haffner, M.C., Zhang, Y., Lee, B.H., Brennen, W.N., Britton, J., Kachhap, S.K., Shim, J.S., Liu, J.O., Nelson, W.G., *et al.* (2011). Disulfiram Is a DNA Demethylating Agent and Inhibits Prostate Cancer Cell Growth. The Prostate *71*, 333.

Liu, Y., McNevin, J., Cao, J., Zhao, H., Genowati, I., Wong, K., McLaughlin, S., McSweyn, M.D., Diem, K., Stevens, C.E., *et al.* (2006). Selection on the Human Immunodeficiency Virus Type 1 Proteome following Primary Infection. Journal of Virology *80*, 9519–9529.

Lorenzo-Redondo, R., Fryer, H.R., Bedford, T., Kim, E.Y., Archer, J., Kosakovsky Pond, S.L., Chung, Y.S., Penugonda, S., Chipman, J.G., Fletcher, C. v., *et al.* (2016). Persistent HIV-1 replication maintains the tissue reservoir during therapy. Nature *530*, 51–56.

Loutfy, M.R., Wu, W., Letchumanan, M., Bondy, L., Antoniou, T., Margolese, S., Zhang, Y., Rueda, S., McGee, F., Peck, R., *et al.* (2013). Systematic Review of HIV Transmission between Heterosexual Serodiscordant Couples where the HIV-Positive Partner Is Fully Suppressed on Antiretroviral Therapy. PLoS ONE *8*.

Lu, H.K., Gray, L.R., Wightman, F., Ellenberg, P., Khoury, G., Cheng, W.-J., Mota, T.M., Wesselingh, S., Gorry, P.R., Cameron, P.U., *et al.* (2014). Ex Vivo Response to Histone Deacetylase (HDAC) Inhibitors of the HIV Long Terminal Repeat (LTR) Derived from HIV-Infected Patients on Antiretroviral Therapy. PLoS ONE *9*, 113341.

Maldarelli, F., Wu, X., Su, L., Simonetti, F.R., Shao, W., Hill, S., Spindler, J., Ferris, A.L., Mellors, J.W., Kearney, M.F., *et al.* (2014). Specific HIV integration sites are linked to clonal expansion and persistence of infected cells. Science (New York, N.Y.) *345*, 179.

Marsden, M.D., Loy, B.A., Wu, X., Ramirez, C.M., Schrier, A.J., Murray, D., Shimizu, A., Ryckbosch, S.M., Near, K.E., Chun, T.W., *et al.* (2017). In vivo activation of latent HIV with a synthetic bryostatin analog effects both latent cell "kick" and "kill" in strategy for virus eradication. PLoS Pathogens *13*.

Marshall, H.M., Ronen, K., Berry, C., Llano, M., Sutherland, H., Saenz, D., Bickmore, W., Poeschla, E., and Bushman, F.D. (2007). Role of PSIP 1/LEDGF/p75 in lentiviral infectivity and integration targeting. PLoS ONE *2*, e1340.

Martinez-Picado*, J., and Deeks, S.G. (2016). Persistent HIV-1 replication during antiretroviral therapy. Current Opinion in HIV and AIDS *11*, 417–423.

Mattapallil, J.J., Douek, D.C., Hill, B., Nishimura, Y., Martin, M., and Roederer, M. (2005). Massive infection and loss of memory CD4+ T cells in multiple tissues during acute SIV infection. Nature *434*, 1093–1097.

McCoombe, S.G., and Short, R. v (2006). Potential HIV-1 target cells in the human penis. AIDS *20*, 1491–1495.

McDonald, D., Wu, L., Bohks, S.M., KewalRamani, V.N., Unutmaz, D., and Hope, T.J. (2003). Recruitment of HIV and its receptors to dendritic cell-T cell junctions. Science *300*, 1295–1297.

McDonald, R.A., Mayers, D.L., Chung, R.C., Wagner, K.F., Ratto-Kim, S., Birx, D.L., and Michael, N.L. (1997). Evolution of human immunodeficiency virus type 1 env sequence variation in patients with diverse rates of disease progression and T-cell function. Journal of Virology *71*, 1871–1879.

Mehandru, S., Poles, M.A., Tenner-Racz, K., Horowitz, A., Hurley, A., Hogan, C., Boden, D., Racz, P., and Markowitz, M. (2004). Primary HIV-1 infection is associated with preferential depletion of CD4+ T lymphocytes from effector sites in the gastrointestinal tract. Journal of Experimental Medicine *200*, 761–770.

Mehandru, S., Poles, M.A., Tenner-Racz, K., Manuelli, V., Jean-Pierre, P., Lopez, P., Shet, A., Low, A., Mohri, H., Boden, D., *et al.* (2007). Mechanisms of Gastrointestinal CD4+ T-Cell Depletion during Acuteand Early Human Immunodeficiency Virus Type 1 Infection. Journal of Virology *81*, 599–612.

Melkova*, Z., Shankaran, P., Madlenakova, M., and Bodor, J. (2017). Current views on HIV-1 latency, persistence, and cure. Folia Microbiologica *62*, 73–87.

Mellors, J.W., Muñoz, A., Giorgi, J. v., Margolick, J.B., Tassoni, C.J., Gupta, P., Kingsley, L.A., Todd, J.A., Saah, A.J., Detels, R., *et al.* (1997). Plasma viral load and CD4+ lymphocytes as prognostic markers of HIV-1 infection. Annals of Internal Medicine *126*, 946–954.

Miller, C.J., Li, Q., Abel, K., Kim, E.-Y., Ma, Z.-M., Wietgrefe, S., la Franco-Scheuch, L., Compton, L., Duan, L., Shore, M.D., *et al.* (2005). Propagation and Dissemination of Infection after Vaginal Transmission of Simian Immunodeficiency Virus. Journal of Virology *79*, 9217–9227.

Muto, A., Hoshino, H., Madisen, L., Yanai, N., Obinata, M., Karasuyama, H., Hayashi, N., Nakauchi, H., Yamamoto, M., Groudine, M., *et al.* (1998). Identification of Bach2 as a B-cell-specific partner for small maf proteins that negatively regulate the immunoglobulin heavy chain gene 3' enhancer. The EMBO Journal *17*, 5734.

Muto, A., Tashiro, S., Tsuchiya, H., Kume, A., Kanno, M., Ito, E., Yamamoto, M., and Igarashi, K. (2002). Activation of Maf/AP-1 Repressor Bach2 by Oxidative Stress Promotes Apoptosis and Its Interaction with Promyelocytic Leukemia Nuclear Bodies *. Journal of Biological Chemistry *277*, 20724–20733.

Muto, A., Tashiro, S., Nakajima, O., Hoshino, H., Takahashi, S., Sakoda, E., Ikebe, D., Yamamoto, M., and Igarashi, K. (2004). The transcriptional programme of antibody class switching involves the repressor Bach2. Nature *429*, 566–571.

Nkeze, J., Li, L., Benko, Z., Li, G., and Zhao, R.Y. (2015). Molecular characterization of HIV-1 genome in fission yeast Schizosaccharomyces pombe. Cell & Bioscience *5*, 47.

Nunoshiba, T., Obata, F., Boss, A.C., Oikawa, S., Mori, T., Kawanishi, S., and Yamamoto, K. (1999). Role of Iron and Superoxide for Generation of Hydroxyl Radical, Oxidative DNA Lesions, and Mutagenesis in Escherichia coli. J. Biol. Chem *274*, 34832–34837.

Oxenius, A., Price, D.A., Easterbrook, P.J., O'Callaghan, C.A., Kelleher, A.D., Whelan, J.A., Sontag, G., Sewell, A.K., and Phillips, R.E. (2000). Early highly active antiretroviral therapy for acute HIV-1 infection preserves immune function of CD8+ and CD4+ T lymphocytes. Proceedings of the National Academy of Sciences of the United States of America *97*, 3382–3387.

Oyake, T., Itoh, K., Motohashi, H., Hayashi, N., Hoshino, H., Nishizawa, M., Yamamoto, M., and Igarashi, K. (1996). Bach proteins belong to a novel family of BTB-basic leucine zipper transcription factors that interact with MafK and regulate transcription through the NF-E2 site. Molecular and Cellular Biology *16*, 6083.

Pardons, M., Fromentin, R., Pagliuzza, A., Routy, J.-P., and Chomont, N. (2019). Latency-Reversing Agents Induce Differential Responses in Distinct Memory CD+ T Cell Subsets in Individuals on Antiretroviral Therapy. Cell Reports *29*, 2783-2795.e5.

Park, E.J., Vujcic, L.K., Anand, R., Theodore, T.S., and Quinnan, G. v. (1998). Mutations in both gp120 and gp41 Are Responsible for the Broad Neutralization Resistance of Variant Human Immunodeficiency Virus Type 1 MN to Antibodies Directed at V3 and Non-V3 Epitopes. Journal of Virology *72*, 7099–7107.

Paz-Bailey, G., Sternberg, M., Puren, A.J., Steele, L., and Lewis, D.A. (2010). Determinants of HIV type 1 shedding from genital ulcers among men in South Africa. Clinical Infectious Diseases *50*, 1060–1067.

Pearson, R., Kim, Y.K., Hokello, J., Lassen, K., Friedman, J., Tyagi, M., and Karn, J. (2008). Epigenetic Silencing of Human Immunodeficiency Virus (HIV) Transcription by Formation of Restrictive Chromatin Structures at the Viral Long Terminal Repeat Drives the Progressive Entry of HIV into Latency. Journal of Virology *82*, 12291.

Pedersen, C., Katzenstein, T., Nielsen, C., Lundgren, J.D., and Gerstoft, J. (1997). Prognostic value of serum HIV-RNA levels at virologic steady state after seroconversion: Relation to CD4 cell count and clinical course of primary infection. Journal of Acquired Immune Deficiency Syndromes and Human Retrovirology *16*, 93–99.

Peeters, M., Honoré, C., Huett, T., Bedjabaga, L., Ossari, S., Bussi, P., Cooper, R.W., and Delaporte, E. (1989). Isolation and partial characterization of an HIV-related virus occurring naturally in chimpanzees in Gabon. AIDS *3*, 625–630.

Pereira, P.J.B., Macedo-Ribeiro, S., Párraga, A., Pérez-Luque, R., Cunningham, O., Darcy, K., Mantle, T.J., and Coll, M. (2001). Structure of human biliverdin IXβ reductase, an early fetal bilirubin IXβ producing enzyme. Nature *8*, 215–220.

Perelson, A.S., Essunger, P., Cao, Y., Vesanen, M., Hurley, A., Saksela, K., Markowitz, M., and Ho, D.D. (1997). Decay characteristics of HIV-1-infected compartments during combination therapy. Nature *387*, 188–191.

Peressin, M., Proust, A., Schmidt, S., Su, B., Lambotin, M., Biedma, M.E., Laumond, G., Decoville, T., Holl, V., and Moog, C. (2014). Efficient transfer of HIV-1 in trans and in cis from Langerhans dendritic cells and macrophages to autologous T lymphocytes. AIDS *28*, 667–677.

Perkins, N.D., Edwards, N.L., Duckett, C.S., Agranoff, A.B., Schmid, R.M., and Nabel, G.J. (1993). A cooperative interaction between NF-kappa B and Sp1 is required for HIV-1 enhancer activation. The EMBO Journal *12*, 3551.

Pilcher*, C.D., Eron, J.J., Galvin, S., Gay, C., and Cohen, M. (2004). Acute HIV revisited: New opportunities for treatment and prevention. Journal of Clinical Investigation *113*, 937–945.

Pinkevych, M., Cromer, D., Tolstrup, M., Grimm, A.J., Cooper, D.A., Lewin, S.R., Søgaard, O.S., Rasmussen, T.A., Kent, S.J., Kelleher, A.D., *et al.* (2015). HIV Reactivation from Latency after Treatment Interruption Occurs on Average Every 5-8 Days—Implications for HIV Remission. PLoS Pathogens *11*, e1005000.

Plantier, J.C., Leoz, M., Dickerson, J.E., de Oliveira, F., Cordonnier, F., Lemée, V., Damond, F., Robertson, D.L., and Simon, F. (2009). A new human immunodeficiency virus derived from gorillas. Nature Medicine *15*, 871–872.

Powers, K.A., Poole, C., Pettifor, A.E., and Cohen, M.S. (2008). Rethinking the heterosexual infectivity of HIV-1: a systematic review and meta-analysis. The Lancet Infectious Diseases *8*, 553–563.

Pyo, C.-W., Yang, Y.L., Yoo, N.-K., and Choi, S.-Y. (2008). Reactive oxygen species activate HIV long terminal repeat via post-translational control of NF-κB. Biochemical and Biophysical Research Communications *376*, 180–185.

Quinn, T.C., Wawer, M.J., Sewankambo, N., Serwadda, D., Li, C., Wabwire-Mangen, F., Meehan, M.O., Lutalo, T., and Gray, R.H. (2000). Viral Load and Heterosexual Transmission of Human Immunodeficiency Virus Type 1. New England Journal of Medicine *342*, 921–929.

Raha, T., Cheng, S.W.G., and Green, M.R. (2005). HIV-1 Tat Stimulates Transcription Complex Assembly through Recruitment of TBP in the Absence of TAFs. PLoS Biology *3*, 0221–0230.

Rasmussen, T.A., Tolstrup, M., Brinkmann, C.R., Olesen, R., Erikstrup, C., Solomon, A., Winckelmann, A., Palmer, S., Dinarello, C., Buzon, M., *et al.* (2014). Panobinostat, a histone deacetylase inhibitor, for latent-virus reactivation in HIV-infected patients on suppressive antiretroviral therapy: a phase 1/2, single group, clinical trial. The Lancet. HIV *1*, e13–e21.

Raymond, S., Saliou, A., Delobel, P., Cazabat, M., Pasquier, C., Jeanne, N., Sauné, K., Massip, P., Marchou, B., and Izopet, J. (2014). Evolution of HIV-1 quasispecies and coreceptor use in cell reservoirs of patients on suppressive antiretroviral therapy. Journal of Antimicrobial Chemotherapy *69*, 2527–2530.

Richman, D.D., Wrin, T., Little, S.J., and Petropoulos, C.J. (2003). Rapid evolution of the neutralizing antibody response to HIV type 1 infection. Proceedings of the National Academy of Sciences of the United States of America *100*, 4144–4149.

del Romero, J., Marincovich, B., Castilla, J., García, S., Campo, J., Hernando, V., and Rodríguez, C. (2002). Evaluating the risk of HIV transmission through unprotected orogenital sex. AIDS *16*, 1296–1297.

del Romero, J., Río, I., Castilla, J., Baza, B., Paredes, V., Vera, M., and Rodríguez, C. (2015). Absence of transmission from HIV-infected individuals with HAART to their heterosexual serodiscordant partners. Enfermedades Infecciosas y Microbiologia Clinica *33*, 666–672.

Rosenbloom, D.I.S., Hill, A.L., Laskey, S.B., and Siliciano, R.F. (2017). Re-evaluating evolution in the HIV reservoir. Nature *551*, E6–E8.

Rustanti, L., Jin, H., Lor, M., Lin, M.H., Rawle, D.J., and Harrich, D. (2017). A mutant Tat protein inhibits infection of human cells by strains from diverse HIV-1 subtypes. Virology Journal 2017 14:1 *14*, 1–11.

Ryter*, S.W. (2021). Significance of Heme and Heme Degradation in the Pathogenesis of Acute Lung and Inflammatory Disorders. International Journal of Molecular Sciences *22*, 5509.

Saba, E., Grivel, J.C., Vanpouille, C., Brichacek, B., Fitzgerald, W., Margolis, L., and Lisco, A. (2010). HIV-1 sexual transmission: Early events of HIV-1 infection of human cervico-vaginal tissue in an optimized ex vivo model. Mucosal Immunology *3*, 280–290.

Sahu, G.K., Paar, D., Frost, S.D.W., Smith, M.M., Weaver, S., and Cloyd, M.W. (2009). Low-level plasma HIVs in patients on prolonged suppressive highly active antiretroviral therapy are produced mostly by cells other than CD4 T-cells. Journal of Medical Virology *81*, 9–15.

Salazar-Gonzalez, J.F., Salazar, M.G., Keele, B.F., Learn, G.H., Giorgi, E.E., Li, H., Decker, J.M., Wang, S., Baalwa, J., Kraus, M.H., *et al.* (2009). Genetic identity, biological phenotype,

and evolutionary pathways of transmitted/founder viruses in acute and early HIV-1 infection. Journal of Experimental Medicine *206*, 1273–1289.

Saleh, S., Solomon, A., Wightman, F., Xhilaga, M., Cameron, P.U., and Lewin, S.R. (2007). CCR7 ligands CCL19 and CCL21 increase permissiveness of resting memory CD4+ T cells to HIV-1 infection: a novel model of HIV-1 latency. Blood *110*, 4161–4164.

Salim, M., Brown-Kipphut, B.A., and Maines, M.D. (2001). Human Biliverdin Reductase Is Autophosphorylated, and Phosphorylation Is Required for Bilirubin Formation. Journal of Biological Chemistry *276*, 10929–10934.

Sallusto, F., Lenig, D., Förster, R., Lipp, M., and Lanzavecchia, A. (1999). Two subsets of memory T lymphocytes with distinct homing potentials and effector functions. Nature *401*, 708–712.

Schreiber, M., Wachsmuth, C., Mqiler, H., Hagen, C., Schmitz, H., and van Lunzen2t, J. (1996). Loss of antibody reactivity directed against the V3 domain of certain human immunodeficiency virus type 1 variants durin 9 disease progression.

Schröder, A.R.W., Shinn, P., Chen, H., Berry, C., Ecker, J.R., and Bushman, F. (2002). HIV-1 Integration in the Human Genome Favors Active Genes and Local Hotspots. Cell *110*, 521–529.

Sedlak, T.W., Saleh, M., Higginson, D.S., Paul, B.D., Juluri, K.R., and Snyder, S.H. (2009). Bilirubin and glutathione have complementary antioxidant and cytoprotective roles. Proceedings of the National Academy of Sciences *106*, 5171–5176.

Semenova, N., Bosnjak, M., Markelc, B., Znidar, K., Cemazar, M., and Heller, L. (2019). Multiple cytosolic DNA sensors bind plasmid DNA after transfection. Nucleic Acids Research *47*, 10235–10246.

Shan, L., Deng, K., Gao, H., Xing, S., Capoferri, A.A., Durand, C.M., Rabi, S.A., Laird, G.M., Kim, M., Hosmane, N.N., *et al.* (2017). Transcriptional Reprogramming during Effector-to-Memory Transition Renders CD4+ T Cells Permissive for Latent HIV-1 Infection. Immunity *47*, 766-775.e3.

Shankaran, P. (2016). Effects of heme arginate in HIV-1 acute infection and in latency reversal.

Shankaran, P., Vlkova, L., Liskova, J., and Melkova, Z. (2011). Heme arginate potentiates latent HIV-1 reactivation while inhibiting the acute infection. Antiviral Research *92*, 434–446.

Shankaran, P., Madlenakova, M., Hajkova, V., Jilich, D., Svobodova, I., Horinek, A., Fujikura, Y., and Melkova, Z. (2017). Effects of heme degradation products on reactivation of latent HIV-1. Acta Virologica *61*, 86–96.

Shaw*, G.M., and Hunter, E. (2012). HIV transmission. Cold Spring Harbor Perspectives in Medicine *2*.

Shepherd, J.C., Jacobson, L.P., Qiao, W., Jamieson, B.D., Phair, J.P., Piazza, P., Quinn, T.C., and Margolick, J.B. (2008). Emergence and persistence of CXCR4-tropic HIV-1 in a population of men from the multicenter AIDS cohort study. Journal of Infectious Diseases *198*, 1104–1112.

Siliciano, J.D., Lai, J., Callender, M., Pitt, E., Zhang, H., Margolick, J.B., Gallant, J.E., Cofrancesco, J., Moore, R.D., Gange, S.J., *et al.* (2007). Stability of the Latent Reservoir for HIV-1 in Patients Receiving Valproic Acid. The Journal of Infectious Diseases *195*, 833–836.

Sivard, P., Dezutter-Dambuyant, C., Kanitakis, J., Mosnier, J.-F., Hamzeh, H., Bechetoille, N., Berthier, O., Sabido, O., Schmitt, D., Genin, C., *et al.* (2003). In vitro reconstructed mucosa-integrating Langerhans' cells. Experimental Dermatology *12*, 346–355.

Sivard, P., Berlier, W., Picard, B., Sabido, O., Genin, C., and Misery, L. (2004). HIV-1 Infection of Langerhans Cells in a Reconstructed Vaginal Mucosa. The Journal of Infectious Diseases *190*, 227–235.

Søgaard, O.S., Graversen, M.E., Leth, S., Olesen, R., Brinkmann, C.R., Nissen, S.K., Kjaer, A.S., Schleimann, M.H., Denton, P.W., Hey-Cunningham, W.J., *et al.* (2015). The Depsipeptide Romidepsin Reverses HIV-1 Latency In Vivo.

Soriano-Sarabia, N., Bateson, R.E., Dahl, N.P., Crooks, A.M., Kuruc, J.D., Margolis, D.M., and Archin, N.M. (2014). Quantitation of Replication-Competent HIV-1 in Populations of Resting CD4 + T Cells . Journal of Virology *88*, 14070–14077.

Spina, C.A., Anderson, J., Archin, N.M., Bosque, A., Chan, J., Famiglietti, M., Greene, W.C., Kashuba, A., Lewin, S.R., Margolis, D.M., *et al.* (2013). An In-Depth Comparison of Latent HIV-1 Reactivation in Multiple Cell Model Systems and Resting CD4+ T Cells from Aviremic Patients. PLoS Pathogens *9*, 1–15.

Spivak, A.M., Andrade, A., Eisele, E., Hoh, R., Bacchetti, P., Bumpus, N.N., Emad, F., Buckheit, R., Ccance-Katz, E.F., Lai, J., *et al.* (2014). A pilot study assessing the safety and latency-reversing activity of disulfiram in HIV-1-infected adults on antiretroviral therapy. Clinical Infectious Diseases *58*, 883–890.

Starcich, B.R., Hahn, B.H., Shaw, G.M., McNeely, P.D., Modrow, S., Wolf, H., Parks, E.S., Parks, W.P., Josephs, S.F., Gallo, R.C., *et al.* (1986). Identification and characterization of conserved and variable regions in the envelope gene of HTLV-III/LAV, the retrovirus of AIDS. Cell *45*, 637–648.

Stevenson, M., Stanwick, T.L., Dempsey, M.P., and Lamonica, C.A. (1990). HIV-1 replication is controlled at the level of T cell activation and proviral integration. The EMBO Journal *9*, 1551–1560.

Suñé, C., and García-Blanco, A.M. (1995). Sp1 Transcription Factor Is Required for In Vitro Basal and Tat-Activated Transcription from the Human Immunodeficiency Virus Type 1 Long Terminal Repeat. Journal of Virology *10*, 6572-6576

Swiggard, W.J., Baytop, C., Yu, J.J., Dai, J., Li, C., Schretzenmair, R., Theodosopoulos, T., and O'Doherty, U. (2005). Human Immunodeficiency Virus Type 1 Can Establish Latent Infection in Resting CD4+ T Cells in the Absence of Activating Stimuli. Journal of Virology *79*, 14179.

Sykiotis*, G.P., and Bohmann, D. (2010). Stress-Activated Cap'n'collar Transcription Factors in Aging and Human Disease. Science Signaling *3*, 112, re3.

Telwatte, S., Kim, P., Chen, T.H., Milush, J.M., Somsouk, M., Deeks, S.G., Hunt, P.W., Wong, J.K., and Yukl, S.A. (2020). Mechanistic differences underlying HIV latency in the gut and blood contribute to differential responses to latency-reversing agents. AIDS (London, England) *34*, 2013–2024.

Tenhunen, R., Marver, H.S., and Schmidt, R. (1969). Microsomal Heme Oxygenase CHARACTERIZATION OF THE ENZYME*. Journal of Biological Chemistry *244*, 6388–6394.

Terahara, K., Iwabuchi, R., Hosokawa, M., Nishikawa, Y., Takeyama, H., Takahashi, Y., and Tsunetsugu-Yokota, Y. (2019). A CCR5+ memory subset within HIV-1-infected primary resting CD4+ T cells is permissive for replication-competent, latently infected viruses in vitro. BMC Research Notes 2019 12:1 *12*, 1–7.

Thome, J.J.C., Yudanin, N., Ohmura, Y., Kubota, M., Grinshpun, B., Sathaliyawala, T., Kato, T., Lerner, H., Shen, Y., and Farber, D.L. (2014). Spatial map of human T cell compartmentalization and maintenance over decades of life. Cell *159*, 814.

Thome, J.J.C., Bickham, K.L., Ohmura, Y., Kubota, M., Matsuoka, N., Gordon, C., Granot, T., Griesemer, A., Lerner, H., Kato, T., *et al.* (2016). Early life compartmentalization of human T cell differentiation and regulatory function in mucosal and lymphoid tissues. Nature Medicine *22*, 72.

Toki, T., Itoh, J., Kitazawa, ichi, Arai, K., Hatakeyama, K., Akasaka, J., Igarashi, K., Nomura, N., Yokoyama, M., Yamamoto, M., *et al.* (1997). Human small Maf proteins form heterodimers with CNC family transcription factors and recognize the NF-E2 motif.

Trejbalova, K., Kovářová, D., Blažková, J., Machala, L., Jilich, D., Weber, J., Kučerová, D., Vencálek, O., Hirsch, I., and Hejnar, J. (2016). Development of 5' LTR DNA methylation of latent HIV-1 provirus in cell line models and in long-term-infected individuals. Clinical Epigenetics *8*, 1–20.

Tripathy, M.K., McManamy, M.E.M., Burch, B.D., Archin, N.M., and Margolis, D.M. (2015). H3K27 Demethylation at the Proviral Promoter Sensitizes Latent HIV to the Effects of Vorinostat in Ex Vivo Cultures of Resting CD4+ T Cells. Journal of Virology *89*, 8392.

Tsai, P., Wu, G., Baker, C.E., Thayer, W.O., Spagnuolo, R.A., Sanchez, R., Barrett, S., Howell, B., Margolis, D., Hazuda, D.J., *et al.* (2016). In vivo analysis of the effect of panobinostat on cell-associated HIV RNA and DNA levels and latent HIV infection. Retrovirology *13*, 1–12.

Tsukumo, S., Unno, M., Muto, A., Takeuchi, A., Kometani, K., Kurosaki, T., Igarashi, K., and Saito, T. (2013). Bach2 maintains T cells in a naive state by suppressing effector memory-related genes. Proceedings of the National Academy of Sciences *110*, 10735–10740.

Tudor, C., Lerner-Marmarosh, N., Engelborghs, Y., Gibbs, P.E.M., and Maines, M.D. (2008). Biliverdin reductase is a transporter of haem into the nucleus and is essential for regulation of HO-1 gene expression by haematin. Biochemical Journal *413*, 405–416.

Turner*, A.-M.W., and Margolis, D.M. (2017). Chromatin Regulation and the Histone Code in HIV Latency. The Yale Journal of Biology and Medicine *90*, 229.

UNAIDS (2000). Report on the global HIV/AIDS epidemic (Geneva).

UNAIDS (2020). UNAIDS report on HIV/AIDS pandemic (Geneva).

Vajdy, M., Veazey, R., Tham, I., deBakker, C., Westmoreland, S., Neutra, M., and Lackner, A. (2001). Early Immunologic Events in Mucosal and Systemic Lymphoid Tissues after Intrarectal Inoculation with Simian Immunodeficiency Virus. The Journal of Infectious Diseases *184*, 1007–1014.

Valladeau, J., Ravel, O., Dezutter-Dambuyant, C., Moore, K., Kleijmeer, M., Liu, Y., Duvert-Frances, V., Vincent, C., Schmitt, D., Davoust, J., *et al.* (2000). Langerin, a novel C-type lectin specific to langerhans cells, is an endocytic receptor that induces the formation of Birbeck granules. Immunity *12*, 71–81.

Varghese, B., Maher, J.E., Peterman, T.A., Branson, B.M., and Steketee, R.W. (2002). Reducing the risk of sexual HIV transmission: Quantifying the per-act risk for HIV on the basis of choice of partner, sex act, and condom use. Sexually Transmitted Diseases *29*, 38–43.

Veazey, R.S., Marx, P.A., and Lackner, A.A. (2003). Vaginal CD4+ T Cells Express High Levels of CCR5 and Are Rapidly Depleted in Simian Immunodeficiency Virus Infection. The Journal of Infectious Diseases *187*, 769–776.

Wagner, T.A., McLaughlin, S., Garg, K., Cheung, C.Y.K., Larsen, B.B., Styrchak, S., Huang, H.C., Edlefsen, P.T., Mullins, J.I., and Frenkel, L.M. (2014). Proliferation of cells with HIV integrated into cancer genes contributes to persistent infection. Science (New York, N.Y.) *345*, 570.

Watanabe-Matsui, M., Muto, A., Matsui, T., Itoh-Nakadai, A., Nakajima, O., Murayama, K., Yamamoto, M., Ikeda-Saito, M., and Igarashi, K. (2011). Heme regulates B-cell differentiation, antibody class switch, and heme oxygenase-1 expression in B cells as a ligand of Bach2. Blood *117*, 5438–5448.

Watanabe-Matsui, M., Matsumoto, T., Matsui, T., Ikeda-Saito, M., Muto, A., Murayama, K., and Igarashi, K. (2015). Heme binds to an intrinsically disordered region of Bach2 and alters its conformation. Archives of Biochemistry and Biophysics *565*, 25–31.

Wei, D.G., Chiang, V., Fyne, E., Balakrishnan, M., Barnes, T., Graupe, M., Hesselgesser, J., Irrinki, A., Murry, J.P., Stepan, G., *et al.* (2014). Histone Deacetylase Inhibitor Romidepsin Induces HIV Expression in CD4 T Cells from Patients on Suppressive Antiretroviral Therapy at Concentrations Achieved by Clinical Dosing. PLOS Pathogens *10*, e1004071.

Westendorp, M.O., Shatrov, V.A., Schulze-Osthoff, K., Frank, R., Kraft, M., Los, M., Krammer, P.H., Droge, W., and Lehmann, V. (1995). HIV-1 Tat potentiates TNF-induced NF-KB activation and cytotoxicity by altering the cellular redox state. The EMBO Journal *14*, 546–554.

de Witte, L., Nabatov, A., Pion, M., Fluitsma, D., de Jong, M.A.W.P., de Gruijl, T., Piguet, V., van Kooyk, Y., and Geijtenbeek, T.B.H. (2007). Langerin is a natural barrier to HIV-1 transmission by Langerhans cells. Nature Medicine *13*, 367–371.

de Witte*, L., Nabatov, A., and Geijtenbeek, T.B.H. (2008). Distinct roles for DC-SIGN+-dendritic cells and Langerhans cells in HIV-1 transmission. Trends in Molecular Medicine *14*, 12–19.

Wolfe, N.D., Switzer, W.M., Carr, J.K., Bhullar, V.B., Shanmugam, V., Tamoufe, U., Prosser, A.T., Torimiro, J.N., Wright, A., Mpoudi-Ngole, E., *et al.* (2004). Naturally acquired simian retrovirus infections in central African hunters. Lancet *363*, 932–937.

Wood, N., Bhattacharya, T., Keele, B.F., Giorgi, E., Liu, M., Gaschen, B., Daniels, M., Ferrari, G., Haynes, B.F., McMichael, A., *et al.* (2009). HIV Evolution in Early Infection: Selection Pressures, Patterns of Insertion and Deletion, and the Impact of APOBEC. PLoS Pathogens *5*, e1000414.

World Health Organization (2019). HIV/AIDS surveillance in Europe (Stockholm).

Wu, L., Paxton, W.A., Kassam, N., Ruffing, N., Rottman, J.B., Sullivan, N., Choe, H., Sodroski, J., Newman, W., Koup, R.A., *et al.* (1997). CCR5 Levels and Expression Pattern Correlate with Infectability by Macrophage-tropic HIV-1, In Vitro. Journal of Experimental Medicine *185*, 1681–1692.

Xing, S., Bullen, C.K., Shroff, N.S., Shan, L., Yang, H.-C., Manucci, J.L., Bhat, S., Zhang, H., Margolick, J.B., Quinn, T.C., *et al.* (2011). Disulfiram Reactivates Latent HIV-1 in a Bcl-2-Transduced Primary CD4 + T Cell Model without Inducing Global T Cell Activation . Journal of Virology *85*, 6060–6064.

Yamada, T., Yamaguchi, Y., Inukai, N., Okamoto, S., Mura, T., and Handa, H. (2006). P-TEFb-mediated phosphorylation of hSpt5 C-terminal repeats is critical for processive transcription elongation. Molecular Cell *21*, 227–237.

Yoshida, C., Yoshida, F., Sears, D.E., Hart, S.M., Ikebe, D., Muto, A., Basu, S., Igarashi, K., and Melo, J. v. (2007). Bcr-Abl signaling through the PI-3/S6 kinase pathway inhibits nuclear translocation of the transcription factor Bach2, which represses the antiapoptotic factor heme oxygenase-1. Blood *109*, 1211–1219.

Yu, K.L., Jung, Y.M., Park, S.H., and You*, S.D.L.& J.C. (2020). Human transcription factor YY1 could upregulate the HIV-1 gene expression. BMB Reports *53*, 248–253.

Zack, A.J., Arrigo, J.S., Weitsman, R.S., Go, S.A., Haislip, A., and Chen, S.Y.I. (1990). HIV-1 Entry into Quiescent Primary Lymphocytes: Molecular Analysis Reveals a Labile, Latent Viral Structure. Cell *61*, 213–222.

Zack, J.A., Cann, A.J., Lugo, J.P., and Chen, I.S.Y. (1988). HIV-1 production from infected peripheral blood T cells after HTLV-I induced mitogenic stimulation. Science *240*, 1026–1029.

Zhang, Z.Q., Schuler, T., Zupancic, M., Wietgrefe, S., Staskus, K.A., Reimann, K.A., Reinhart, T.A., Rogan, M., Cavert, W., Miller, C.J., *et al.* (1999). Sexual transmission and propagation of SIV and HIV in resting and activated CD4+ T cells. Science *286*, 1353–1357.

Zhuang, J., Jetzt, A.E., Sun, G., Yu, H., Klarmann, G., Ron, Y., Preston, B.D., and Dougherty, J.P. (2002). Human Immunodeficiency Virus Type 1 Recombination: Rate, Fidelity, and Putative Hot Spots. Journal of Virology *76*, 11273–11282.

---

*secondary citation